NASA TECHNICAL NOTE

NASA TN D-6006

LUNAR ORBITER FLIGHT VIBRATION DATA AND COMPARISONS WITH ENVIRONMENTAL SPECIFICATIONS

by Sherman A. Clevenson

Langley Research Center
Hampton, Va. 23365

NATIONAL AERONAUTICS AND SPACE ADMINISTRATION • WASHINGTON, D. C. • SEPTEMBER 1970

1. Report No.	2. Government Accession No.
NASA TN D-6006	

4. Title and Subtitle

LUNAR ORBITER FLIGHT VIBRATION DATA AND COMPARISONS WITH ENVIRONMENTAL SPECIFICATIONS

5. Report Date: September 1970

6. Performing Organization Code:

7. Author(s)

Sherman A. Clevenson

8. Performing Organization Report No.: L-6594

9. Performing Organization Name and Address

NASA Langley Research Center
Hampton, Va. 23365

10. Work Unit No.: 814-11-00-03

11. Contract or Grant No.:

12. Sponsoring Agency Name and Address

National Aeronautics and Space Administration
Washington, D. C. 20546

13. Type of Report and Period Covered: Technical Note

14. Sponsoring Agency Code:

15. Supplementary Notes

16. Abstract

This paper presents detailed flight-measured vibration data obtained during the five successful flights of Lunar Orbiter and compares these data with vibration levels specified as flight acceptance requirements. Measured flight vibration data on these flights were lower than those measured on previous flights of the Atlas-Agena launch vehicle and thus the flight acceptance random vibration test levels substantially exceeded the flight measurements. This paper also discusses the derivation of the flight requirements.

17. Key Words (Suggested by Author(s))	18. Distribution Statement
Vibration predictions Flight vibration measurements Lunar Orbiter	Unclassified – Unlimited

19. Security Classif. (of this report)	20. Security Classif. (of this page)	21. No. of Pages	22. Price*
Unclassified	Unclassified	68	$3.00

*For sale by the Clearinghouse for Federal Scientific and Technical Information
Springfield, Virginia 22151

LUNAR ORBITER FLIGHT VIBRATION DATA AND COMPARISONS WITH ENVIRONMENTAL SPECIFICATIONS

By Sherman A. Clevenson
Langley Research Center

SUMMARY

This paper presents requirements and philosophies of flight acceptance testing. Detailed vibration measurements, including peak acceleration levels and predominant frequencies that occurred during various transients, are given for five flights of Lunar Orbiter. Results of power spectral density analyses for lift-off and transonic speed conditions are presented. Results of shock spectrum analyses are shown for the various transients during launch and ascent. Discussions are given in an appendix for some unusual on-pad vibrations prior to ignition of the launch vehicle. Flight data are compared with preflight predictions, namely, vibration levels from flight acceptance tests (FAT) and results of a regression analysis. The FAT random vibration levels are considered severe, since the measured flight inputs were lower than expected. Results of the regression analysis predicted the random vibration environment very conservatively; therefore, the analysis requires further development.

INTRODUCTION

A spacecraft is subjected to a large number of environments during its lifetime. It is desirable to show through ground-test studies prior to flight that the spacecraft can withstand loads which result from these environments. Most ground environments encountered can be determined with a high level of confidence. However, the vibration environment imposed during the ascent phase of launch through spacecraft separation is determined with a much lower level of confidence because of the differences between spacecraft, differences between launch vehicles, and the scarcity of applicable vibration data. Flight measurements are seldom available for identical spacecraft and launch vehicles. In particular, the vibration response from the various transient inputs during launch are very difficult to predict.

Qualification tests are usually made on development and flight hardware to insure that adequate margins are present in the spacecraft. To assure that a spacecraft will withstand the prelaunch, launch, and ascent environments, flight acceptance tests (FAT) are conducted. The general approach in establishing FAT levels (not to exceed expected

flight levels) has been to depend on previous flight vibration data obtained with other spacecraft on the same or similar launch vehicles. However, the amount and quality of applicable flight data have generally been very limited.

The Lunar Orbiter project provided a unique opportunity to obtain data of the type needed on five flights with essentially identical spacecraft and launch vehicles (Atlas-Agenas). During each flight of Lunar Orbiter, the vibration measurements during launch and ascent were obtained with accelerometers which allowed the determination of peak vibration data for critical conditions of lift-off, transonic speeds, booster engine cutoff, booster engine staging, sustainer engine cutoff, vernier engine cutoff and jettison of horizon sensor fairing, shroud jettison, Atlas-Agena separation, Agena first and second ignitions and burnouts, and spacecraft separation. These measurements when compared with the results of ground environmental testing would indicate the appropriateness of the preflight environmental flight acceptance test.

The purpose of this paper is to present flight vibration measurements obtained during the launchings of five Lunar Orbiters and to compare these data with requirements from flight acceptance vibration tests. In addition, these data are compared with the results of a recently completed regression analysis technique intended to predict the random vibration levels for any spacecraft. The philosophy of FAT requirements and the determination of the various test levels are also discussed.

DESIGNATIONS

$A_{r,t}$ accelerometer located at the Agena forward ring in the transverse direction

$A_{r,l}$ accelerometer located at the Agena forward ring in the longitudinal (thrust) direction

$A_{r,\theta}$ accelerometer located at the Agena forward ring in the tangential direction

$A_{r,\phi}$ accelerometer located at the Agena forward ring in the tangential direction 180^{o} from $A_{r,\theta}$

$A_{s,t}$ accelerometer located at the base of the oxidizer tank in the spacecraft in the transverse direction

$A_{s,l}$ accelerometer located at the base of the photographic subsystem in the spacecraft in the longitudinal direction

$A_{a,t}$	accelerometer located at the spacecraft adapter in the transverse direction
$A_{a,l}$	accelerometer located at the spacecraft adapter in the longitudinal direction
BECO	booster engine cutoff
BES	booster engine staging
FAT	flight acceptance tests
f	frequency, Hz
g	acceleration due to gravity, earth gravity units
g_p	peak acceleration, earth gravity units
g_{p-p}	double-amplitude acceleration (peak to peak), earth gravity units
lox	liquid oxygen
Q	amplification factor
RP-1	rocket propellant
SECO	sustainer engine cutoff
VECO	vernier engine cutoff

TEST AND DATA ANALYSIS

Mission

The Lunar Orbiter program was managed by the NASA Langley Research Center under the direction of the Office of Space Science and Applications. The spacecraft was designed and fabricated by The Boeing Company as prime contractor. Eastman Kodak Company (camera system) and Radio Corporation of America (power and communication systems) were the principal subcontractors. The NASA Lewis Research Center was responsible for the launch vehicle, and the Kennedy Space Center supervised the launch operation. Prime vehicle contractors were Convair Division of General Dynamics Corp. for the Atlas, and Lockheed Missiles and Space Company for the Agena.

Spacecraft Description

The Lunar Orbiter spacecraft had a nominal weight of 3759 newtons and was designed to be mounted within an aerodynamic nose shroud on top of the Atlas-Agena launch vehicle. During launch, the solar panels were folded under the spacecraft base and the antennas were held against the side of the structure. In this configuration, the spacecraft was approximately 1.52 meters in diameter and 1.68 meters long. With the solar panels and antennas deployed after injection into the translunar trajectory, the maximum span was increased to approximately 5.64 meters along the antenna booms and 3.66 meters across the solar panels. (See fig. 1.)

Philosophy and Requirements of Flight Acceptance Tests

The philosophy for the flight acceptance test (FAT) requirements of flight items prior to Lunar Orbiter flight was to conduct spacecraft tests at levels up to but not exceeding any that would be experienced in flight. This is in contrast to the philosophy of making the requirements for flight acceptance tests very low in order to assess workmanship in construction. If the spacecraft can successfully withstand the expected flight environment before flight, one can be assured that it will withstand the actual flight environment. It should be understood that a prototype spacecraft would have had prior qualification tests at levels which were higher than FAT requirements to show that the design was adequate. Qualification test philosophy is not discussed herein.

Sinusoidal vibrations.- Sinusoidal vibration tests were designed to subject the spacecraft to vibration levels that would occur because of the in-flight quasi-sinusoidal excitation caused by the various transient excitations. The levels were based on shock spectrum analyses of previous flight transients. The sinusoidal test levels pertaining to the flight acceptance tests were basically derived after a detailed review of vibration measurements of about 25 previous Atlas- and Thor-Agena flights. (See ref. 1.) The flight data which had the greatest vibration levels from only six flights were used as the bases for determining shock spectrum response levels for various values of Q. The amplification factor Q of the response of the mass of a single-degree-of-freedom system is equal to the reciprocal of 2 times the ratio of the damping C of the system to the critical damping C_{cr} of the system $\frac{1}{2C/C_{cr}}$. The shock spectrum response levels were obtained by using the flight transients measured in the spacecraft adapter as inputs to single-degree-of-freedom systems, the natural frequencies of which varied discretely from 10 to 1000 Hz. The amplitudes of peak response for each system were connected to form the shock spectrum results for each assumed value of Q. To obtain the equivalent sinusoidal test levels for the system with assumed values of Q, the response values from the shock spectrum results were divided by the Q used. The resulting equivalent sinusoidal spectrum levels were statistically evaluated to determine the 95-percent levels, and since these values were determined from only six flights, they were enveloped. In

order that essentially all systems be subjected to flight vibration levels, the enveloped $Q = 5$ lines were used as the basis of the flight acceptance test levels. Because of the limited data and since only a single-degree-of-freedom system was considered, an uncertainty multiplying factor of 1.25 was applied to obtain the FAT requirements. These resulting FAT levels for both the longitudinal and transverse directions are shown in figure 2(a).

Random vibrations.- The flight acceptance test requirement for random excitation was determined from an enveloping of the power spectral density plots obtained from applicable flight data of all previous Agena flights for both lift-off and transonic speeds. Only one FAT test for both lift-off and transonic speeds was required at these enveloped test levels. Because of the enveloping, the overall rms acceleration level is high. A high overall rms test level is not too objectionable for test purposes in that the spacecraft acts as a filter and responds primarily at its own resonances. The FAT random test levels are shown in figure 2(b).

Flight Vibration Measurements

Instrumentation.- All flight vibration data were transmitted continuously during lift-off and ascent by utilizing the telemetry of the Agena vehicle. Eight accelerometers were used (fig. 3 and table 1): four were mounted near the Agena forward ring (approximately station 247) to measure the longitudinal ($A_{r,l}$), tangential ($A_{r,\theta}$ and $A_{r,\phi}$), and transverse ($A_{r,t}$) responses of the Agena forward ring; two were installed in the spacecraft adapter (approximately station 238) to measure longitudinal ($A_{a,l}$) and transverse ($A_{a,t}$) excitation to be considered as inputs to the spacecraft; and two were installed within the spacecraft to measure spacecraft response, one to measure longitudinal ($A_{s,l}$) acceleration at the foot of the photographic subsystem (approximately station 235) and one to measure transverse ($A_{s,t}$) accelerations at the base of the oxidizer tank (approximately station 205). The two accelerometers in the spacecraft for measuring spacecraft response were used during both FAT and flight tests. Table 1 presents the flight instrumentation list, in which the acceleration identification, telemeter channel, direction of response, location, accelerometer frequency response and calibration range, and telemeter frequency response are given. In order to extend the frequency range for the Lunar Orbiter vibration data, the standard telemetry playback filters were replaced with filters that had 3 times the frequency bandwidth characteristics of the standard filters. The wider bandwidth allowed more noise but was considered to be acceptable.

Flight data.- Nominal flight time histories for the eight accelerometers are given in figure 4 for the first 400 seconds of flight (through Agena first ignition). Although the time scale is too compressed for accurate analyses of the data, the response characteristics are as expected with bursts of acceleration occurring on the record. Some of the significant events are indicated in the figure, and actual flight times for Lunar Orbiter V

are given in table 2. The longitudinal and transverse accelerometers in the spacecraft adapter ($A_{a,l}$ and $A_{a,t}$) were responsive to the higher frequencies and indicated the largest vibrations. Acceleration magnitudes and frequencies were obtained from high-speed oscillograph recordings.

Data Analyses

The method of data analysis depended on the desired form of the results. The real-time analog data of instantaneous vibration level as a function of time were obtained on oscillograph records. Amplitudes and frequencies were determined to over 1000 Hz. For some channels, data were analyzed above the frequency where the instrumentation was linear. However, in these instances correction factors were applied. To obtain power spectral density values and shock spectra, the data were digitized at the rate of 8000 and 7000 samples per second, respectively, and stored on magnetic tape. The tapes were used as inputs to a digital computer program to obtain autocorrelation, probability density, and power spectra functions and to a separate program to obtain shock spectra.

Regression Analysis Technique for Predicting Vibration Levels

Previous studies which utilized regression analyses have been made for aircraft and airborne missiles. Mahaffey and Smith (ref. 2) presented one of the earliest documented procedures, followed by Brust and Himelblau (ref. 3). Piersol and van der Laan developed a general prediction rule for all classes of military aircraft (ref. 4). Piersol and van der Laan recently developed a new procedure for predicting the random environment for generalized spacecraft (ref. 5). The procedure of reference 5 utilized a regression analysis of flight vibration data which were compiled by Langley Research Center for the following launch vehicles: Agena (excluding Lunar Oribiter), Atlas (E and F series), Minuteman, Saturn I, Thor, Thor-Asset, Thor-Delta, and Titans I, II, IIA, and IIIC. The flight data were generally in the form of power spectra for lift-off, a Mach number of 1, and maximum dynamic pressure. The basic approach of this regression analysis assumed that the power spectrum for the vibration environment in a spacecraft was described by the linear equation of the form

$$G(f) = b_1(f)\,x_1 + b_2(f)\,x_2 + \ldots b_N(f)\,x_N = \sum_{i=1}^{N} b_i(f)\,x_i$$

where $G(f)$ is the average power spectral density, $b_i(f)$ is the coefficient of the ith parameter, and x_i is the ith parameter being used to describe the vibration.

Regression analyses were made to predict the vibration environment in both the longitudinal (thrust) and transverse axes. The primary parameters which the analysis determined as significant were air density, nozzle exit area, exhaust gas velocity, ambient and local speeds of sound, surface weight density, and dynamic pressure. By substituting

appropriate values in expressions in reference 5, prediction curves with a 97.5-percent upper prediction limit were established for lift-off, transonic flight, and maximum dynamic pressure conditions for the Lunar Orbiter spacecraft. The upper prediction limit is the same as a confidence limit. Therefore, whenever a vibration occurs, the vibration level will be below the predicted value 97.5 percent of the time.

RESULTS AND DISCUSSION OF FLIGHT MEASUREMENTS

The results and discussion are presented in four sections and in an appendix. The first three sections present flight data. The first section concerns real-time measurements of acceleration levels and frequencies at various times during the launch phase and includes a discussion of measured torsional oscillations. The second section deals with random vibrations; specifically, acceleration power spectral densities determined from the spacecraft measured inputs and responses during the lift-off and transonic speed regimes. The third section presents transient phenomenon; specifically, representative acceleration shock spectra results for many of the flight transients. The fourth section contains comparisons of flight measurements with flight acceptance test levels and with the results of predictions based on a regression analysis. Some of these comparisons and results were presented in reference 6. Other flight vibration measurements are given in reference 7. The appendix consists of a discussion of some unusually high vibrations that occurred during the simulated launchings of the first three Lunar Orbiter spacecraft. (Simulated launch, a complete countdown with the exception of lift-off, is conducted one week prior to the actual launching to check out all systems.) The following list indicates those items to be found in this part of the paper:

SECTION	SUBJECT	TABLE	FIGURE
1	Measurements:		
	Real time	2-3	4-5
2	Random vibration:	3	6-15
	Power spectra		6-13
	Probability		14
	Autocorrelation		15
3	Transient vibration:		16-35
	Shroud jettison		16-19
	Agena first ignition		20-23
	Agena first burnout		24-27
	Agena second ignition		28-31
	Agena second burnout		32-35
4	Comparison of results:		36-45
	Sinusoidal vibration:		36-38
	Base of spacecraft (inputs)		36
	Within spacecraft (responses)		37-38
	Random vibration:		39-45
	Base of spacecraft (inputs)		39-43
	Within spacecraft (responses)		44-45
Appendix	Vibrations during simulated launch	4	

Table 5 is an index to the conditions discussed, the comparisons made, and the corresponding figures.

Section 1: Real-Time Measurements

Peak acceleration levels at each event.- Peak acceleration levels and predominant frequencies for each event are included in table 3. From this table it may be noted that peak vibration levels and response frequencies are similar for many of these events from flight to flight for the five flights of Lunar Orbiter.

In some instances, flight data were not available. For example, during the flight of Lunar Orbiter I no signal was received from accelerometer $A_{S,t}$. Another example is that at the time of spacecraft separation, accelerometers $A_{r,l}$, $A_{S,t}$, and $A_{S,l}$ were switched to dash-pot-type position indicators to record the spacecraft separation. Thus, no vibration data were recorded for this event on accelerometers $A_{r,l}$, $A_{S,t}$, and $A_{S,l}$. In addition, since the telemeter was in the Agena, after separation no further vibration data were available from the spacecraft or spacecraft adapter.

Torsional oscillations.- Special attention was given to measuring the torsional vibrations that occurred during booster engine cutoff (BECO) of the Atlas-Agena launch vehicle. On all previous Ranger flights (Atlas-Agena launch vehicle) sustained torsional oscillations as high as $10g_{p-p}$ for as many as 15 cycles had occurred at BECO. These linear vibration measurements of torsional oscillation were made near the circumference (0.76-meter radius) of the Agena with a pair of accelerometers located 180° apart. The corresponding rotational acceleration was ± 64.4 rad/sec^2. Therefore, all Lunar Orbiter flights were instrumented (accelerometers $A_{r,\theta}$ and $A_{r,\phi}$) to measure this oscillation. A typical flight response is shown in figure 5. The flight results for the five Lunar Orbiter flights are given in table 3. A torsional acceleration level of $2.3g_{p-p}$ measured on Lunar Orbiter I was the highest vibration level measured on the five Lunar Orbiter flights. This vibration level was much less than the level of $15g_{p-p}$ that was applied to the spacecraft during qualification testing. No torsional FAT was required.

Section 2: Random Vibrations

Normally, high vibration levels for more than a few seconds occur at lift-off and then again during the time 55 to 70 seconds after lift-off. (See fig. 4). These levels are attributed to random excitation. At lift-off the vibration is attributed to engine noise and acoustic coupling, and during the 55 to 70 seconds after lift-off (transonic speeds and maximum dynamic pressure) the vibration is attributed to aerodynamic buffeting.

Power spectral density analyses were made with data recorded from accelerometers $A_{S,t}$ and $A_{S,l}$ (in the spacecraft) and $A_{a,l}$ and $A_{a,t}$ (at the base of the spacecraft) for both lift-off and transonic speed conditions. In addition, probability density coefficients and autocorrelation functions were determined. The power spectral density plots are given in figures 6 to 13. Random vibration data were not available for all channels

for the same reasons that some transient data are not included. However, for the presented data, good repetition occurs in frequency content, trends, and magnitudes. Thus, the data are shown collectively rather than as separate curves. In general, all spectral density levels were considerably lower than expected. (See fig. 2(b).) The responses within the spacecraft (accelerometers $A_{s,t}$ and $A_{s,l}$) had much less magnitude than those measured at the base of the spacecraft (accelerometers $A_{a,l}$ and $A_{a,t}$), with the possible exception of the response in the longitudinal direction (accelerometers $A_{s,l}$ and $A_{a,l}$) at 400 Hz at lift-off (figs. 7 and 9).

To study the nature of the random vibrations, probability density analyses (histograms) were made for each channel for both lift-off and transonic speed conditions. (See, for example, fig. 14.) After digitizing the data, the number of times an amplitude occurred in a specified narrow band of amplitudes was determined. These data were standardized to an area of 1 and compared with the normal (Gaussian) probability density function (ref. 7). One example of these many plots is shown in figure 14. The general trend of the solid curve is closely followed by the flight data, and therefore for practical purposes, the flight data may be considered to have a normal probability distribution.

An example of further determination of the characteristics of the random vibrations is given in figure 15 where the autocorrelation function is shown. The figure represents a narrow-band random vibration whose center frequency is 940 Hz. (See ref. 8.) Examples of the autocorrelation functions for data obtained with accelerometers $A_{a,t}$ and $A_{a,l}$ were all of this nature although the center frequency was not always as clearly indicated. Data obtained with accelerometer $A_{s,l}$ had the same type of autocorrelation function with a center frequency of approximately 400 Hz. Accelerometer $A_{s,t}$, in general, had very little response; thus the plots of probability density and autocorrelation functions indicated that the random vibration was neither narrow-band nor had a Gaussian distribution.

Section 3: Transient Vibrations

The transients which occurred at lift-off and transonic speeds were of sufficient duration to be analyzed as random vibrations, as reported in the previous section. The vibration magnitudes at booster engine cutoff, booster engine staging, sustainer engine cutoff and spacecraft separation were considerably smaller than those that occurred during Agena ignitions and burnouts as well as shroud jettisons; thus, no further analyses were made on transients related to the Atlas booster. Although high accelerations were measured at the time of vernier engine cutoff (VECO), these accelerations were due to the small pyrotechnic charges used to jettison the horizon sensor fairings at the same time as VECO. Thus, no further analyses were conducted on the VECO data.

Shock spectrum analyses were made for transient responses measured with accelerometers $A_{s,l}$, $A_{s,t}$ (spacecraft responses), $A_{a,t}$, and $A_{a,l}$ (spacecraft inputs) that occurred during the times of shroud jettison and Agena first and second ignitions and burnouts for Lunar Orbiter flights I and II. The results of these two sets of data were in good agreement. No shock spectra analyses were made for Lunar Orbiters III, IV, or V, and only the data for Lunar Orbiter I will be shown.

Figures 16 to 19 show the shock spectrum results at shroud jettison for accelerometers $A_{s,t}$, $A_{s,l}$, $A_{a,t}$, and $A_{a,l}$, respectively. The results obtained for Agena first ignition are shown in figures 20 to 23; for Agena first burnout, figures 24 to 27; for Agena second ignition, figures 28 to 31; and for Agena second burnout, figures 32 to 35. Prior to Lunar Orbiter flights, shock spectrum results had been obtained by Lockheed Missiles and Space Company for values of Q equal to 5, 10, and 33. The Lunar Orbiter data were reduced in a similar manner. The shock spectrum values for $Q = 10$ and 33 are included in these figures for reference only, since acceleration values from the $Q = 5$ data were previously used as the basis of the sinusoidal FAT. (In some instances as indicated in figures 27, 32, 33, 34, and 35, some shock spectrum response levels were not calculated.) The figures show that the peak acceleration responses occurred at approximately the expected frequencies; namely, those that were resonances of the system. Some of these results are used in the comparisons to follow.

Section 4: Comparison of Results

Two comparisons of the flight data are made: (1) with the flight acceptance test levels and (2) with the results of a regression analysis for predicting flight vibration levels.

Sinusoidal vibrations.- To obtain equivalent sinusoidal levels, the more severe shock spectrum outputs (for $Q = 5$) from accelerometers $A_{a,l}$ and $A_{a,t}$ which indicated the spacecraft inputs were divided by 5, the same Q used in determining the FAT levels. These flight values are compared with FAT in figure 36. At frequencies above 90 Hz in the longitudinal direction and above 50 Hz in the transverse direction equivalent sinusoidal flight levels exceed the FAT requirements. These data indicate that the FAT levels for sinusoidal vibration are not conservative. A look at the response data within the spacecraft leads to a similar conclusion.

Figures 37 and 38 present the measured responses during flight and during FAT at two positions within the spacecraft (Lunar Orbiter V). Superimposed on the FAT measurements are peak responses measured from the various flight transients as determined by narrow-band analyses (conducted by The Boeing Company). The narrow-band analyses consisted of passing the transient signal through band-pass filters whose band widths were 2 to 15 Hz, 12 to 30 Hz, 20 to 50 Hz, and 40 to 80 Hz. By measuring

the amplitude of the resulting sinusoids, acceleration levels were determined and are shown in the figures. From figure 37 it appears that the required sinusoidal FAT levels in the transverse direction resulted in spacecraft responses similar to those measured in flight. For tests in the longitudinal direction (fig. 38), it appears that the sinusoidal FAT levels resulted in spacecraft responses that were not as high as those measured in flight. When it is remembered that for the flight data only the sinusoidal component of the peak response during the transient is shown and that the actual FAT consisted of slow-sweep sinusoidal tests where many hundreds of cycles occur near the peak amplitude, the undertest was not serious.

Random vibration.- The random flight-measured vibrations can also be compared with FAT levels for the conditions both as inputs to the spacecraft and as output vibrations within the spacecraft, and with the results of a new prediction technique based on a regression-type analysis. Measurements obtained at lift-off and during transonic speeds are considered to be of sufficient duration to analyze as random vibration.

The flight results are compared with FAT specifications and the results of regression analyses in figures 39 to 43 for both lift-off and transonic speeds in the longitudinal and transverse directions. The FAT levels were determined from an enveloping of the flight data of previous Agena flights for both lift-off and transonic speeds. Therefore, the overall test levels (rms) were expected to be high. Only one test was required.

During the flights of Lunar Orbiter, the random inputs as measured in the longitudinal and transverse directions were more than an order of magnitude less than the values predicted with both the regression analysis and the flight acceptance levels (FAT) throughout the vibration spectrum. The rms accelerations were expected to be lower in flight than the FAT levels, and the maximum levels of the power spectral density in flight were not expected to exceed the FAT spectral density levels. The spectral density levels from flight measurements, however, were considerably lower than the FAT levels. These low levels may have been due to the ogive metallic nose fairing (same fairing as used on Mariner IV, which also had low random excitation). The random vibration test level had been based on measurement from launch vehicles that had nose fairings composed of phenolic and plastics and had somewhat different shapes. A nose fairing identical to the fairing of Mariners I, II, and III was planned to be used on Lunar Orbiter until the fairing failure on Mariner III. The replacement nose fairing for Mariner IV was used for the Lunar Orbiters. This fairing was all metallic. The overall rms vibration on Mariner IV was approximately 2g as compared with more than 5g on Mariners I and II. The rms vibration levels from the launches of other Atlas-Agenas with non-ogive fairings were greater than 8g. Since the flight input vibration levels to the spacecraft were much lower than expected, the responses within the spacecraft would be expected to be proportionally less.

Regression analysis.- The spectrum shape of the results from the regression analysis indicates maximum energy levels in the 300- to 600-Hz octave band, whereas the flight data peak at higher frequencies. (See composite, fig. 43.) In addition, octave band values of the results from the regression analysis are compared with 20-Hz bandwidth values of flight data. Thus, this new method has predicted the measured environment of the Lunar Orbiter spacecraft very conservatively. Thus, the regression analysis requires further development. However, since many more pertinent variables are considered in the regression analysis than in other prediction methods, it appears that the method could be used as a first step for any new or untried launch vehicle. As evidenced by the comparison of the shape of the spectra (fig. 43) between FAT requirements and flight data, the use of previous flight data from the same launch vehicle still appears to be the better way of estimating FAT requirements. Enveloping of the data results in a certain amount of conservatism which is considered necessary in view of the many unknown responses in flight and because of the difference in responses from spacecraft to spacecraft.

Comparison of spacecraft responses with ground measurements.- Comparisons of the responses within the spacecraft due to the application of the FAT random vibration requirements with the measurements obtained during the flight of Lunar Orbiter V are shown in figures 44 and 45 for excitation in the transverse and longitudinal directions, respectively. The upper curves show the spacecraft responses (power spectral density) due to the application of the FAT random inputs, and the lower curves are the results of spectral density analyses of the flight data. These data were reduced by The Boeing Company to 2000 Hz with appropriate corrections beyond the linear range of the telemeter. Data reduction at the Langley Research Center resulted in similar results in the range of analyses to 400 Hz. (For example, compare figs. 6 and 10 with fig. 44, and figs. 7 and 11 with fig. 45.) These data indicate that the trends of the responses within the spacecraft in flight are the same as those that occur during FAT. Since the flight vibration inputs were more than an order of magnitude less than FAT vibration levels, the responses within the spacecraft were accordingly less by an order of magnitude.

CONCLUSIONS

Detailed vibration measurements from five flights of Lunar Orbiter, including peak acceleration levels and predominant frequencies that occurred during various transients and results of power spectral density analyses during lift-off and transient speed conditions, have been presented. Results from shock spectrum analyses have been given for the various transients during launch and ascent. The torsional oscillations during booster engine cutoff have been shown to be smaller than those measured on previous spacecraft. Some unusual on-pad vibrations prior to ignition of the launch vehicle have

been discussed in an appendix. Flight acceptance test (FAT) requirements and philosophy for Lunar Orbiter spacecraft have been discussed and compared with flight data. From the results and discussions given herein, the following conclusions are made:

1. At frequencies above 90 Hz in the longitudinal direction and above 50 Hz in the transverse direction, equivalent sinusoidal flight levels exceeded the FAT requirements.

2. Measured flight vibration data on these flights were lower than those measured on previous flights and thus the flight acceptance random vibration test levels substantially exceeded the flight measured values.

3. The random vibration flight data were compared with the results of a new prediction method based on a regression analysis. The new method yields random vibration levels that are overly conservative and thus the procedure needs refinement.

4. Responses within the spacecraft during flight were compared with responses measured within the spacecraft during FAT. The trends of the responses with frequency within the spacecraft in flight were the same as those occurring during FAT. Since the flight input levels were less than expected, correspondingly, the responses were also less during flight than those measured during FAT.

5. The flight-measured random vibration data appeared very consistent for all five flights, and the shock spectrum results were consistent for the two flights investigated.

Langley Research Center,
National Aeronautics and Space Administration,
Hampton, Va., June 22, 1970.

APPENDIX

VIBRATIONS DURING SIMULATED LAUNCH

Approximately 1 week prior to flight, a simulated launch was conducted in which the entire countdown progressed up to actual vehicle launch with the exception that the firing switch was not closed and the Agena booster was not fueled. However, the Atlas booster was fueled with both RP-1 and lox. During the filling of the lox tank for the simulated launch of Lunar Orbiter III, large oscillations occurred at the base of the photographic subsystem (accelerometer $A_{s,l}$); the peak vibration was $6.7g_{p-p}$ at 25.8 Hz. (See table 4.) It was determined that the vibration resulted from forces generated by the motions of the lox tank relief valve which automatically controls the tank pressure. Shifting to manual operation during actual prelaunch countdown eliminated the high response of the photographic subsystem. A reexamination of the simulated launch records for Lunar Orbiters I and II indicated a very low vibration level. Prelaunch recordings during fueling for Lunar Orbiters I and II had not been made. Vibration levels during both simulated launch and prelaunch of Lunar Orbiters IV and V (with manual control of the lox relief valve) were observed to be very low.

REFERENCES

1. Houston, A. D.: Study To Define Agena Vibration and Acoustic Environment. LMSC-A824787, Lockheed Missiles and Space Co., Aug. 17, 1966.

2. Mahaffey, P. T.; and Smith, K. W.: Method for Predicting Environmental Vibration Levels in Jet Powered Vehicles. Noise Contr., vol. 6, no. 4, July-Aug. 1960, pp. 20-26.

3. Brust, J. M.; and Himelblau, H.: Comparison of Predicted and Measured Vibration Environments for Skybolt Guidance Equipment. Shock Vib. Bull., No. 33, Pt. III, U.S. Dep. Def., Mar. 1964, pp. 231-280.

4. Piersol, A. G.; and van der Laan, W. F.: Statistical Analyses of Flight Vibration and Acoustic Data. AFFDL-TR-68-92, U.S. Air Force, June 1968. (Available from DDC as AD847706.)

5. Piersol, A. G.; and Van der Laan, W. F.: A Method for Predicting Launch Vehicle Vibration Levels in the Region of the Spacecraft Adaptor. NASA CR-1227, 1969.

6. Clevenson, Sherman A.: Lunar Orbiter Flight Vibrations With Comparisons to Flight Acceptance Requirements and Predictions Based on a New Generalized Regression Analysis. Shock Vib. Bull., Bull. 39, Pt. 6, U.S. Dept. Def., Mar. 1969, pp. 119-132.

7. Anon: Flight Performance of Atlas-Agena Launch Vehicles in Support of the Lunar Orbiter Missions III, IV, and V. NASA TM X-1859, 1969.

8. Bendat, Julius S.; and Piersol, Allan G.: Measurement and Analysis of Random Data. John Wiley & Sons, Inc., c.1966, pp. 16-21, 160-161.

TABLE 1.- FLIGHT INSTRUMENTATION LIST

Accelerometer	Channel	Direction of measured acceleration	Location	Accelerometer frequency response, Hz	Accelerometer calibration range, g	Channel frequency response,[a] Hz
$A_{r,t}$	8	Transverse	Agena forward ring	0 to 320	±5	135
$A_{r,l}$	9	Longitudinal	Agena forward ring	0 to 400	-4 to +12	180
$A_{r,\theta}$	10	Tangential	Agena forward ring	0 to 320	±5	240
$A_{r,\phi}$	11	Tangential	Agena forward ring	0 to 320	±5	330
$A_{s,t}$	12	Transverse	Spacecraft	5 to 2500	±10	540
$A_{s,l}$	13	Longitudinal	Spacecraft	5 to 2500	±10	660
$A_{a,l}$	17	Longitudinal	Spacecraft adapter	10 to 5000	±20	2370
$A_{a,t}$	18	Transverse	Spacecraft adapter	10 to 5000	±20	3150

[a]With filters having 3 times the frequency response of standard filters.

TABLE 2.- SEQUENCE OF SIGNIFICANT FLIGHT EVENTS

FOR LUNAR ORBITER V

Event	Flight time, sec
Lift-off 22:33:00.352 G.m.t.	0
Mach number 1	49.0
Maximum dynamic pressure	62.0
Booster engine cutoff (BECO)	128.6
Booster engine staging (BES)	131.7
Sustainer engine cutoff (SECO)	288.6
Vernier engine cutoff (VECO)	307.9
Uncage gyroscope	307.9
Jettison horizon sensor fairings	307.9
Fire shroud ejection squibs	310.3
Fire Atlas-Agena separation squibs	312.4
Initiate Agena first burn sequence	369.3
Steady-state thrust 90 percent	370.45
Agena first burn cutoff	523.58
Initiate Agena second burn sequence	1879.4
Steady-state thrust 90 percent	1880.11
Agena second burn cutoff	1967.6
Fire ejection squibs (spacecraft)	2133.42
Initiate yaw maneuver	2136.39
Stop yaw maneuver	2196.27
Initiate retrofire	2733.5
Retrorocket burnout	2750.5

TABLE 3.- ACCELERATIONS AND APPROXIMATE FREQUENCIES OF FLIGHT TRANSIENTS

Accelerometer	Lunar Orbiter I		II		III		IV		V	
	g_{p-p}	f, Hz	g_{p-p}	f, Hz	g_{p-p}	f, Hz	g_{p-p}	f, Hz	g_{p-p}	f, Hz
Lift-off										
$A_{r,t}$	2.5	3.0	1.4	5.5	0.5	(a)	(b)	(b)	0.6	5
$A_{r,l}$	.7	(a)	1.6	42.0	.5	(a)	(b)	(b)	1.1	5
$A_{r,\theta}$	1.0	(a)	.9	82.0	.5	(a)	(b)	(b)	1.0	(a)
$A_{r,\phi}$	1.0	(a)	1.2	570.0	1.5	(a)	(b)	(b)	1.0	(a)
$A_{s,t}$	(b)	(b)	3.1	5.5	.5	(a)	(b)	(b)	1.7	(a)
$A_{s,l}$	1.0	520	1.9	400.0	1.5	(a)	(b)	(b)	1.4	5
$A_{a,l}$	14.0	1000	12.8	960.0	26.0	1000	(b)	(b)	17.0	1000
$A_{a,t}$	14.0	1000	10.5	960.0	10.0	1000	(b)	(b)	12.0	900
Transonic speeds										
$A_{r,t}$	2.8	3.0	0.9	29.0	2.5	(a)	1.8	(a)	2.4	(a)
$A_{r,l}$	1.3	(a)	2.0	34.0	1.5	(a)	1.2	(a)	3.0	(a)
$A_{r,\theta}$	1.0	56.0	.8	(a)	.5	(a)	1.4	(a)	1.0	(a)
$A_{r,\phi}$	1.3	91.0	.6	(a)	.8	(a)	1.0	(a)	1.3	(a)
$A_{s,t}$	(b)	(b)	.6	(a)	(a)	(a)	.1	(a)	.7	(a)
$A_{s,l}$	.8	500	1.7	(a)	.6	400	.3	400	.7	(a)
$A_{a,l}$	12.0	1000	8.8	960.0	26.0	1000	14.0	1000	17.0	1000
$A_{a,t}$	12.5	1000	6.5	960.0	11.0	1000	7.0	1000	17.0	1000
Booster engine cutoff										
$A_{r,t}$	1.1	9.9	0.1	62	(a)	(a)	0.3	(a)	0.3	(a)
$A_{r,l}$	3.9	(a)	.9	15	(a)	(a)	1.2	15	.7	(a)
$A_{r,\theta}$	1.9	66.0	.9	63	1.0	64	1.4	61	1.7	65
$A_{r,\phi}$	2.3	66.0	1.2	63	1.6	67	1.7	62	2.0	65
$A_{s,t}$	(b)	(b)	.5	(a)	1.0	(a)	.7	(a)	.7	(a)
$A_{s,l}$	3.0	1.2	.7	34	1.0	(a)	1.4	59	1.4	19
	1.5	16.0	1.9	14	1.0	(a)	1.4	59	1.4	19
	1.0	65.0								
$A_{a,l}$	.1	1000	.2	960	.5	(a)	.5	1000	1.3	(a)
$A_{a,t}$	.1	1000	.4	960	.5	(a)	.5	1000	1.2	(a)
Booster engine staging										
$A_{r,t}$	0.5	(a)	0.5	38	0.5	(a)	0.6	(a)	0.7	38
$A_{r,l}$	.4	(a)	.5	32	.3	(a)	.7	35	.5	38
$A_{r,\theta}$	2.5	390	1.2	69	.5	(a)	.9	71	.7	(a)
$A_{r,\phi}$	3.0	390	1.0	35	.9	(a)	.8	71	1.0	(a)
$A_{s,t}$	(b)	(b)	1.5	35	1.0	(a)	1.4	35	1.7	34
$A_{s,l}$	1.0	(a)	.5	444	.7	400	1.4	35	1.1	(a)
$A_{a,l}$	.6	(a)	3.7	950	4.0	1000	1.7	1000	2.4	1000
$A_{a,t}$	.6	(a)	1.4	950	2.0	1000	1.4	1000	1.7	(a)

[a]Low signal amplitude or less than 2 cycles for frequency analysis.

[b]No data available, either from lack of appropriate flight tape or from electronic difficulties.

TABLE 3.- ACCELERATIONS AND APPROXIMATE FREQUENCIES OF FLIGHT TRANSIENTS – Continued

Accelerometer	Lunar Orbiter I		II		III		IV		V	
	g_{p-p}	f, Hz	g_{p-p}	f, Hz	g_{p-p}	f, Hz	g_{p-p}	f, Hz	g_{p-p}	f, Hz
Sustainer engine cutoff										
$A_{r,t}$	0.3	(a)	(a)	(a)	0.5	(a)	0.2	(a)	0.2	(a)
$A_{r,l}$	2.6	(a)	(a)	(a)	.4	(a)	.6	(a)	.4	(a)
$A_{r,\theta}$	.2	(a)	0.2	(a)	.3	82	.4	80	.2	(a)
$A_{r,\phi}$	.4	80	.2	(a)	.6	82	.4	80	.2	(a)
$A_{s,t}$	(b)	(b)	.5	(a)	.4	(a)	1.0	(a)	1.0	(a)
$A_{s,l}$	1.2	(a)	.8	81	.4	(a)	1.4	(a)	1.4	24
$A_{a,l}$	.7	(a)	(a)	(a)	.6	(a)	.7	(a)	.2	(a)
$A_{a,t}$	.7	(a)	(a)	(a)	.6	(a)	.8	(a)	.2	(a)
VECO and sensor fairing jettison										
$A_{r,t}$	4.7	(c)	4.5	(c)	4.0	(c)	3.1	(c)	3.5	(c)
$A_{r,l}$	5.9	(c)	4.0	(c)	6.4	(c)	5.4	(c)	5.5	(c)
$A_{r,\theta}$	4.0	(c)	1.1	(c)	.6	(a)	1.9	(c)	1.3	110
$A_{r,\phi}$	5.0	(c)	2.7	(c)	2.5	(a)	3.5	(c)	3.3	110
$A_{s,t}$	(b)	(b)	.9	100	.5	(a)	1.0	(a)	.7	(a)
$A_{s,l}$	1.5	460	5.2	400	2.0	(a)	2.8	(a)	2.8	175
$A_{a,l}$	20.0	990	13.0	960	34.0	1000	29.0	1000	28.0	900
$A_{a,t}$	20.0	990	10.5	960	38.0	1000	31.0	1000	33.0	900
Shroud jettison										
$A_{r,t}$	3.8	(c)	3.1	(c)	2.5	(c)	3.6	(c)	3.5	(c)
$A_{r,l}$	5.6	(c)	4.9	(c)	6.4	(c)	5.8	(c)	7.0	(c)
$A_{r,\theta}$	1.9	100	2.1	(c)	2.0	(c)	2.5	(c)	1.3	(c)
$A_{r,\phi}$	1.7	68	1.9	(c)	2.5	(c)	2.8	(c)	2.6	(c)
			3.0	133						
$A_{s,t}$	(b)	(b)	1.0	(a)	.6	(a)	.6	(a)	.7	(a)
$A_{s,l}$	4.0	490	4.8	400	3.0	400	2.8	(a)	3.5	(a)
$A_{a,l}$	24.0	1000	36.7	960	38.0	1000	35.0	900	28.0	1000
$A_{a,t}$	24.0	1000	31.9	960	36.0	1000	32.0	900	14.0	1000
Atlas-Agena separation										
$A_{r,t}$	1.3	(c)	2.4	(c)	3.2	(c)	2.1	(c)	1.3	(c)
$A_{r,l}$	4.1	(c)	3.2	(c)	3.5	(c)	3.4	(c)	4.1	(c)
$A_{r,\theta}$	1.1	(c)	2.7	(c)	1.7	(c)	3.5	(c)	1.5	(c)
$A_{r,\phi}$	1.6	(c)	2.1	(c)	2.0	(c)	1.8	(c)	2.1	(c)
$A_{s,t}$	(b)	(b)	.5	(a)	.6	(a)	.4	(a)	.3	(a)
$A_{s,l}$	1.4	40	2.5	400	2.0	400	1.8	(a)	1.4	40
$A_{a,l}$	32.0	1000	36.7	960	38.0	1000	32.0	1000	32.0	1000
$A_{a,t}$	23.0	1000	23.8	960	36.0	1000	33.0	1000	23.0	1000

[a]Low signal amplitude or less than 2 cycles for frequency analysis.

[b]No data available, either from lack of appropriate flight tape or from electronic difficulties.

[c]Peak amplitude of pulse.

TABLE 3.- ACCELERATIONS AND APPROXIMATE FREQUENCIES OF FLIGHT TRANSIENTS – Continued

Accelerometer	Lunar Orbiter									
	I		II		III		IV		V	
	g_{p-p}	f, Hz	g_{p-p}	f, Hz	g_{p-p}	f, Hz	g_{p-p}	f, Hz	g_{p-p}	f, Hz
Agena first ignition										
$A_{r,t}$	1.0	(a)	0.2	(a)	(a)	(a)	0.4	(a)	0.2	(a)
$A_{r,l}$	1.6	100	1.2	(c)	(a)	(a)	.4	(a)	.9	(a)
$A_{r,\theta}$	1.3	(a)	1.2	(c)	0.6	(a)	.3	(a)	.3	(a)
$A_{r,\phi}$	1.0	(a)	.2	(a)	(a)	(a)	.4	(a)	.4	(a)
$A_{s,t}$	(b)	(b)	1.0	(a)	(a)	(a)	.7	(a)	1.0	(a)
$A_{s,l}$	1.0	440	1.4	400	1.1	390	.7	(a)	1.4	(a)
$A_{a,l}$	10.0	1000	11.0	960	22.8	1000	4.2	700	4.2	(a)
$A_{a,t}$	9.5	1000	6.6	960	8.2	1000	2.2	(a)	1.6	(a)
Agena first burnout										
$A_{r,t}$	0.5	55	0.4	(a)	2.14	43	0.7	(a)	0.7	(a)
$A_{r,l}$	.7	86	.6	75	.8	73	2.0	(c)	1.7	(c)
$A_{r,\theta}$	.8	85	.7	(c)	.5	73	.7	(a)	.7	(a)
$A_{r,\phi}$	.8	430	.7	(a)	2.9	(a)	.7	(a)	.7	(a)
$A_{s,t}$	(b)	(b)	.7	40	1.9	43	2.1	400	2.1	(a)
$A_{s,l}$	2.0	80	3.9	(c)	2.8	(c)	3.5	(c)	3.0	(c)
	2.5	430	1.1	400						
$A_{a,l}$	2.0	1000	3.0	960	5.3	925	2.5	800	2.8	950
$A_{a,t}$	1.5	1000	1.9	960	2.0	875	1.3	800	1.6	(a)
Agena second ignition										
$A_{r,t}$	0.6	80	0.7	50	3.0	(c)	0.7	(a)	0.4	(a)
$A_{r,l}$	.4	100	.4	125	1.2	22	2.5	(c)	2.5	(c)
$A_{r,\theta}$	.5	80	.5	125	.7	22	.5	(a)	.4	(a)
$A_{r,\phi}$	.7	(a)	.8	125	2.8	(c)	.8	(a)	.7	(a)
$A_{s,t}$	(b)	(b)	1.8	35	1.4	42	1.7	400	1.5	(a)
$A_{s,l}$	3.5	(a)	5.1	(c)	2.9	(c)	3.5	(c)	3.5	(c)
			1.1	400						
$A_{a,l}$	2.0	1000	7.0	(c)	2.8	1000	2.0	800	1.6	1000
			1.5	960						
$A_{a,t}$	1.5	1000	1.0	960	2.0	1000	1.5	800	1.3	(a)
Agena second burnout										
$A_{r,t}$	0.9	58	0.7	50	2.8	50	0.8	(a)	0.7	50
$A_{r,l}$	1.5	86	1.2	72	4.0	(c)	4.8	(a)	5.0	(c)
$A_{r,\theta}$	.9	(a)	.7	(a)	.7	(a)	.9	(a)	.7	70
$A_{r,\phi}$	1.0	(a)	.9	(a)	3.4	(c)	.9	(a)	.7	(a)
$A_{s,t}$	(b)	(b)	2.5	50	2.8	(a)	3.0	400	3.0	38
$A_{s,l}$	7.8	(c)	11.0	(c)	7.6	(c)	7.0	(c)	7.5	(c)
	4.3	350	1.8	400						
$A_{a,l}$	3.0	1000	5.0	(c)	5.7	950	4.5	900	6.4	900
			4.0	960						
$A_{a,t}$	3.0	1000	2.8	960	4.6	950	4.5	900	2.5	(a)

[a]Low signal frequency or less than 2 cycles for frequency analysis.

[b]No data available, either from lack of appropriate flight tape or from electronic difficulties.

[c]Peak amplitude of pulse.

TABLE 3.- ACCELERATIONS AND APPROXIMATE FREQUENCIES OF FLIGHT TRANSIENTS – Concluded

Accelerometer	Lunar Orbiter									
	I		II		III		IV		V	
	g_{p-p}	f, Hz	g_{p-p}	f, Hz	g_{p-p}	f, Hz	g_{p-p}	f, Hz	g_{p-p}	f, Hz
	Spacecraft separation									
$A_{r,t}$	2.5	25	2.3 4.0	(c) 0.76	3.71	57	2.1	(c)	3.5	(c)
$A_{r,l}$	(d)	(d)	(d)	(d)	(d)	(d)	(d)	(d)	(d)	(d)
$A_{r,\theta}$	1.0	104	2.2	(c)	1.6	44	1.8	(c)	.6	(c)
$A_{r,\phi}$	.8	82	2.1	(c)	1.7	173	1.8	(c)	1.3	(c)
$A_{s,t}$	(d)	(d)	(d)	(d)	(d)	(d)	(d)	(d)	(d)	(d)
$A_{s,l}$	(d)	(d)	(d)	(d)	(d)	(d)	(d)	(d)	(d)	(d)
$A_{a,l}$	20.0	1000	36.8	960	40	850	46	800	20	800
$A_{a,t}$	20.0	1000	42.5	960	40	850	(b)	(b)	(b)	(b)

[b]No data available, either from lack of appropriate flight tape or from electronic difficulties.

[c]Peak amplitude of pulse.

[d]Prior to separation, these channels were switched to position indicators to show separation.

TABLE 4.- VIBRATION MEASUREMENTS DURING SIMULATED LAUNCH AND PRELAUNCH FOR LUNAR ORBITER III

Accelerometer	Simulated launch, g_{p-p}		Prelaunch, g_{p-p}	
	Frequency			
	25.8 Hz	26.5 Hz	24.8 Hz	27.7 Hz
$A_{r,t}$	0.14	0.27	----	----
$A_{r,l}$	1.9	1.4	0.09	----
$A_{r,\theta}$	.11	.07	.06	----
$A_{r,\phi}$	.09	.09	.32	0.15
$A_{s,t}$	.57	.38	.07	----
$A_{s,l}$	6.7	4.6	.35	.57
$A_{a,l}$	3.7	2.7	----	----
$A_{a,t}$	1.5	1.1	----	----

TABLE 5.- INDEX TO FIGURES[a] [b]

Event	Spacecraft response		Spacecraft input	
	$A_{s,t}$	$A_{s,l}$	$A_{a,t}$	$A_{a,l}$
Lift-off	6,A;44,E	7,A;45,E	8,A;41,D;43,D	9,A;39,D;43,D
Transonic speeds	10,A;44,E	11,A;45,E	12,A;14,B 15,C;42,D;43,D	13,A;40,D;43,D
BECO	37,H	38,H		
SECO	37,H	38,H		
VECO and fairing ejections	--------	--------	----------	----------
Shroud jettison	16,F	17,F	18,F;36,G	19,F;36,G
Atlas-Agena separation			36,G	36,G
Agena first ignition	20,F;37,H	21,F;38,H	22,F	23,F
Agena first burnout	24,F;37,H	25,F;38,H	26,F;36,G	27,F;36,G
Agena second ignition	28,F;37,H	29,F;38,H	30,F	31,F
Agena second burnout	32,F;37,H	33,F;38,H	34,F;36,G	35,F;36,G

[a]Only representative shock spectrum data for transients creating the higher vibration levels have been shown.

[b]Numbers refer to figures. Letters refer to the type of flight data or kind of comparison as follows:

- A — Power spectral data.
- B — Probability data.
- C — Autocorrelation data.
- D — Comparison of power spectral data (A) with FAT and results of regression analysis.
- E — Comparison of spacecraft response with FAT response.
- F — Shock spectrum data.
- G — Comparison of equivalent sine inputs with FAT.
- H — Comparison of narrow-band spacecraft response with response measured during FAT.

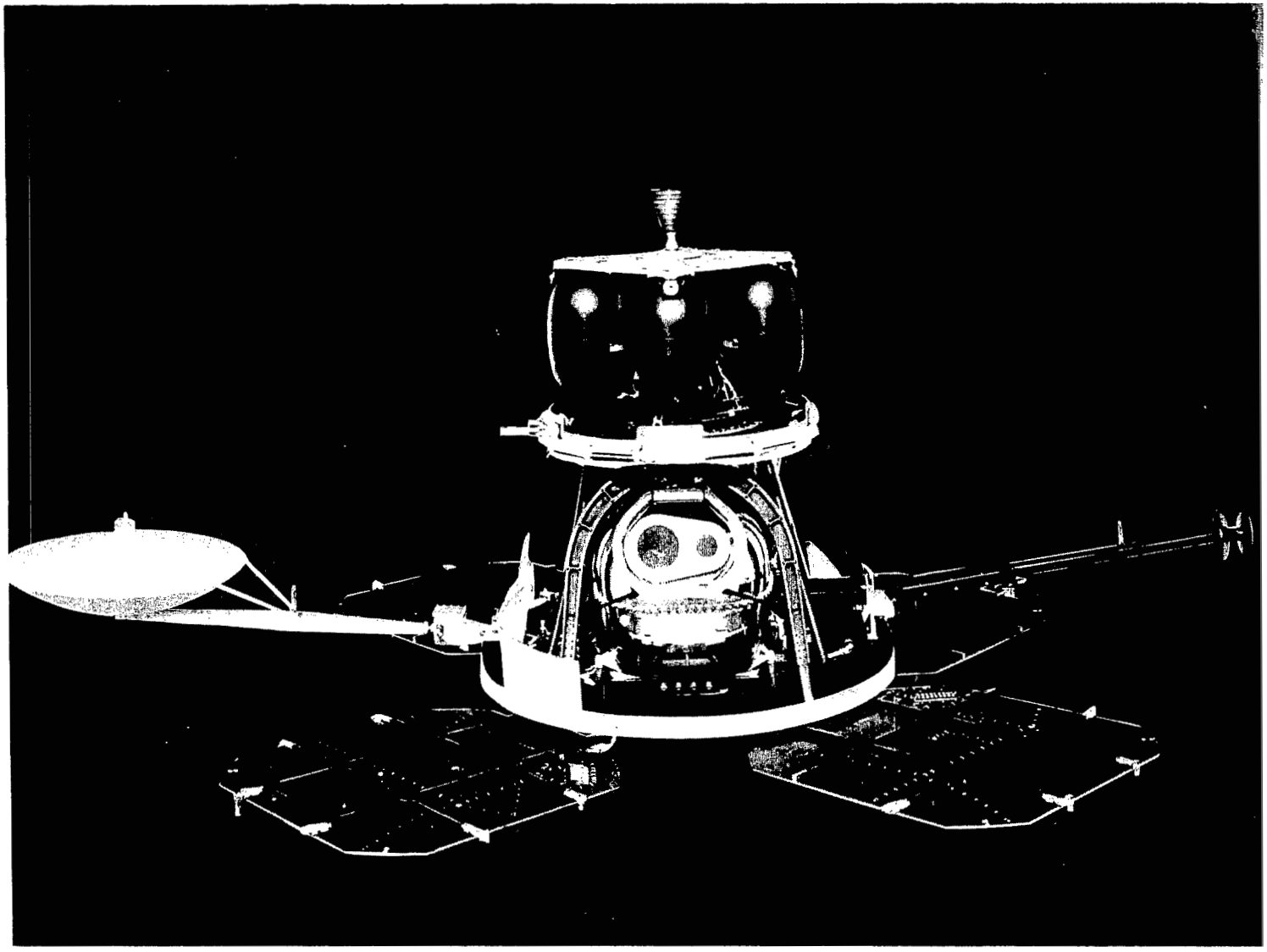

Figure 1.- Lunar Orbiter spacecraft without its thermal blanket.

L-68-3840

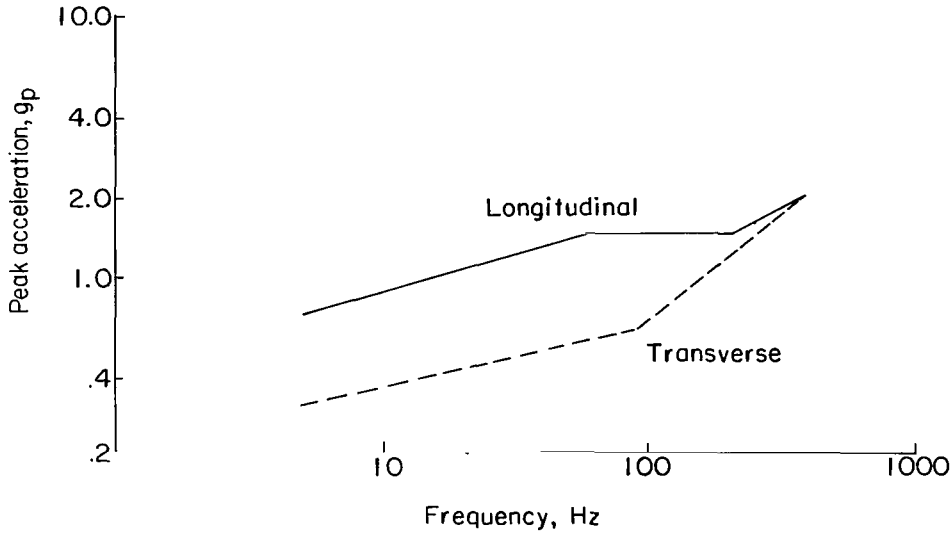

(a) Sinusoidal.

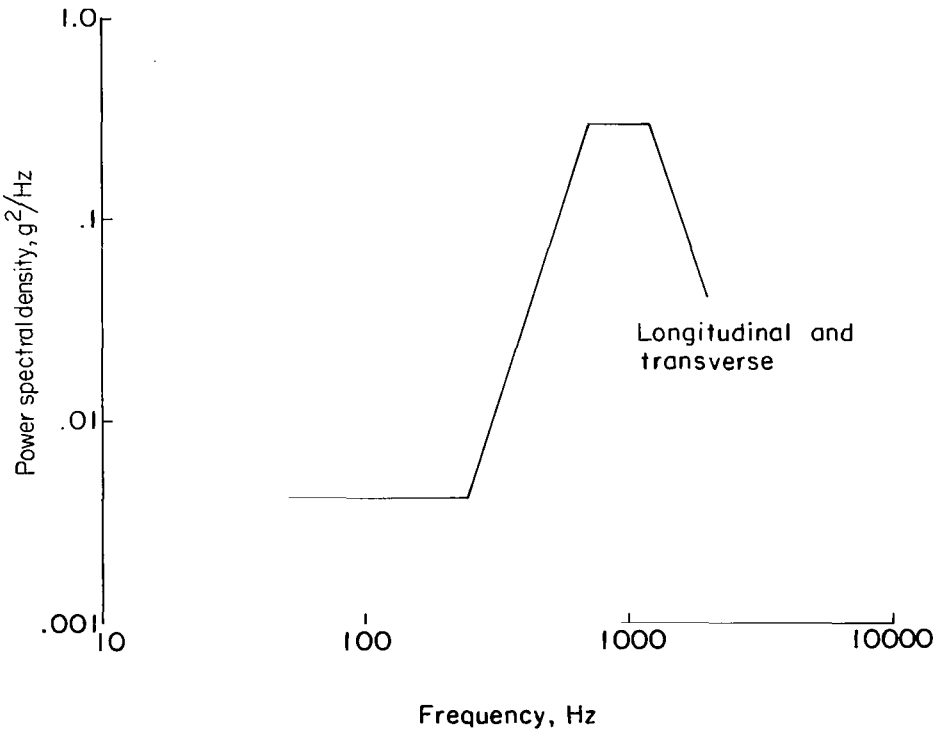

(b) Random.

Figure 2.- Flight acceptance test levels.

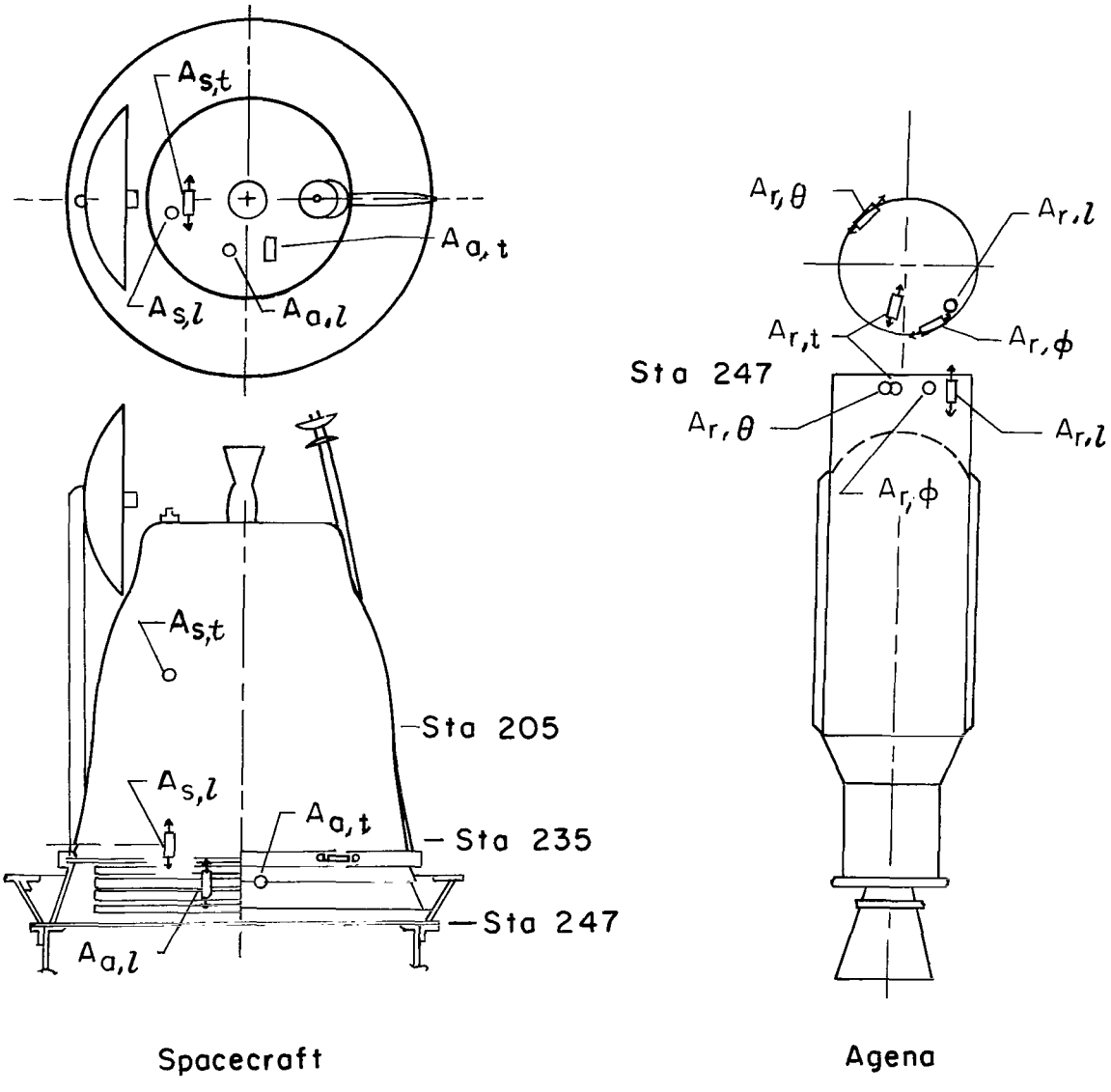

Figure 3.- Accelerometer locations. Spacecraft in undeployed condition.

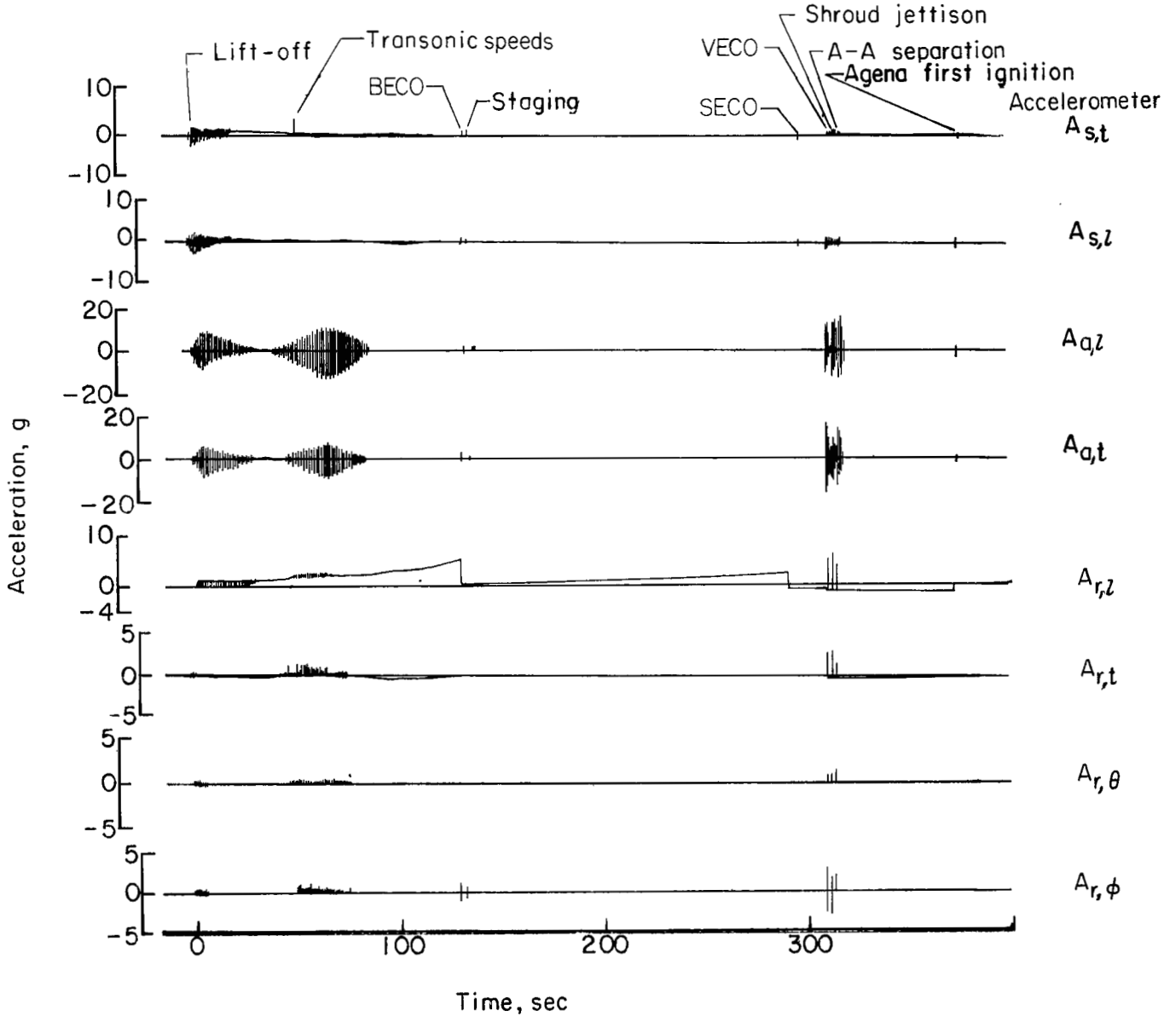

Figure 4.- Nominal flight time history.

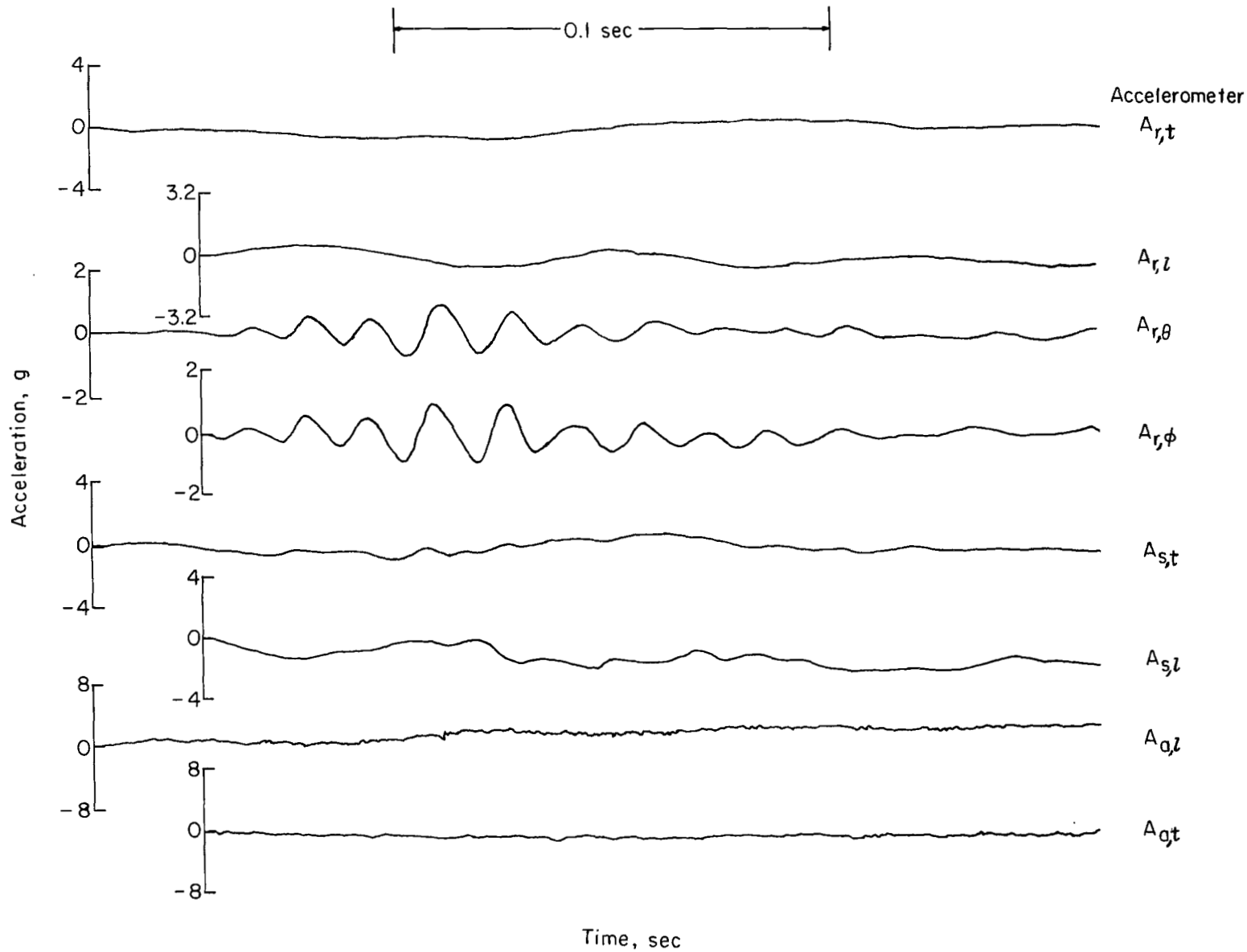

Figure 5.- Response at booster engine cutoff. Lunar Orbiter V.

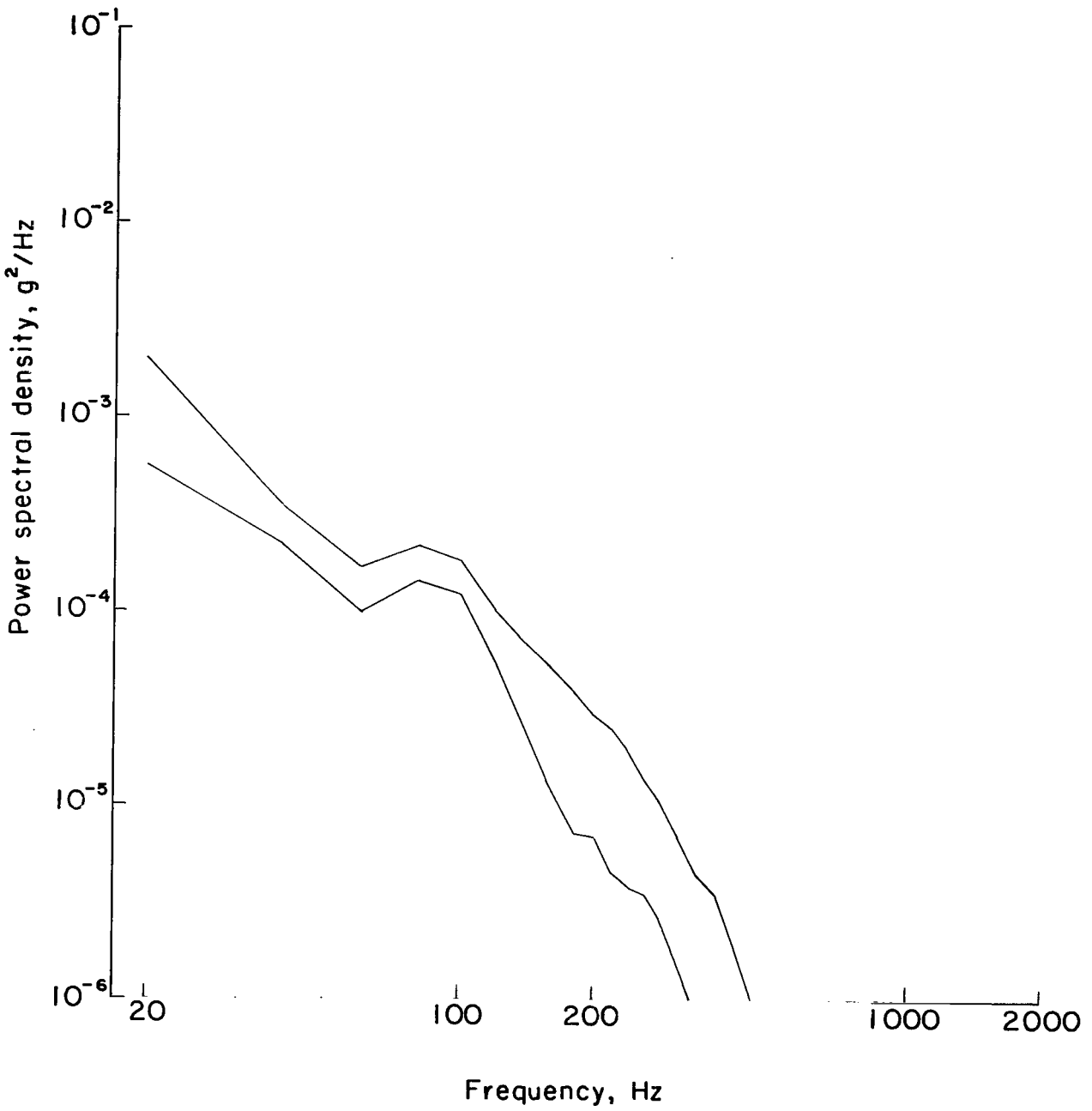

Figure 6.- Range of power spectral densities for Lunar Orbiters II, III, and V at lift-off. Accelerometer $A_{s,t}$; transverse response to spacecraft.

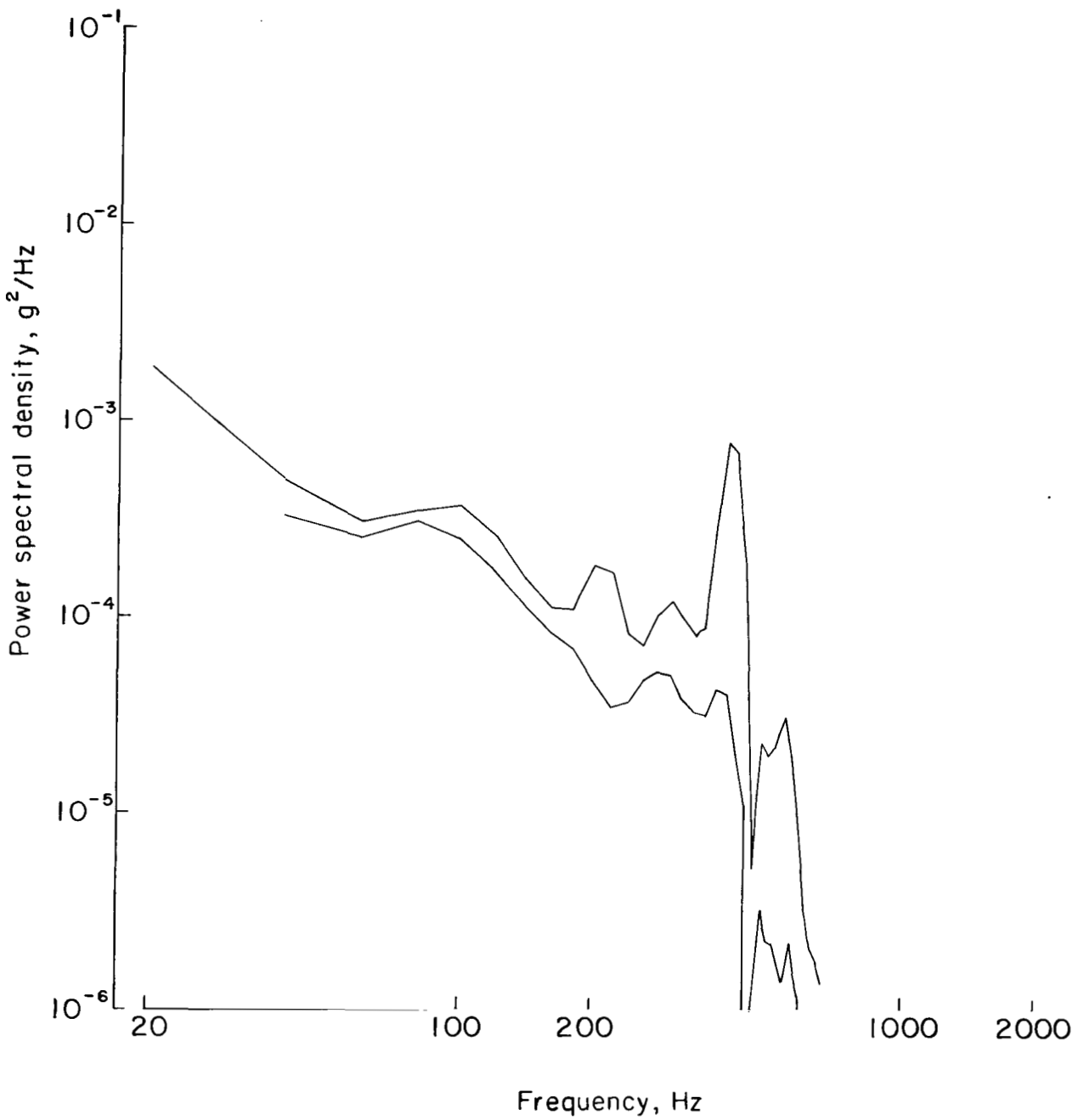

Figure 7.- Range of power spectral densities for Lunar Orbiters I, II, III, and V at lift-off. Accelerometer $A_{s,l}$; longitudinal response in spacecraft.

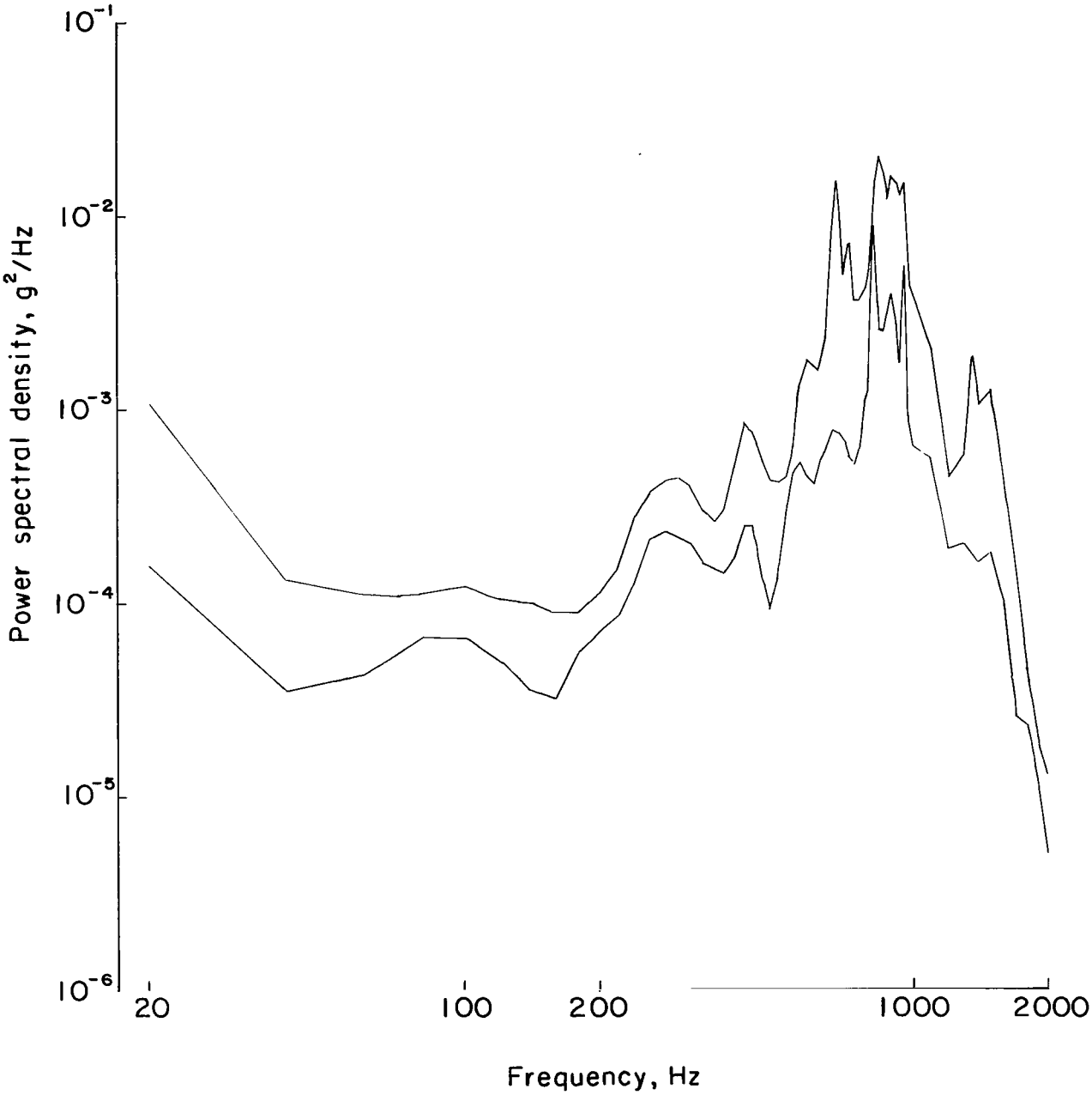

Figure 8.- Range of power spectral densities for Lunar Orbiters I, II, III, and V at lift-off. Accelerometer $A_{a,t}$; transverse input to spacecraft.

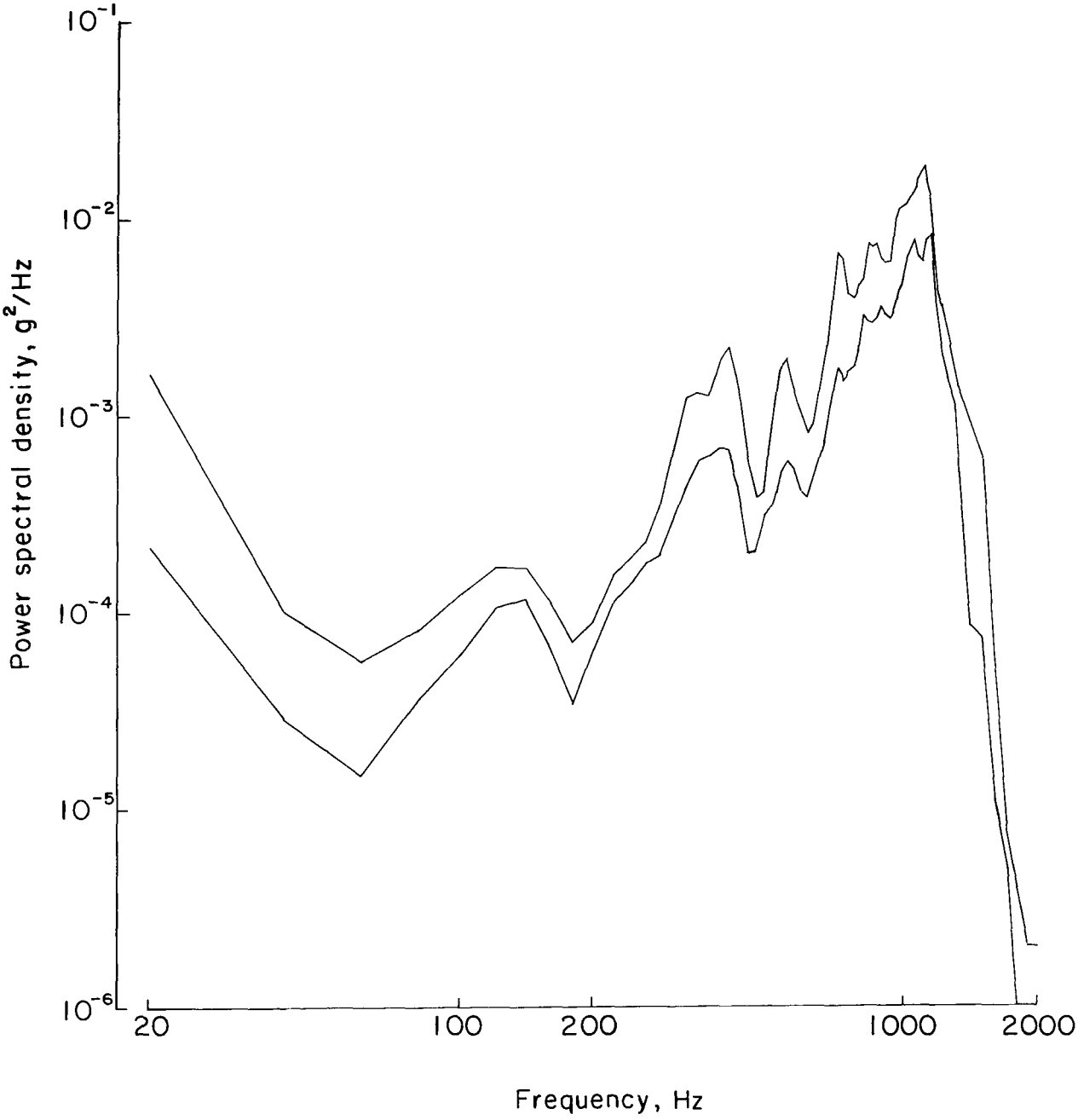

Figure 9.- Range of power spectral densities for Lunar Orbiters I, II, III, and V at lift-off. Accelerometer $A_{a,l}$; longitudinal response to spacecraft.

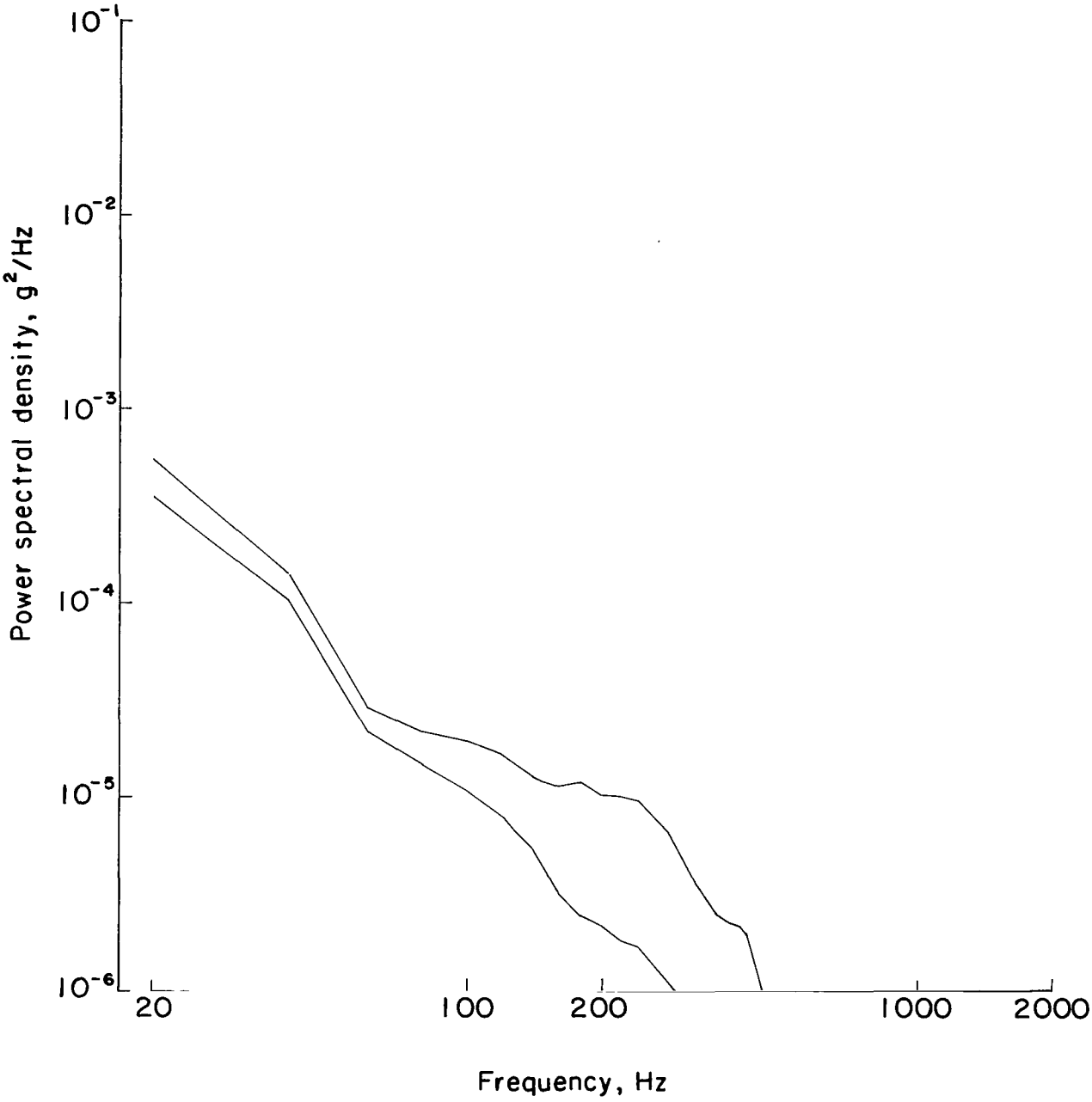

Figure 10.- Range of power spectral densities for Lunar Orbiters II, III, IV, and V at transonic speeds. Accelerometer $A_{s,t}$; transverse response in spacecraft.

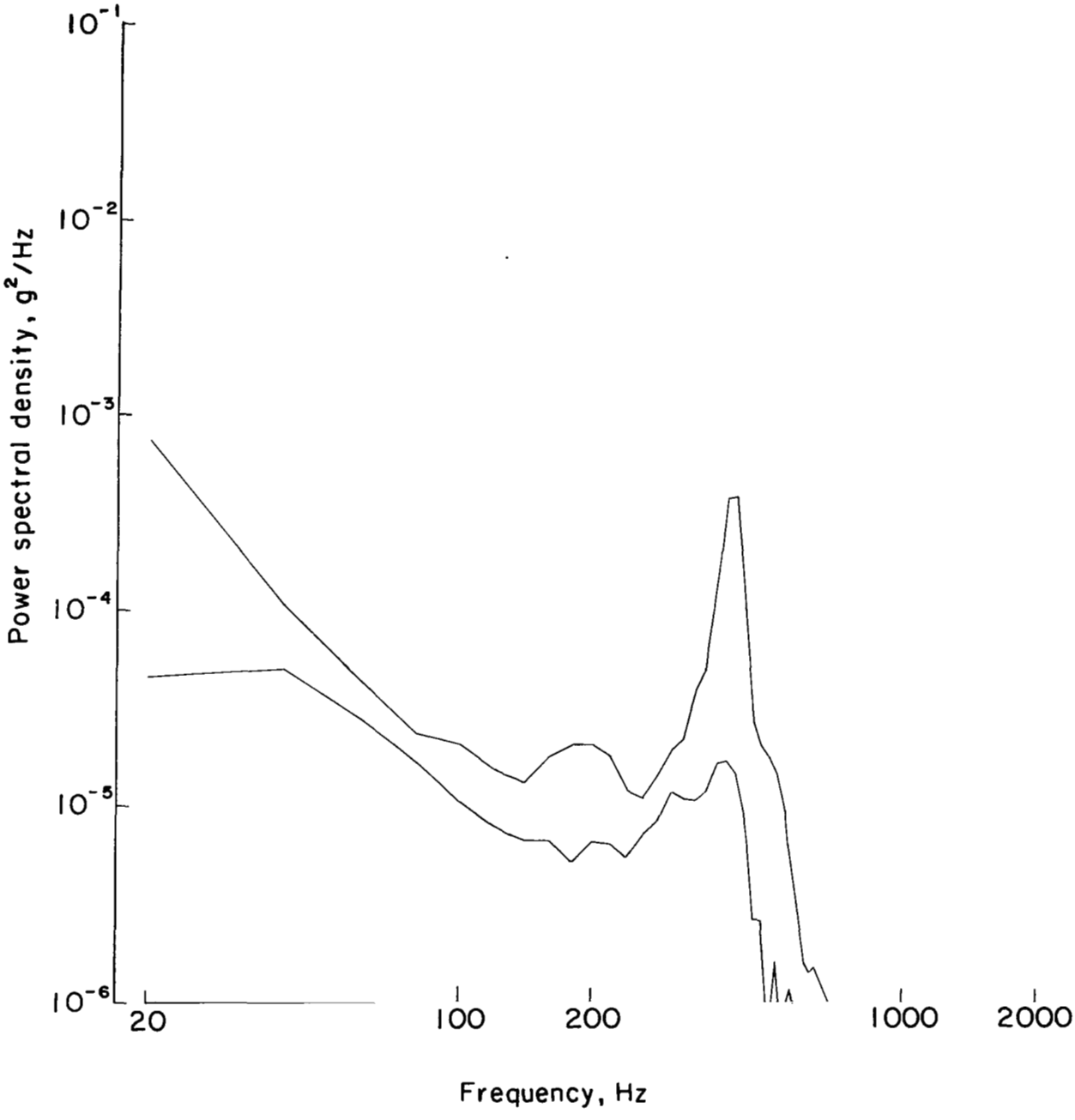

Figure 11.- Range of power spectral densities for Lunar Orbiters I, II, III, IV, and V at transonic speeds. Accelerometer $A_{s,l}$; longitudinal response in spacecraft.

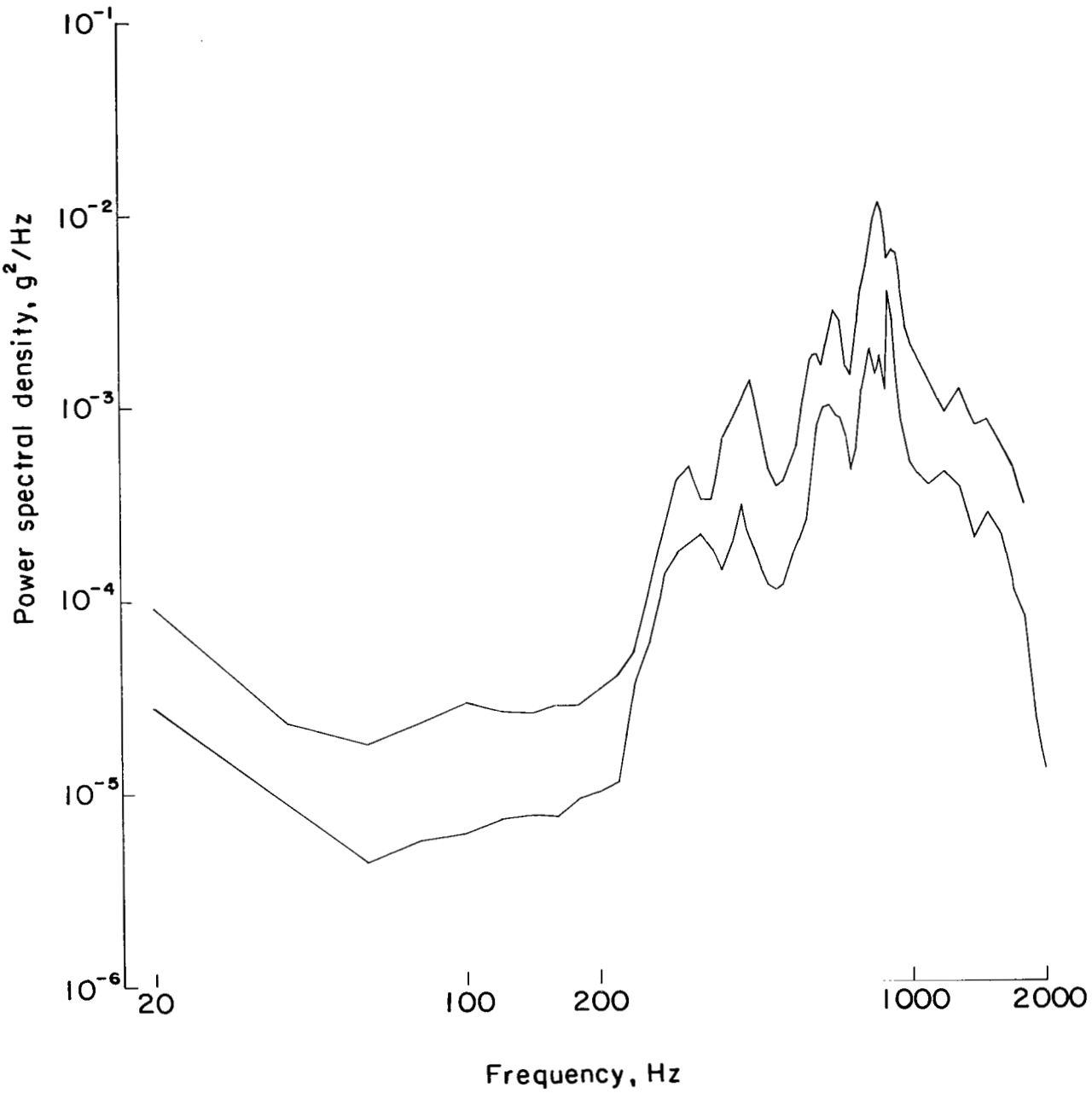

Figure 12.- Range of power spectral densities for Lunar Orbiters I, II, III, IV, and V at transonic speeds. Accelerometer $A_{a,t}$: transverse input to spacecraft.

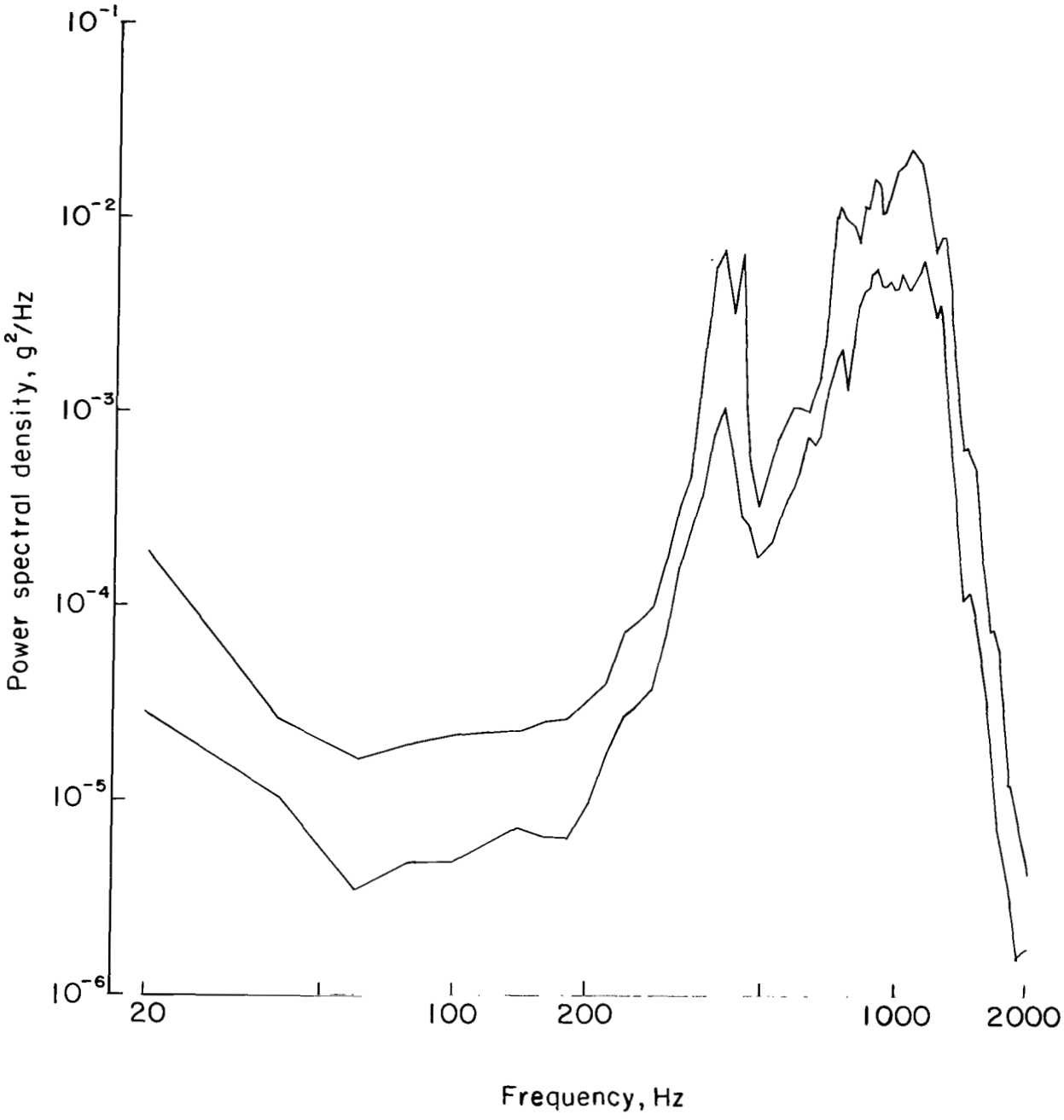

Figure 13.- Range of power spectral densities for Lunar Orbiters I, II, III, IV, and V at transonic speeds. Accelerometer $A_{a,l}$; longitudinal input to spacecraft.

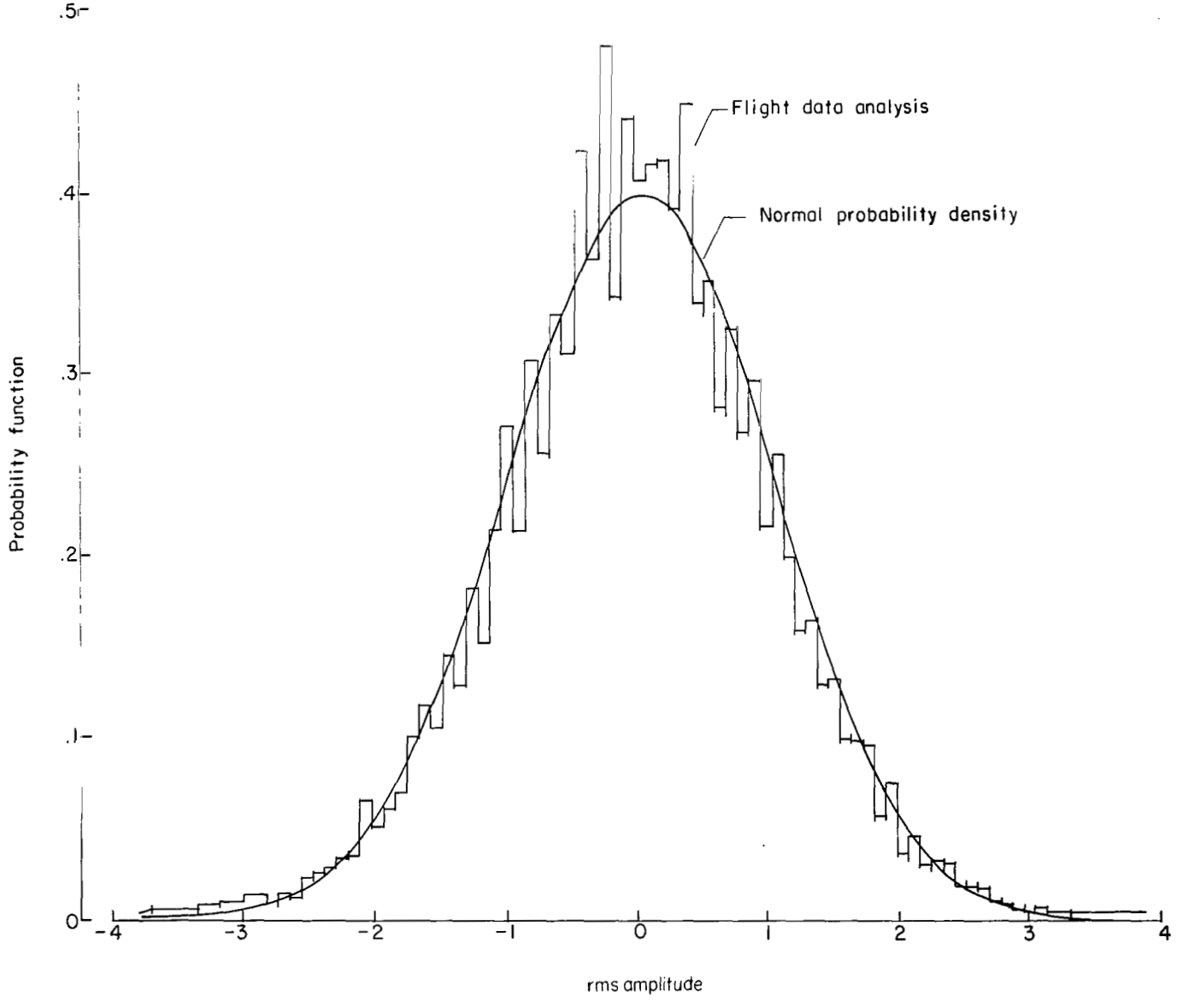

Figure 14.- Example of probability analysis in the transverse direction at lift-off for Lunar Orbiter V. Accelerometer $A_{a,t}$.

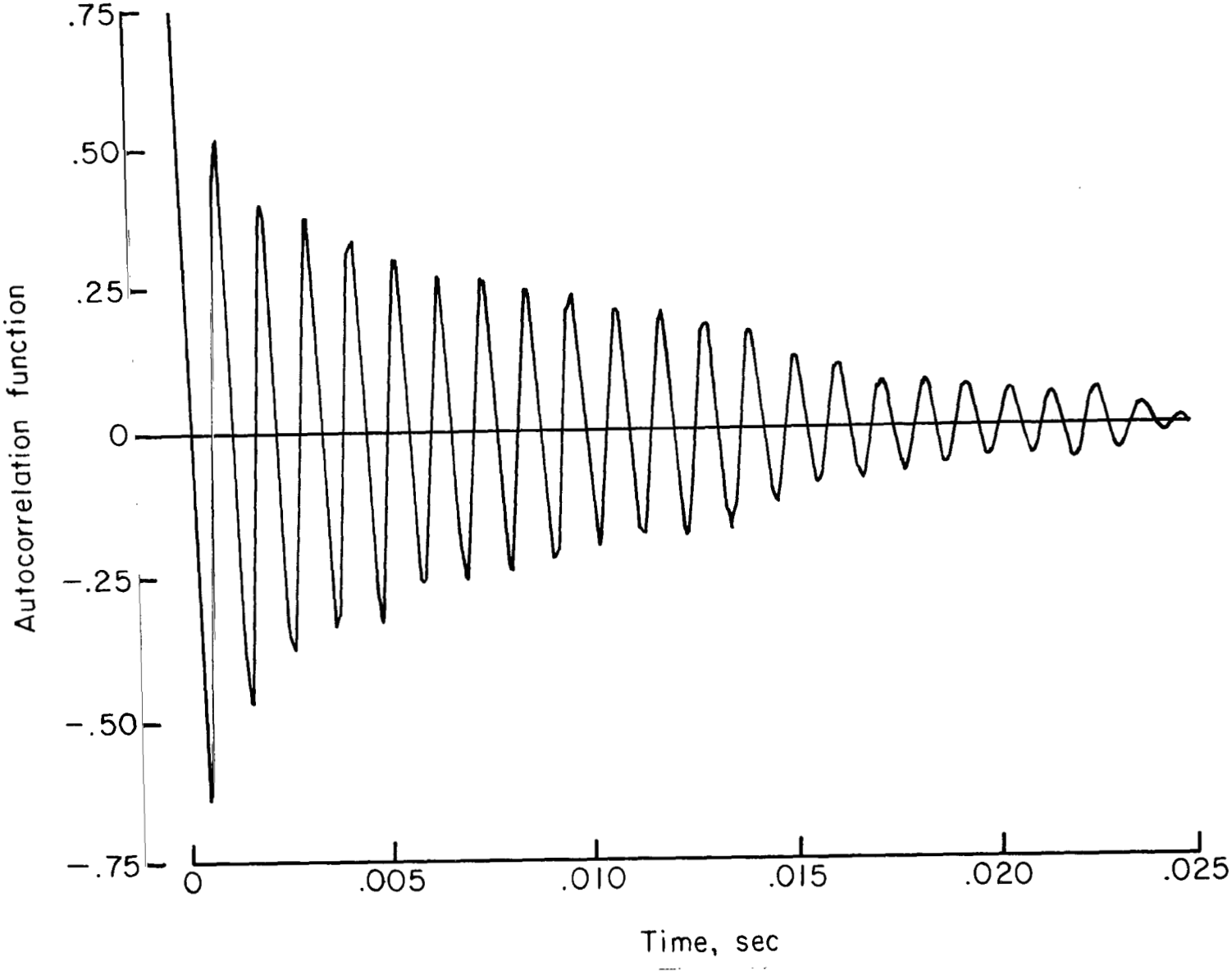

Figure 15.- Example of autocorrelation function in the transverse direction at lift-off for Lunar Orbiter V. Accelerometer $A_{a,t}$.

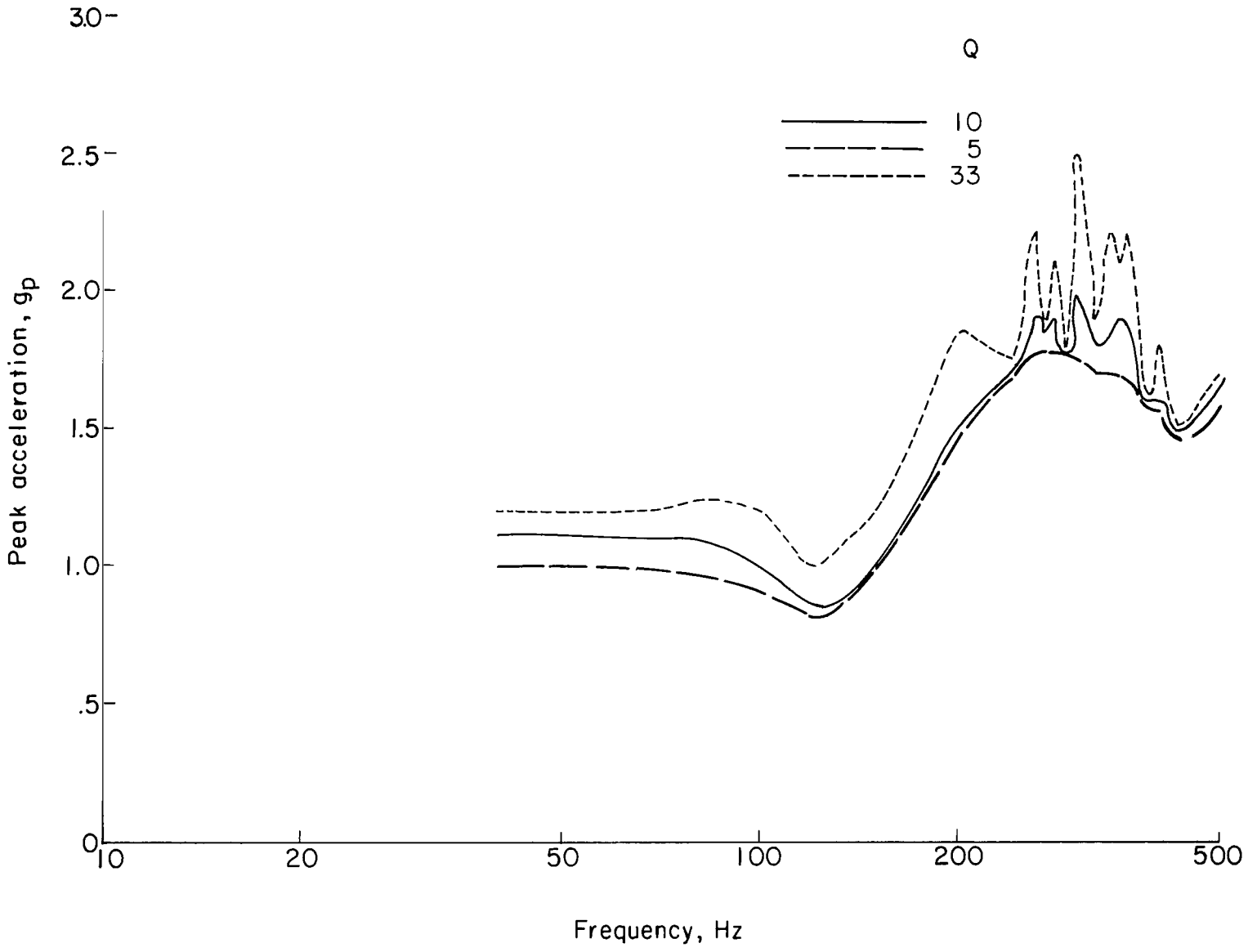

Figure 16.- Shock spectrum analysis of accelerometer $A_{s,t}$ at shroud jettison.

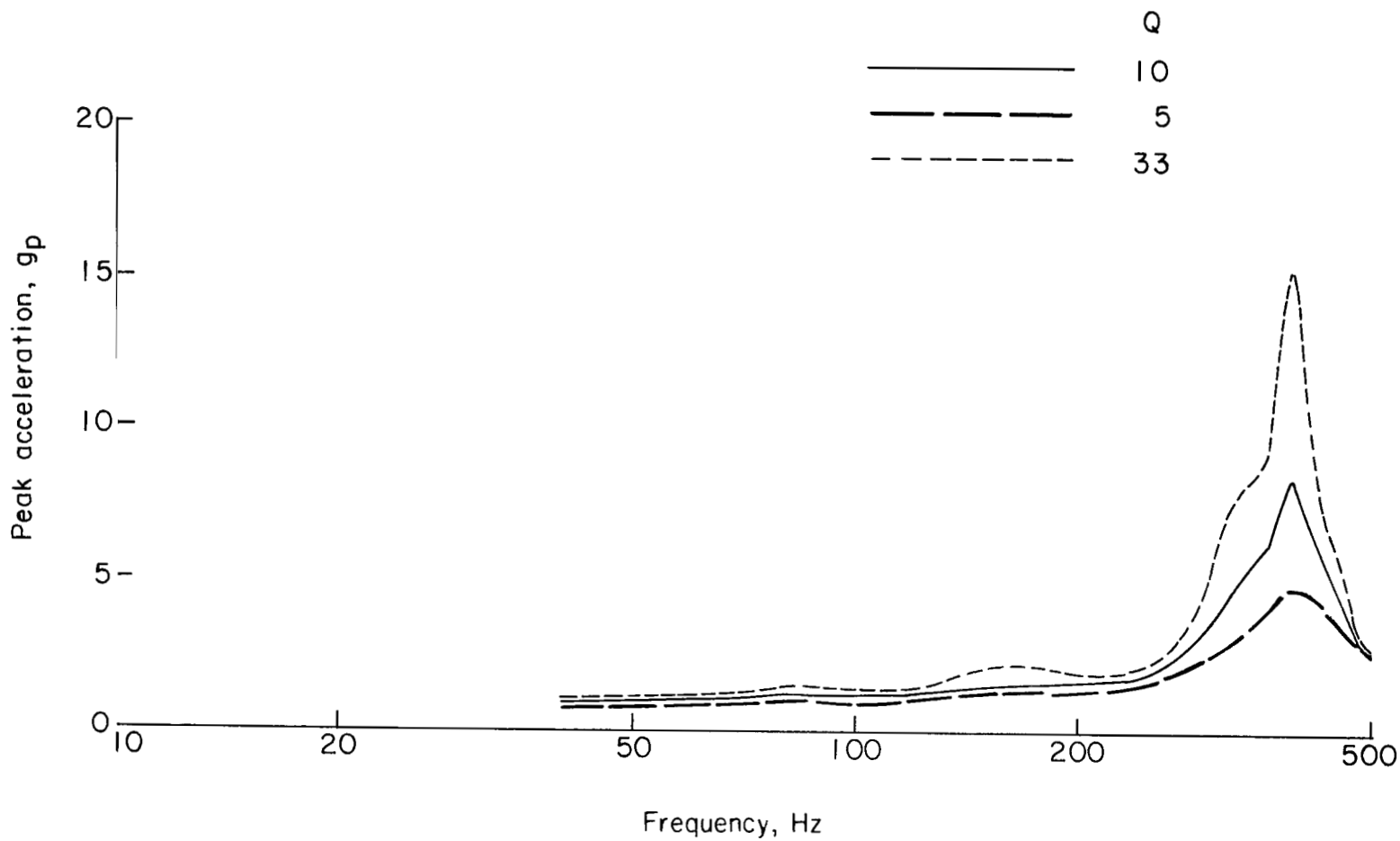

Figure 17.- Shock spectrum analysis of accelerometer $A_{s,l}$ at shroud jettison.

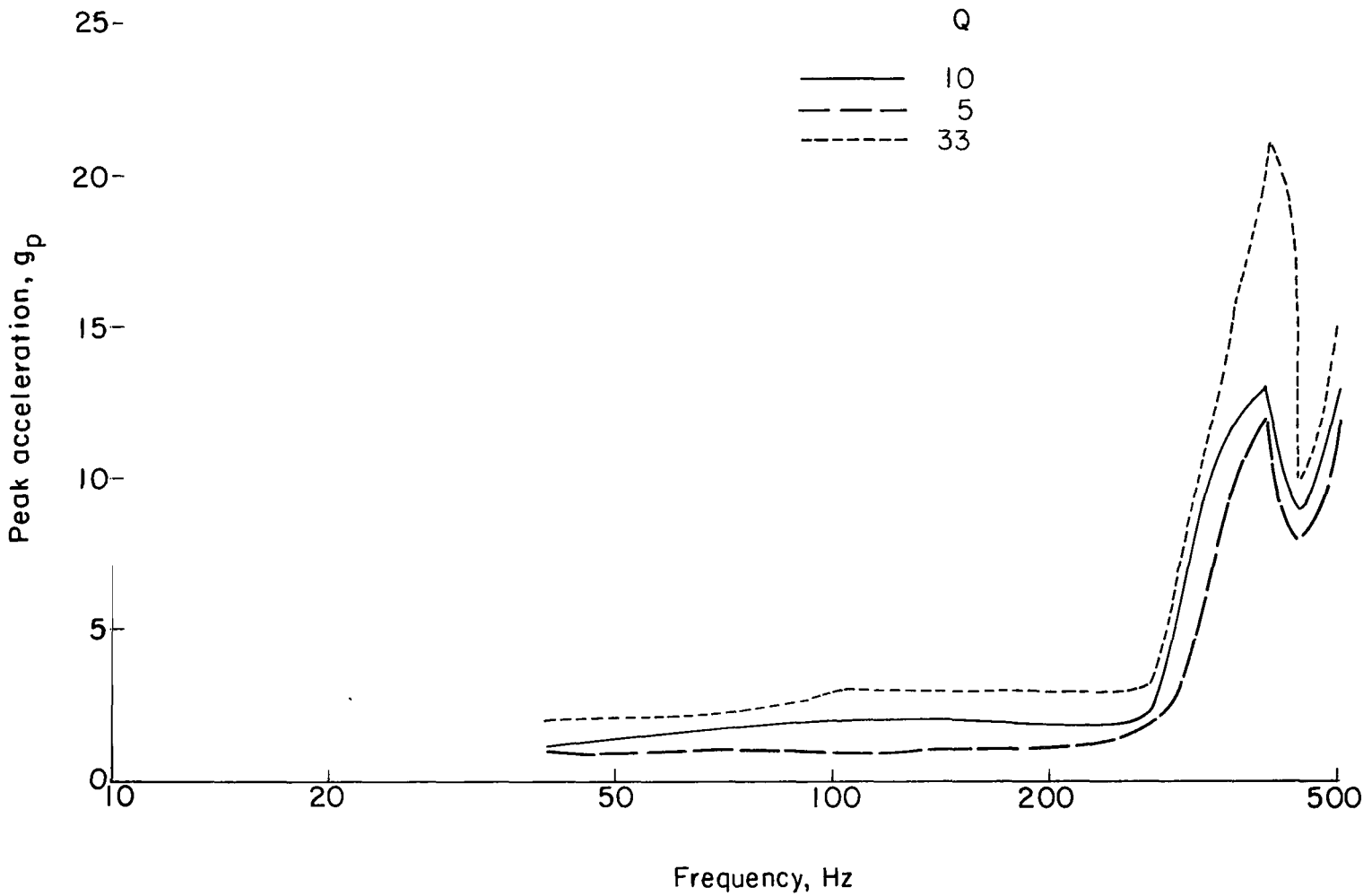

Figure 18.- Shock spectrum analysis of accelerometer $A_{a,t}$ at shroud jettison.

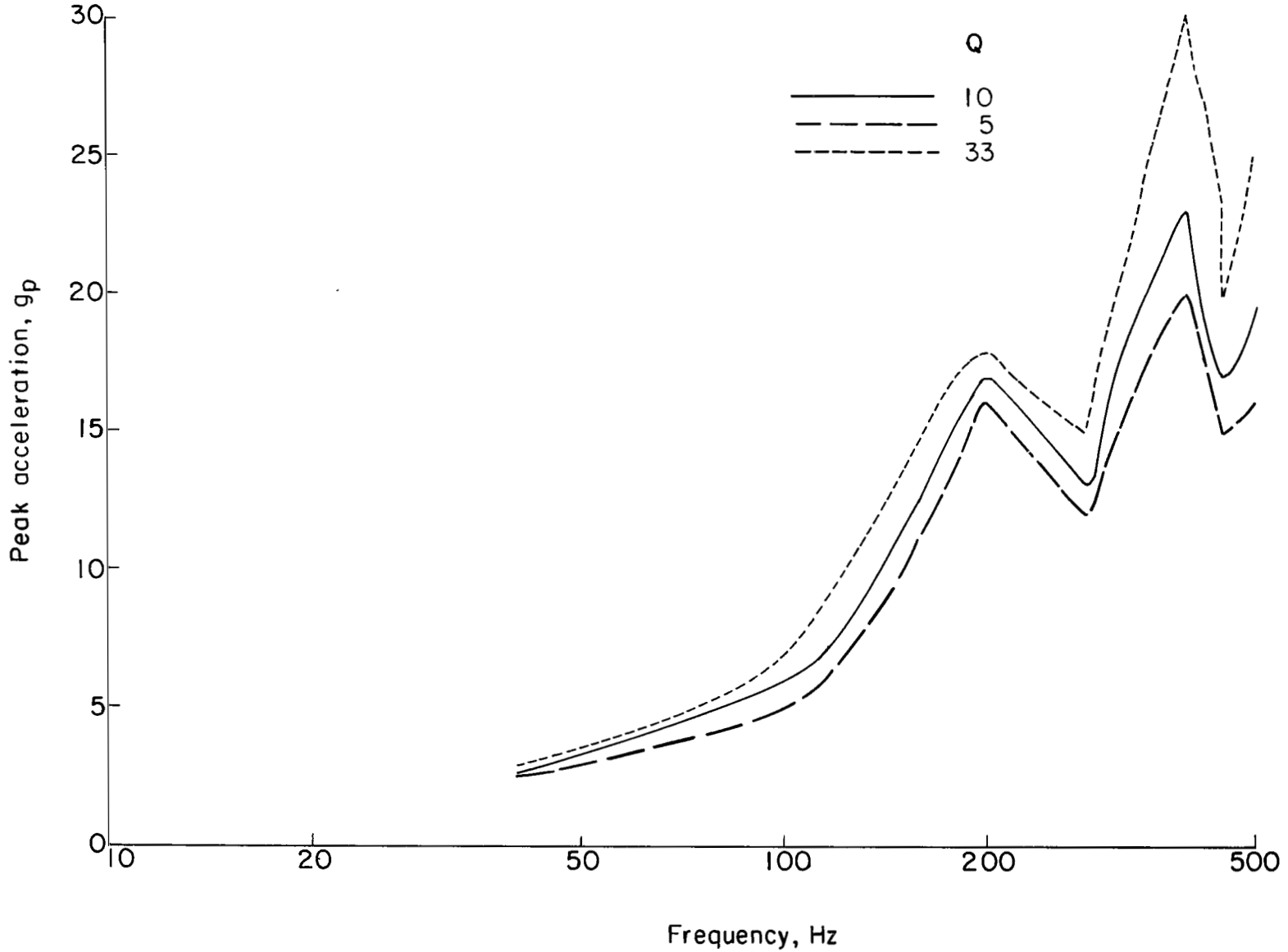

Figure 19.- Shock spectrum analysis of accelerometer $A_{a,l}$ at shroud jettison.

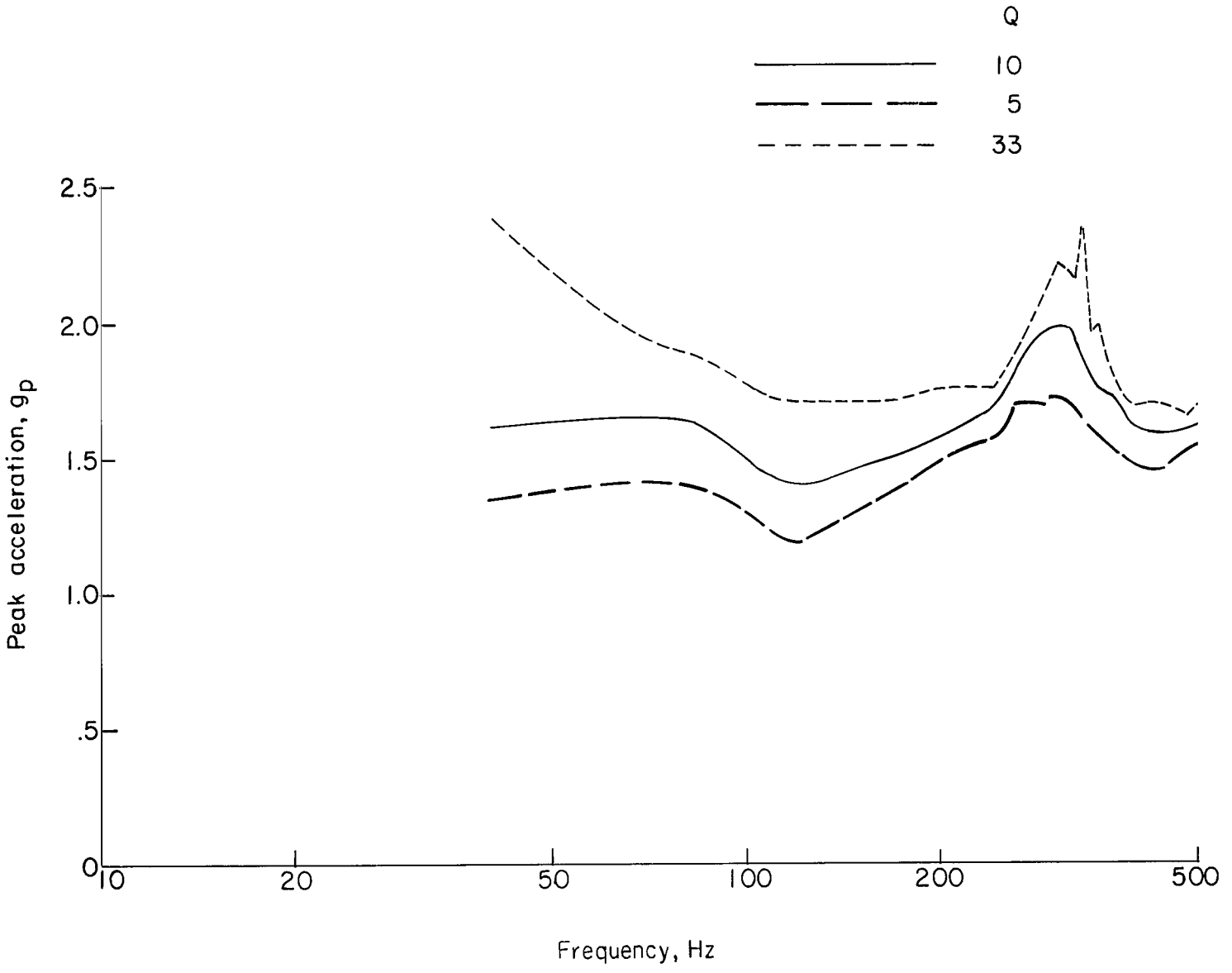

Figure 20.- Shock spectrum analysis of accelerometer $A_{s,t}$ at Agena first ignition.

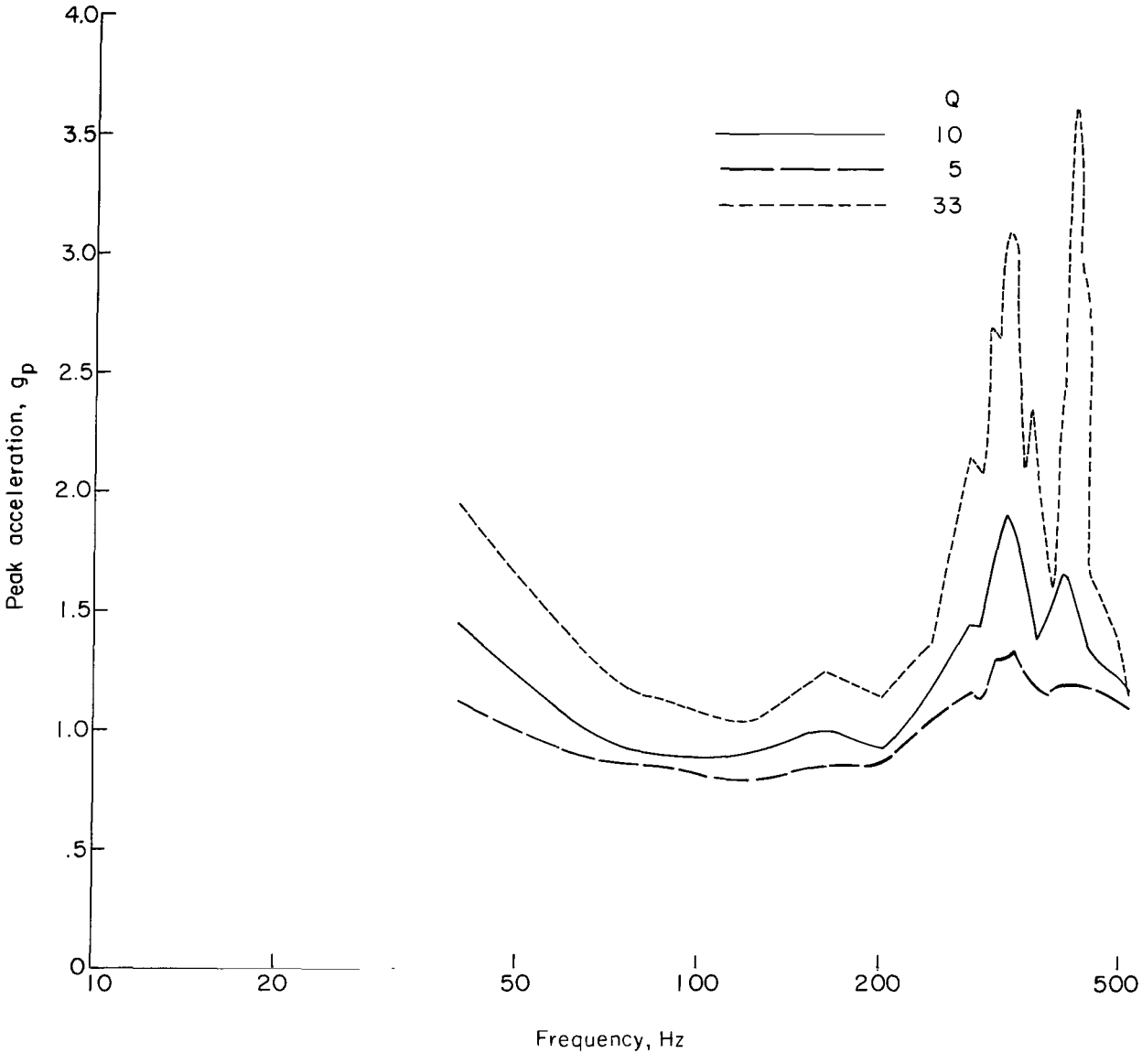

Figure 21.- Shock spectrum analysis of accelerometer $A_{s,l}$ at Agena first ignition.

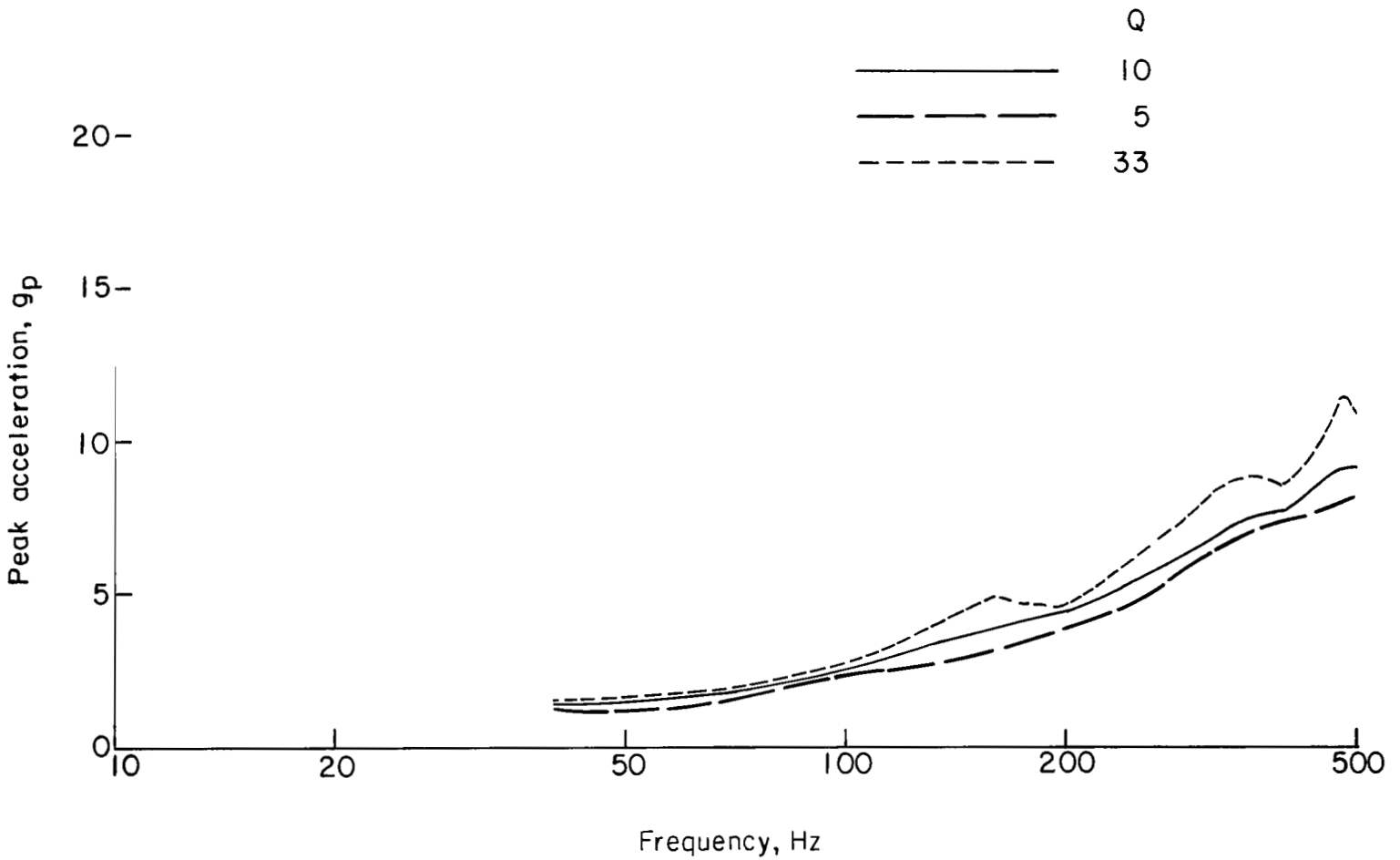

Figure 22.- Shock spectrum analysis of accelerometer $A_{a,t}$ at Agena first ignition.

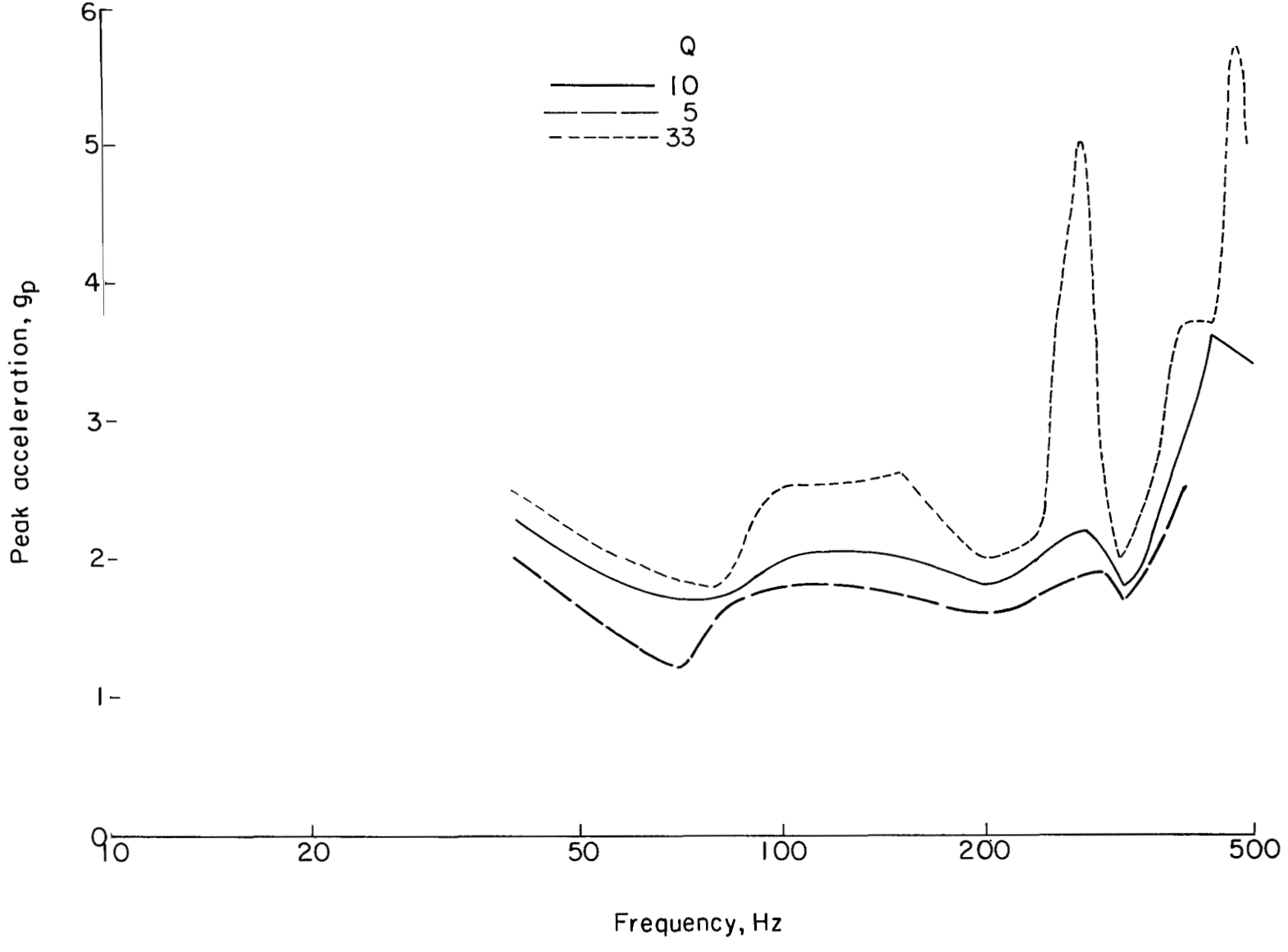

Figure 23.- Shock spectrum analysis of accelerometer $A_{a,l}$ at Agena first ignition.

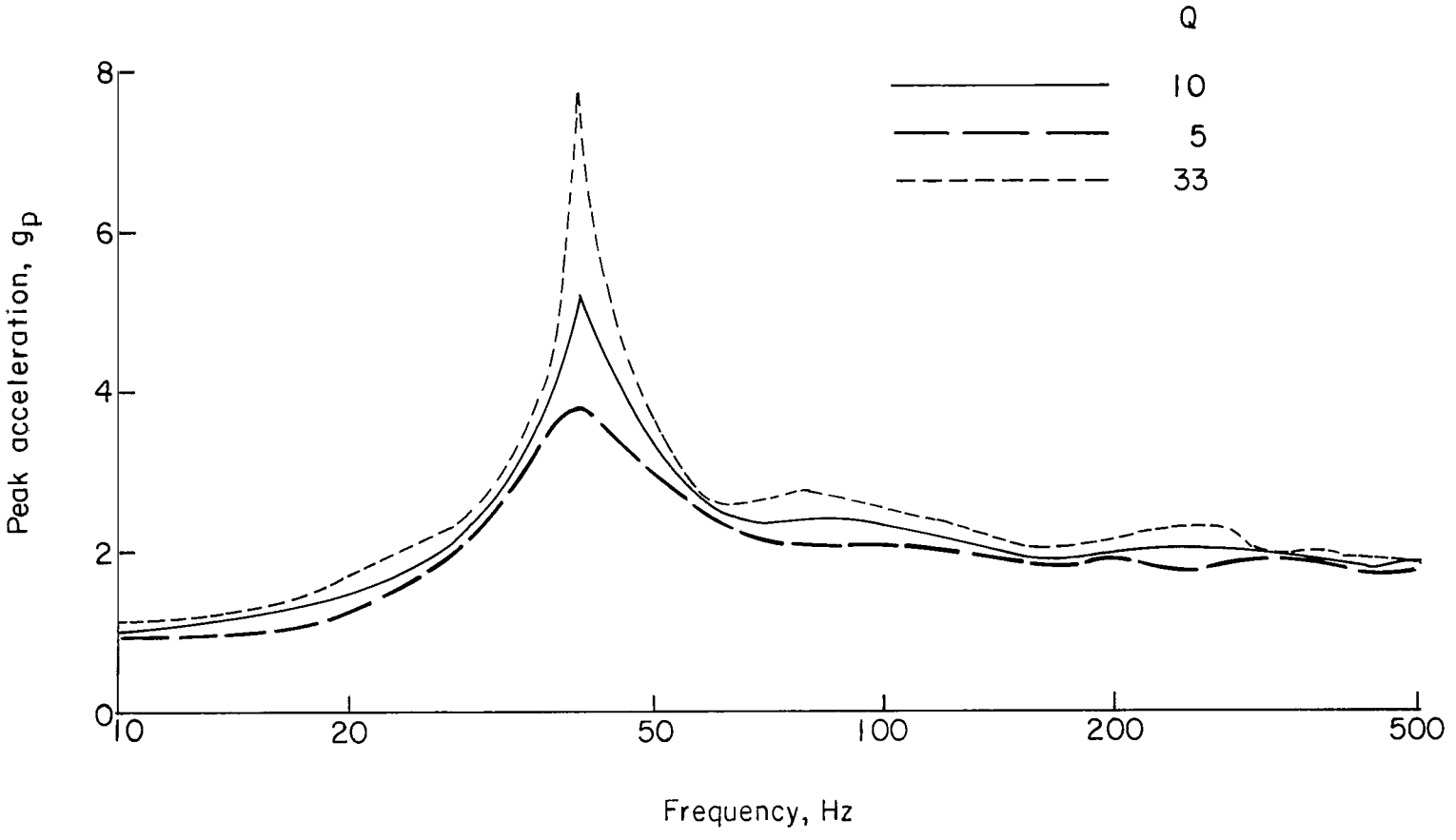

Figure 24.- Shock spectrum analysis of accelerometer $A_{s,t}$ at Agena first burnout.

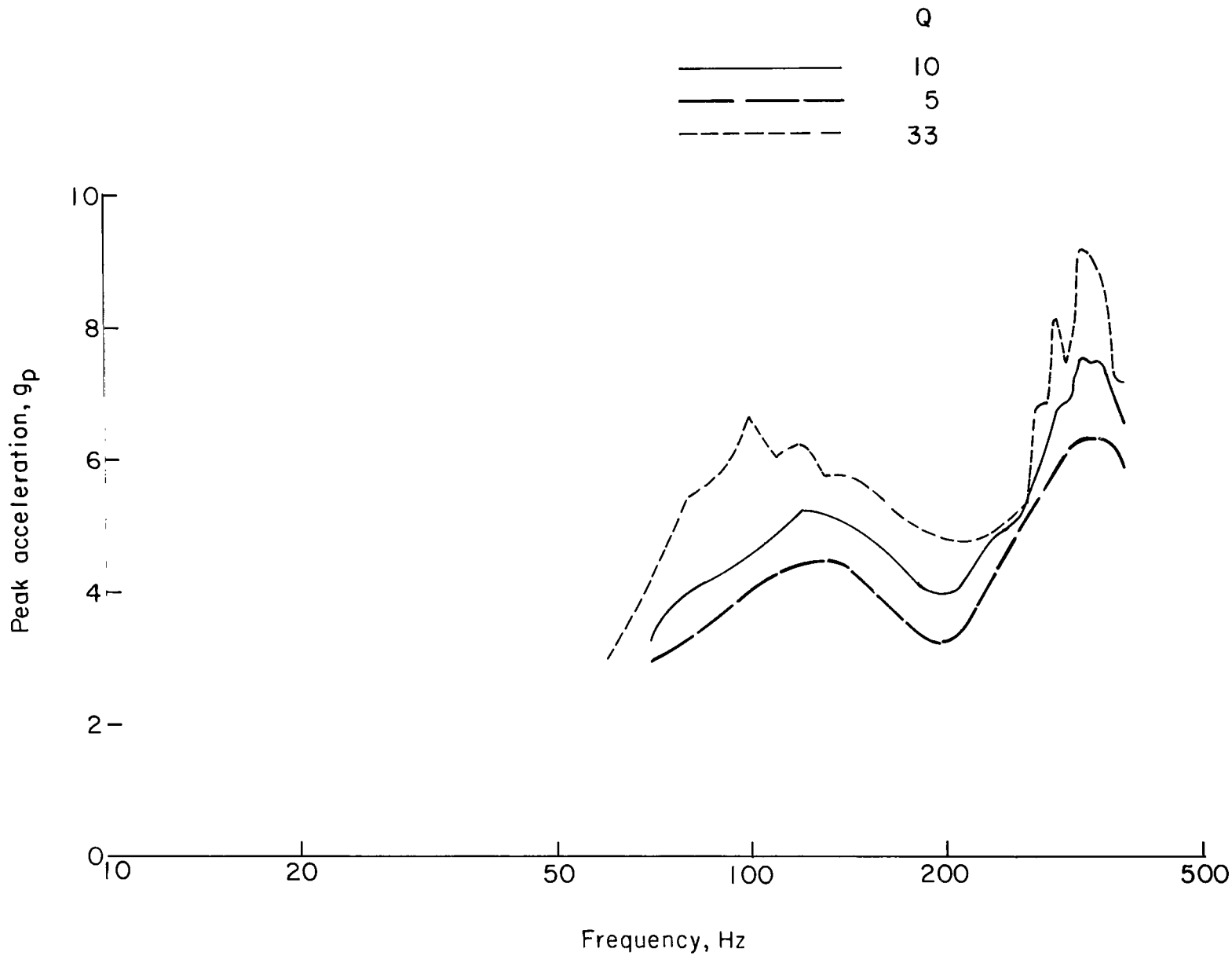

Figure 25.- Shock spectrum analysis of accelerometer $A_{s,l}$ at Agena first burnout.

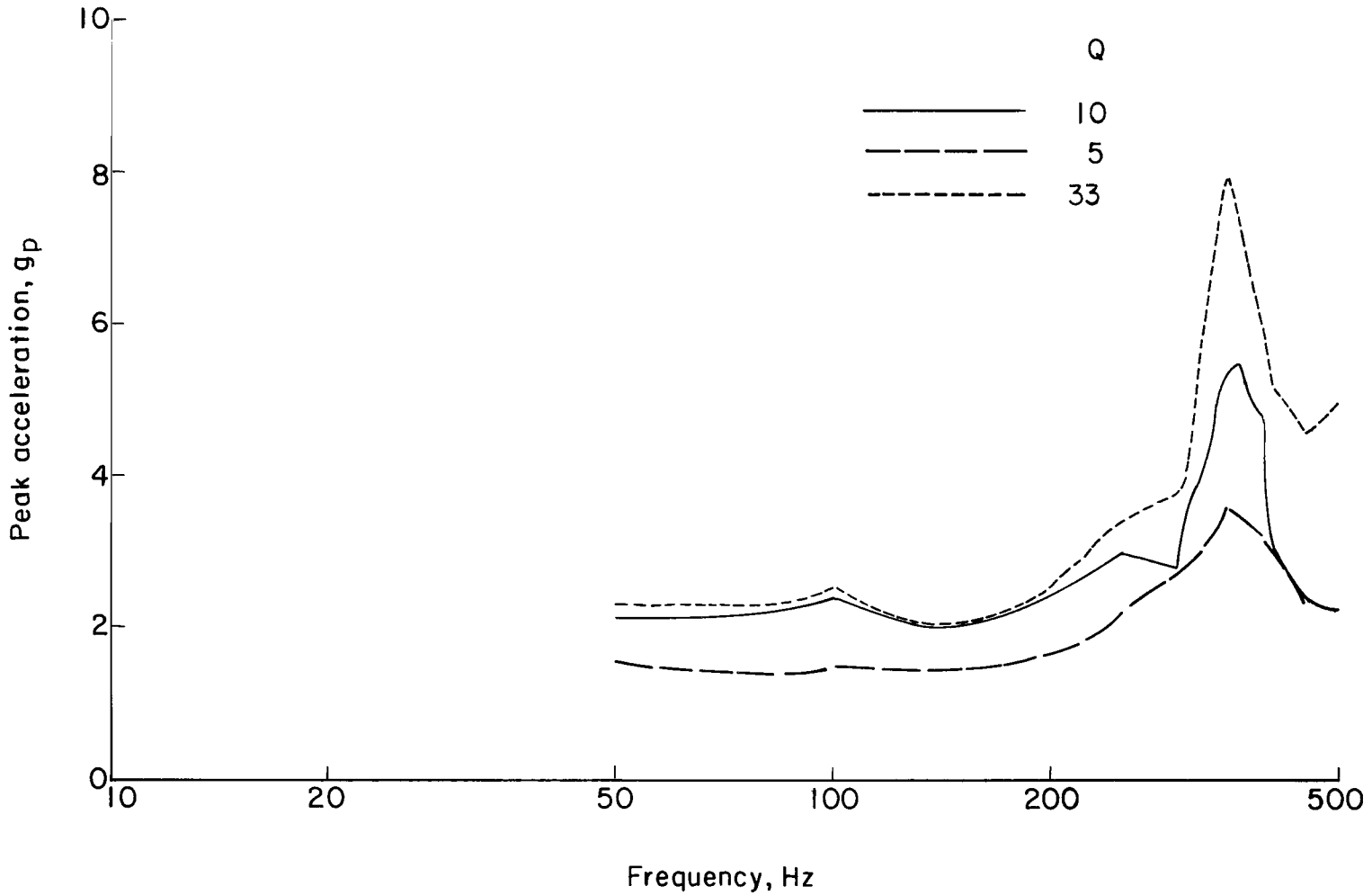

Figure 26.- Shock spectrum analysis of accelerometer $A_{a,t}$ at Agena first burnout.

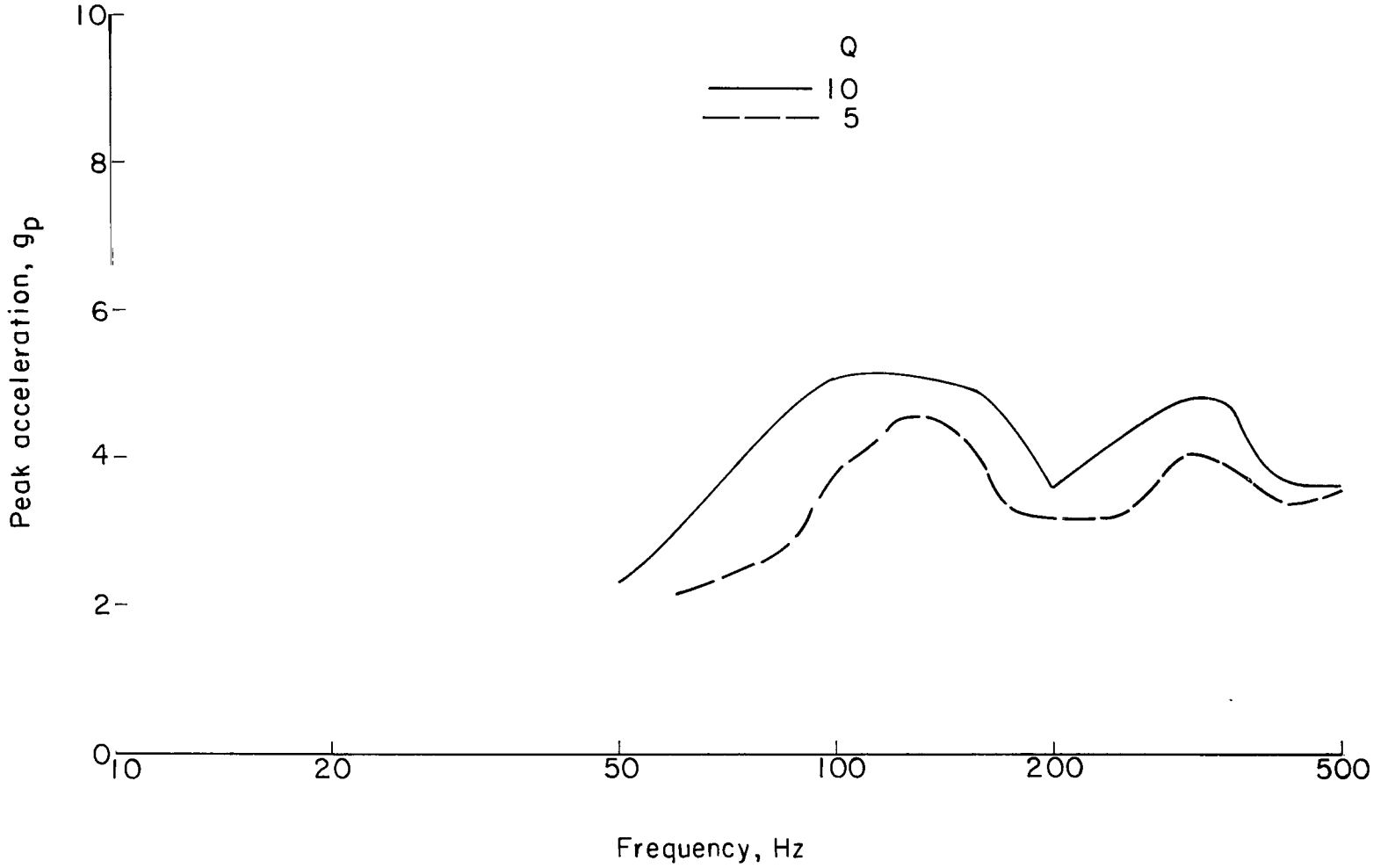

Figure 27.- Shock spectrum analysis of accelerometer $A_{a,l}$ at Agena first burnout.

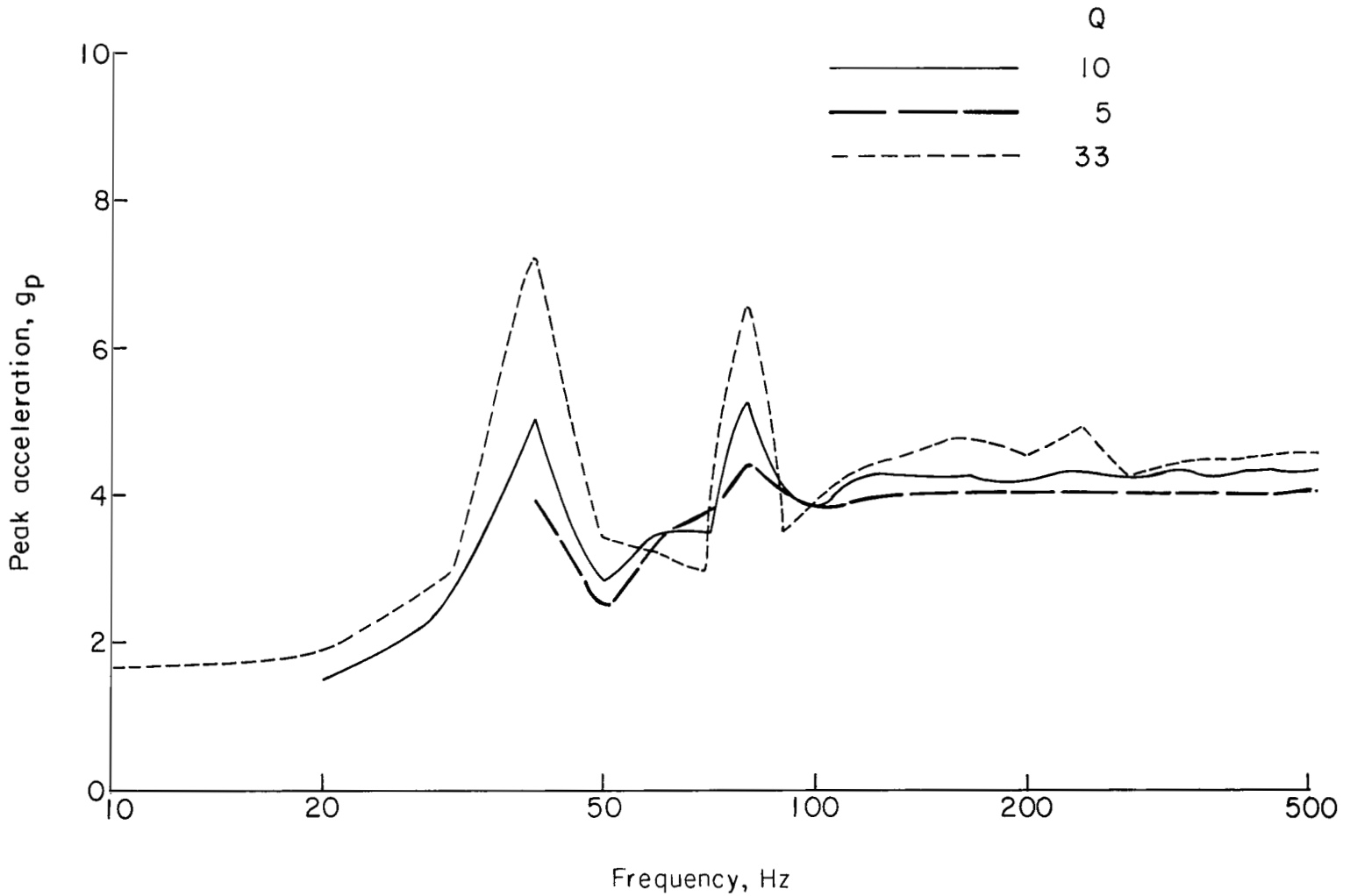

Figure 28.- Shock spectrum analysis of accelerometer $A_{s,t}$ at Agena second ignition.

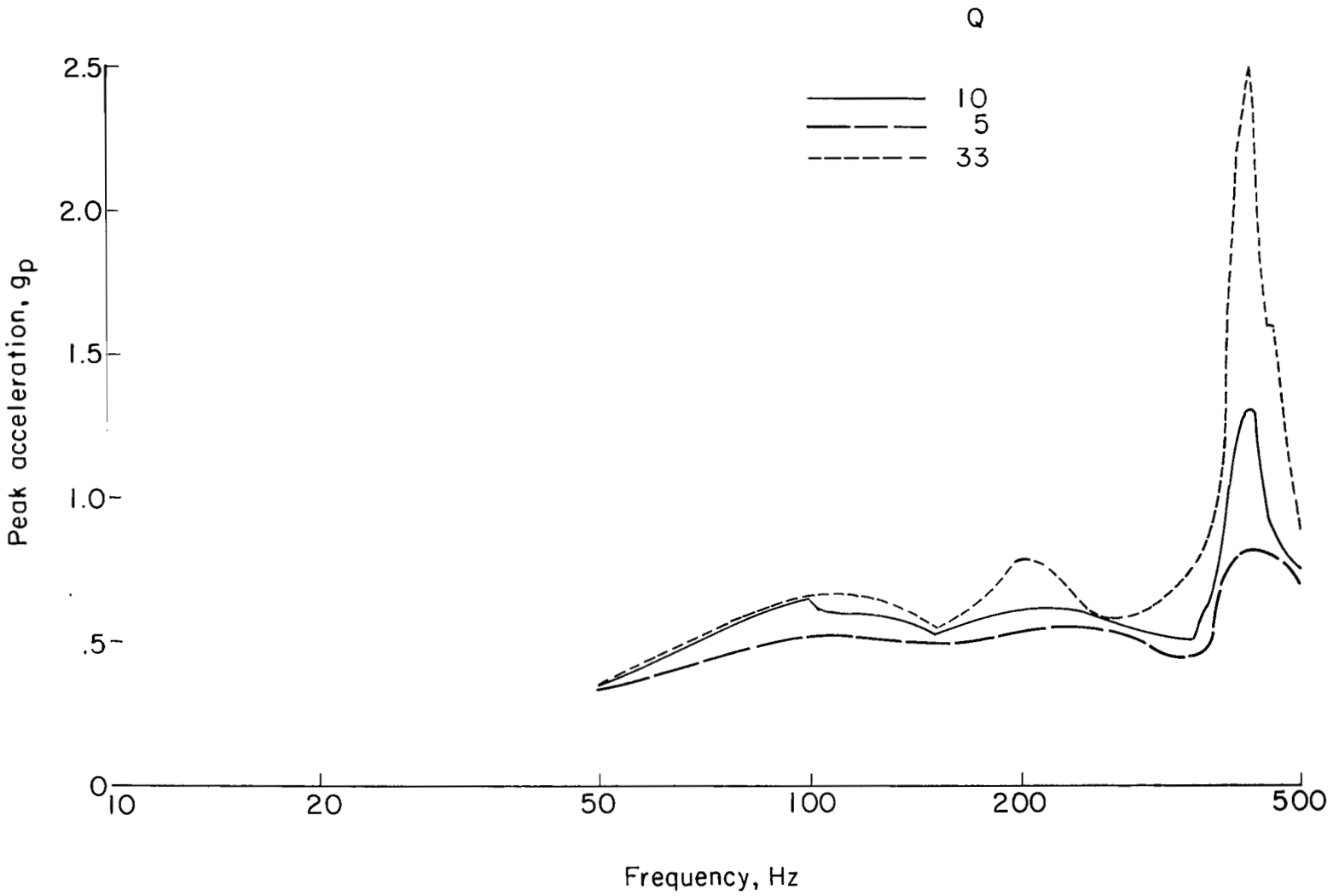

Figure 29.- Shock spectrum analysis of accelerometer $A_{s,l}$ at Agena second ignition.

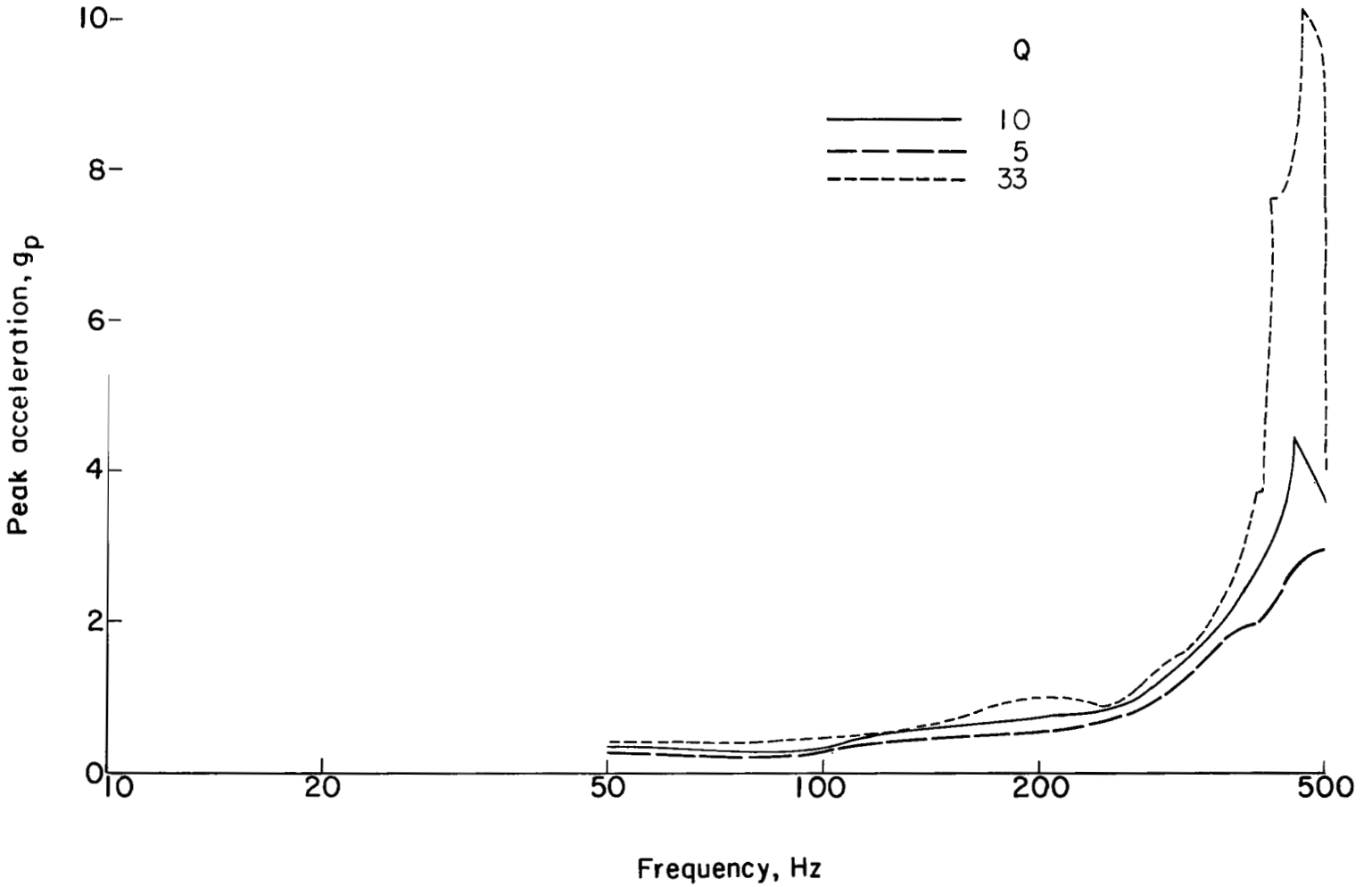

Figure 30.- Shock spectrum analysis of accelerometer $A_{a,t}$ at Agena second ignition.

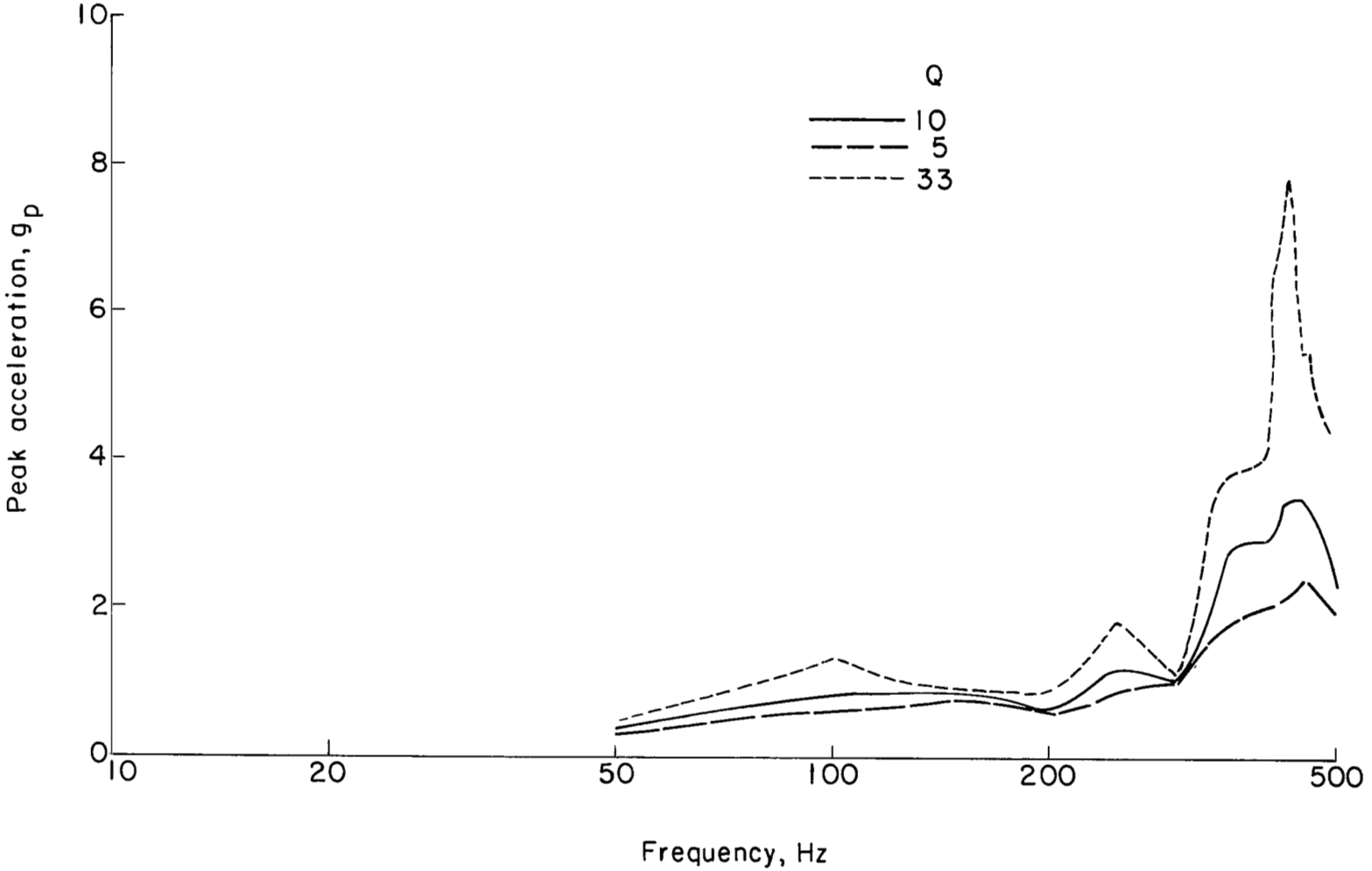

Figure 31.- Shock spectrum analysis of accelerometer $A_{a,l}$ at Agena second ignition.

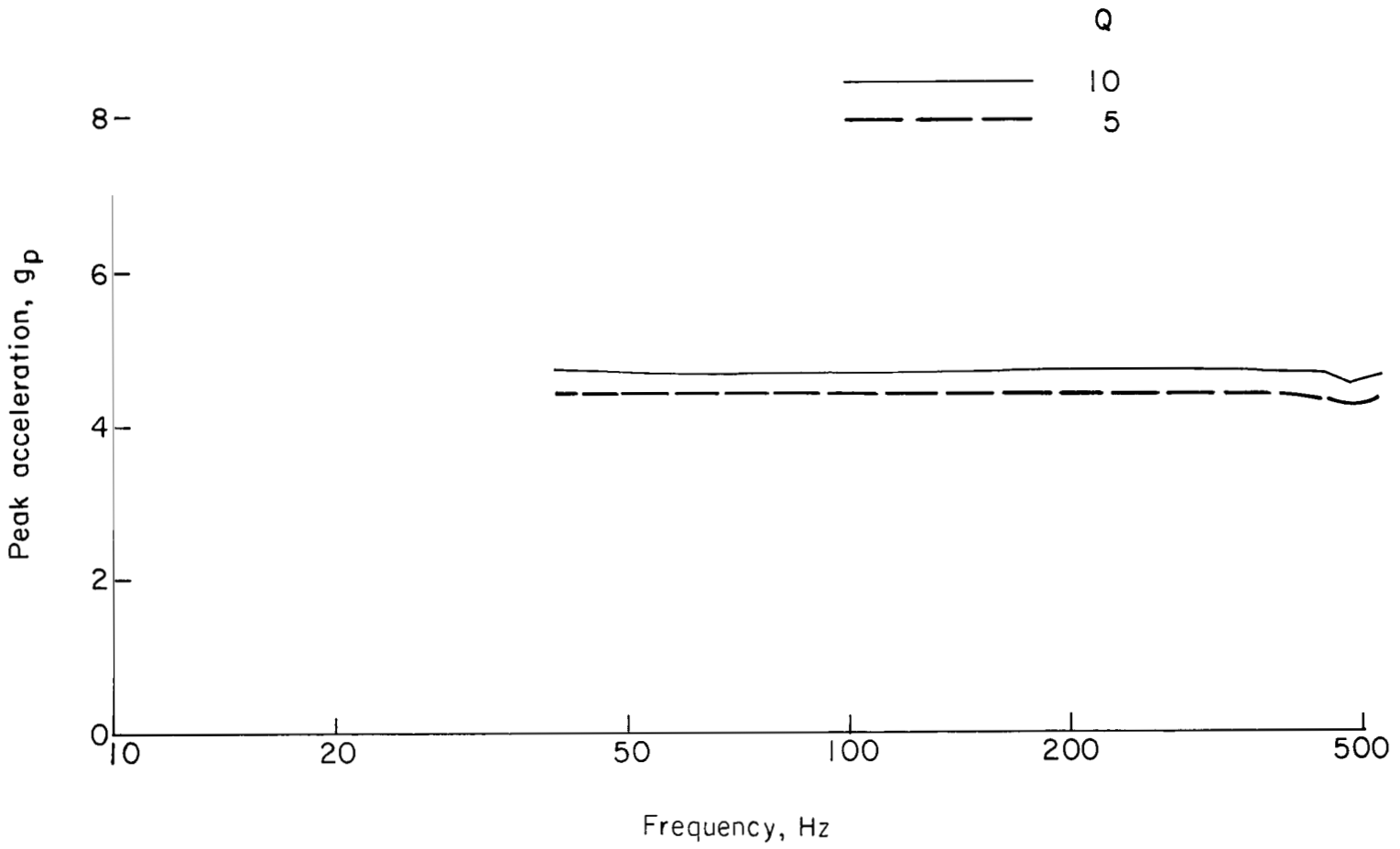

Figure 32.- Shock spectrum analysis of accelerometer $A_{s,t}$ at Agena second burnout.

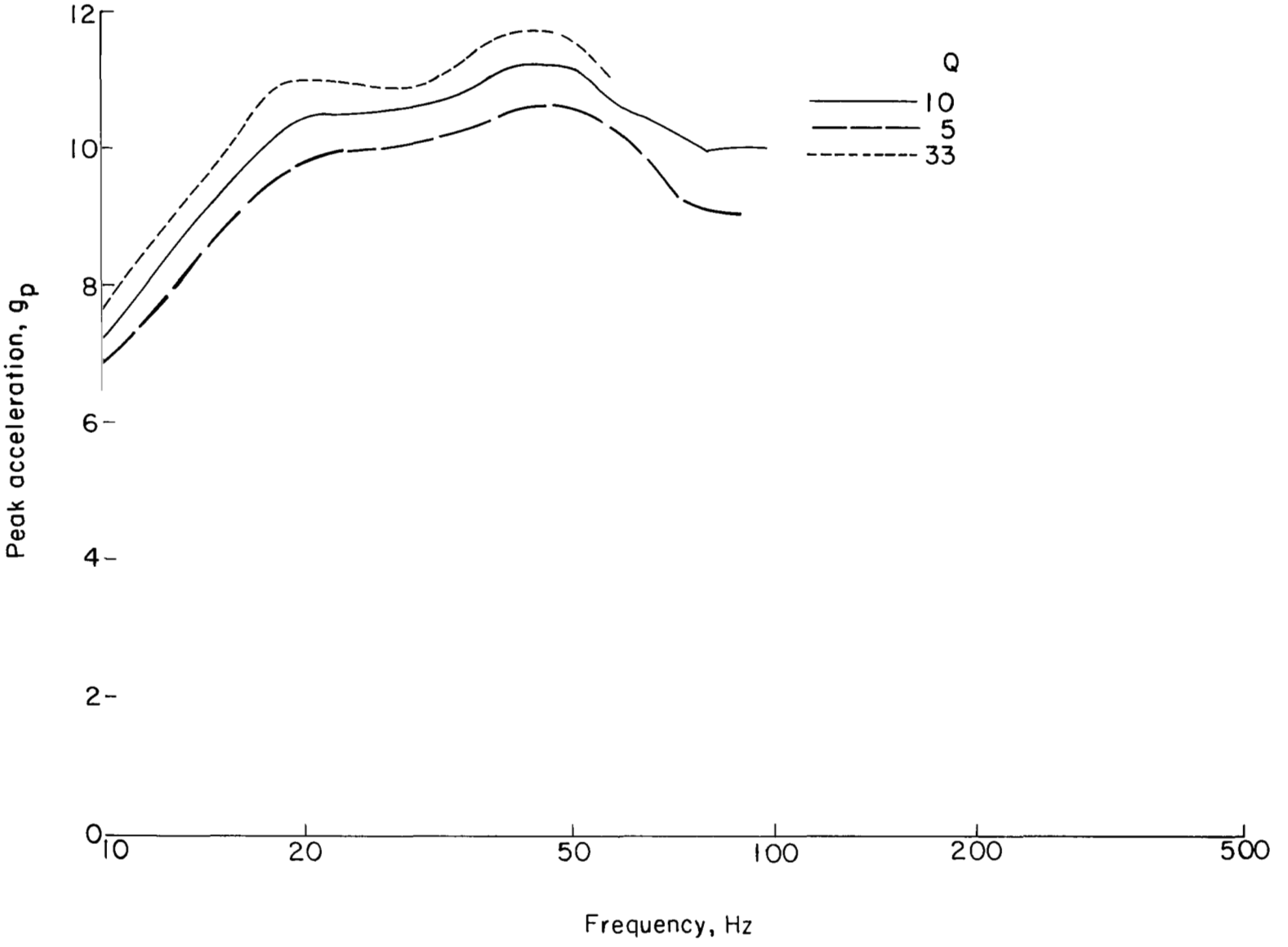

Figure 33.- Shock spectrum analysis of accelerometer $A_{s,l}$ at Agena second burnout.

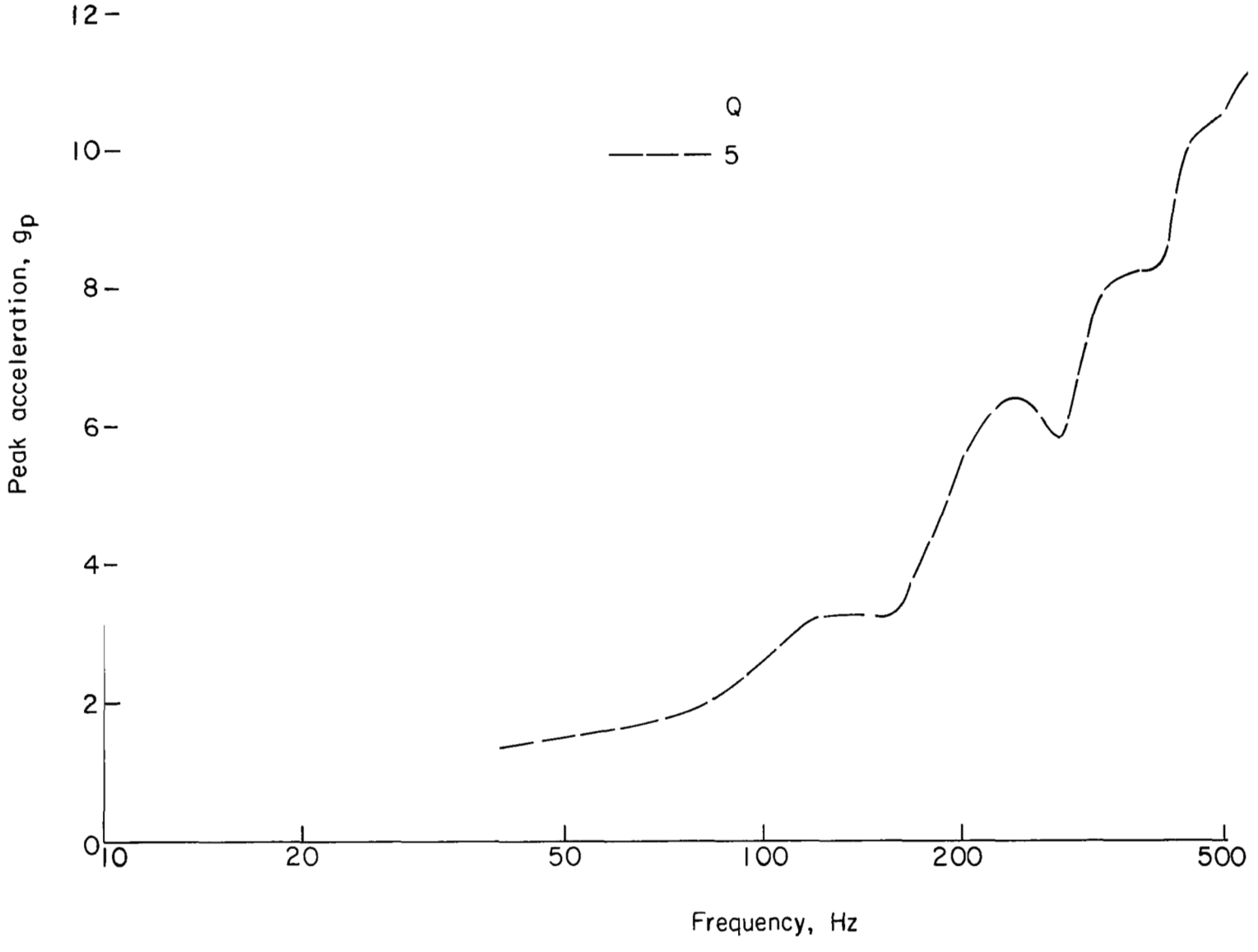

Figure 34.- Shock spectrum analysis of accelerometer $A_{a,t}$ at Agena second burnout.

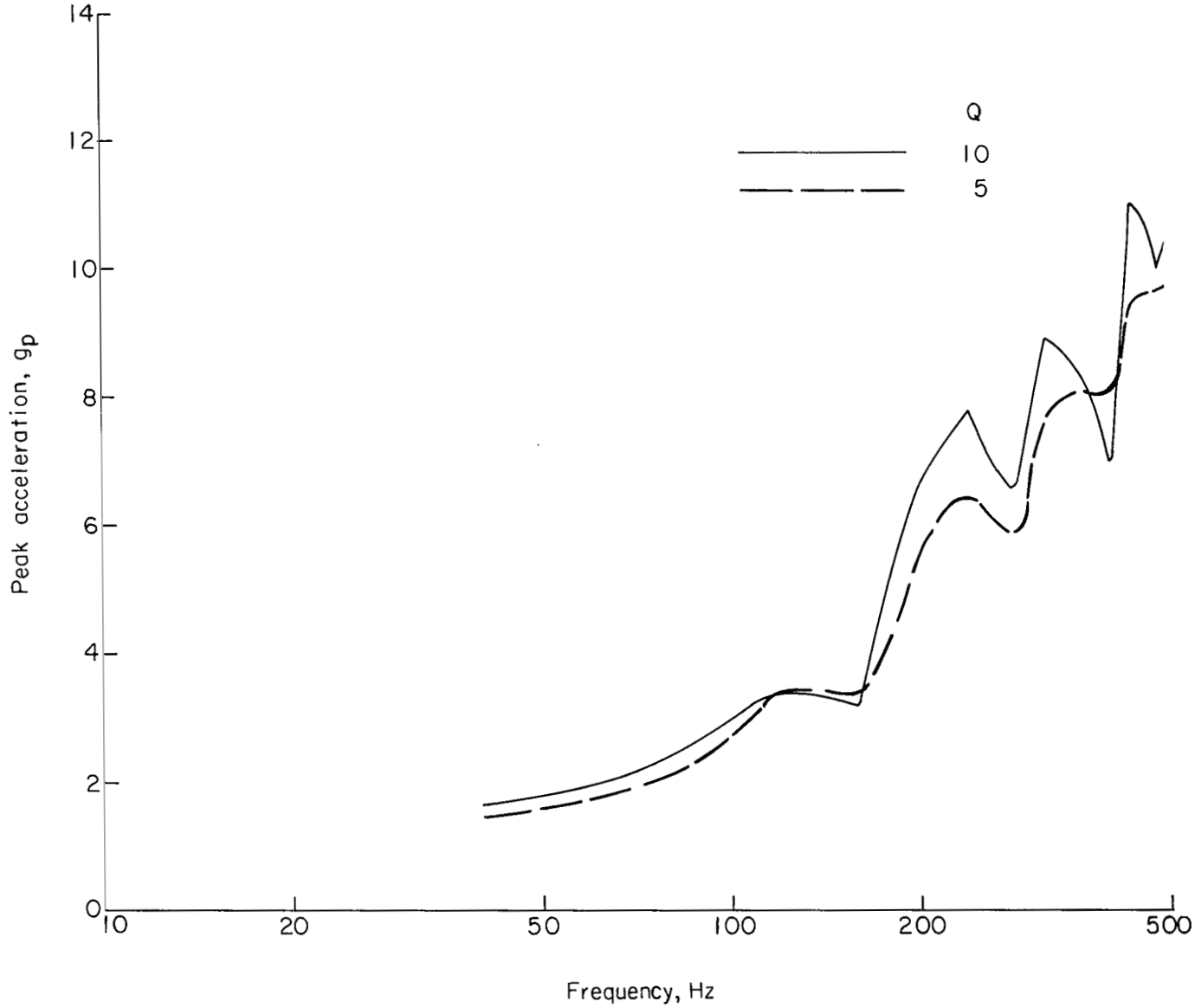

Figure 35.- Shock spectrum analysis of accelerometer $A_{a,l}$ at Agena second burnout.

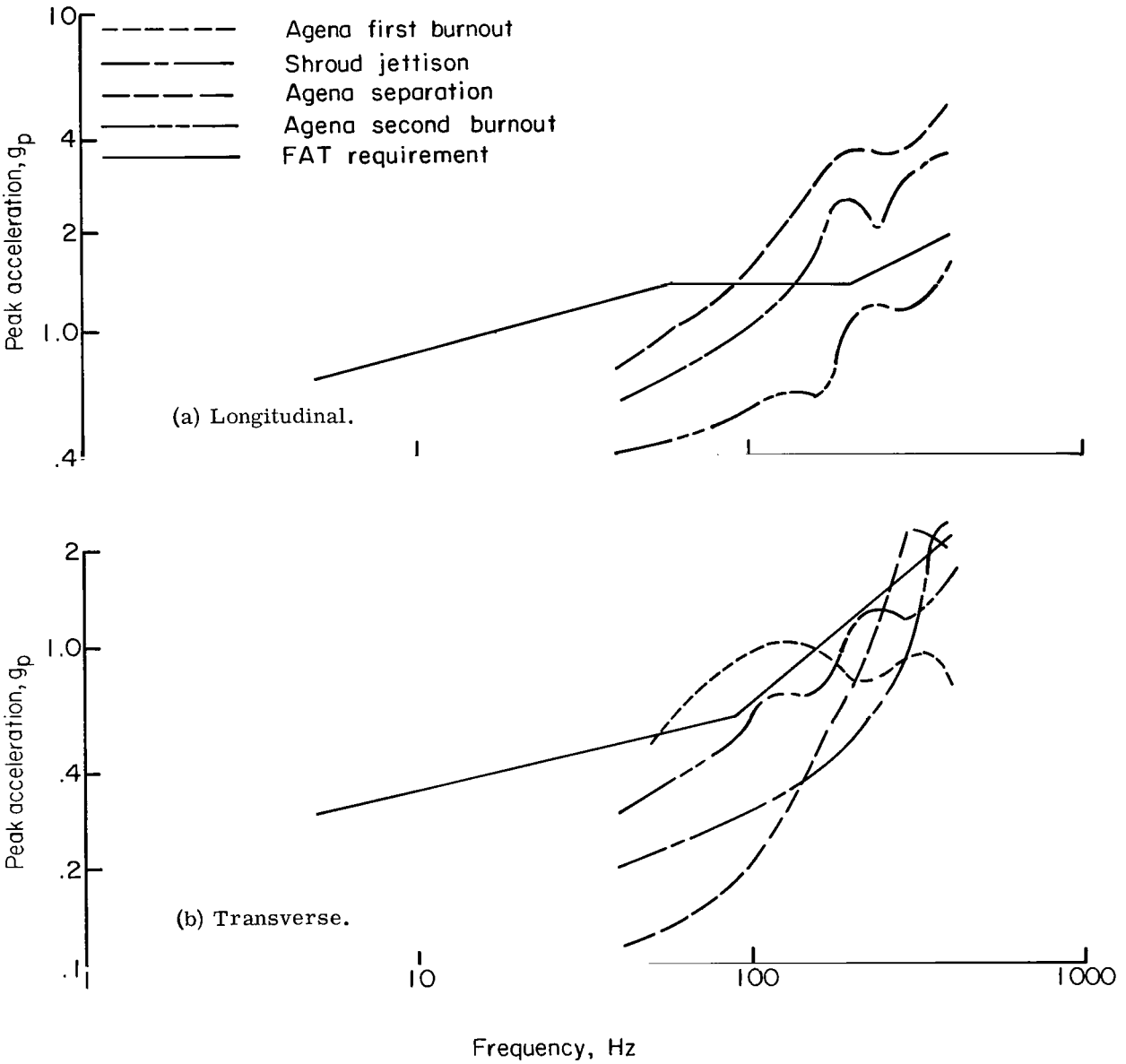

Figure 36.- Comparison of sinusoidal FAT requirements with equivalent sinusoidal levels of shock spectra from flight data. Q = 5.

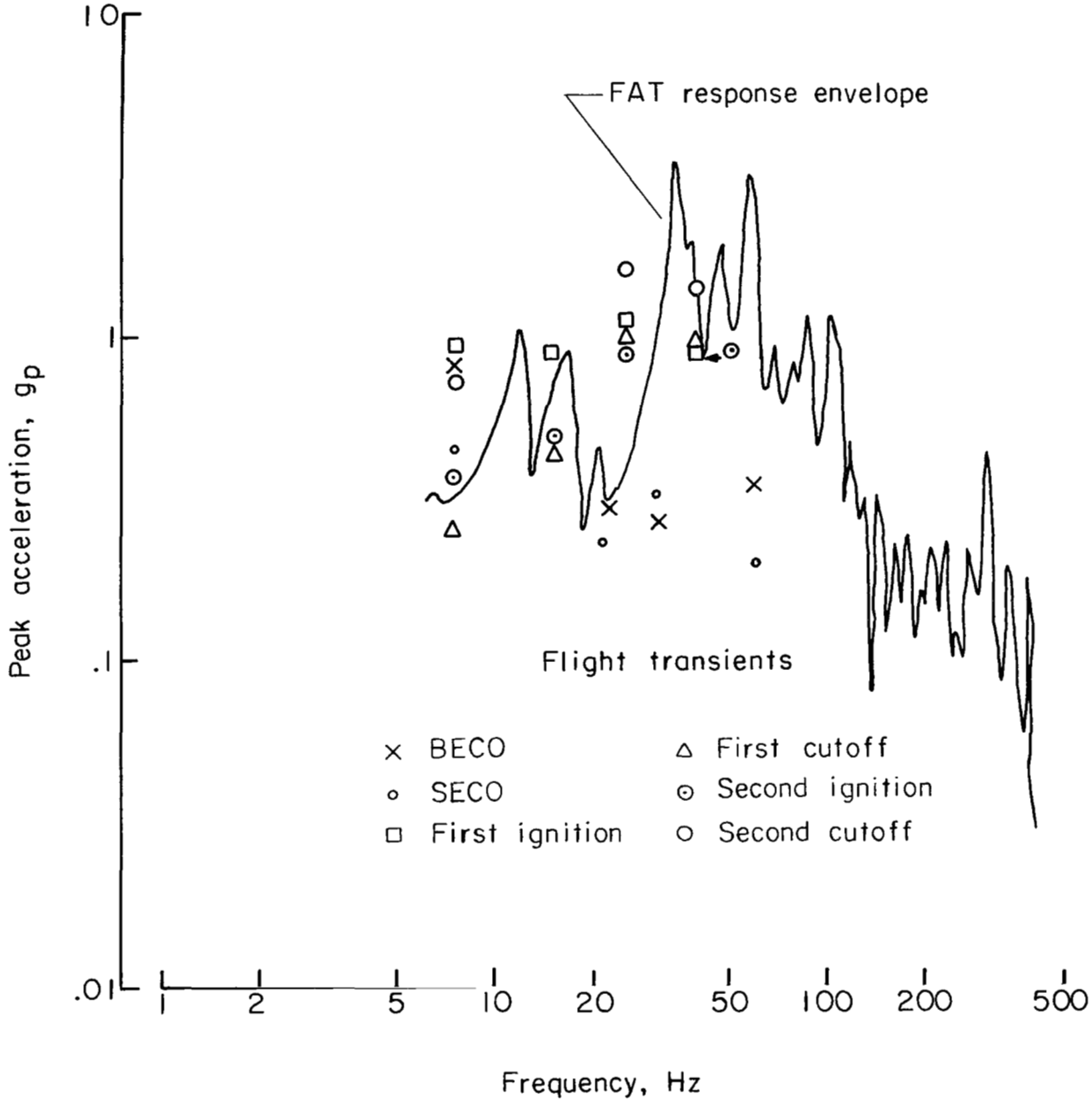

Figure 37.- Comparison of spacecraft transverse response $(A_{s,t})$ due to sinusoidal FAT and flight inputs. Lunar Orbiter V.

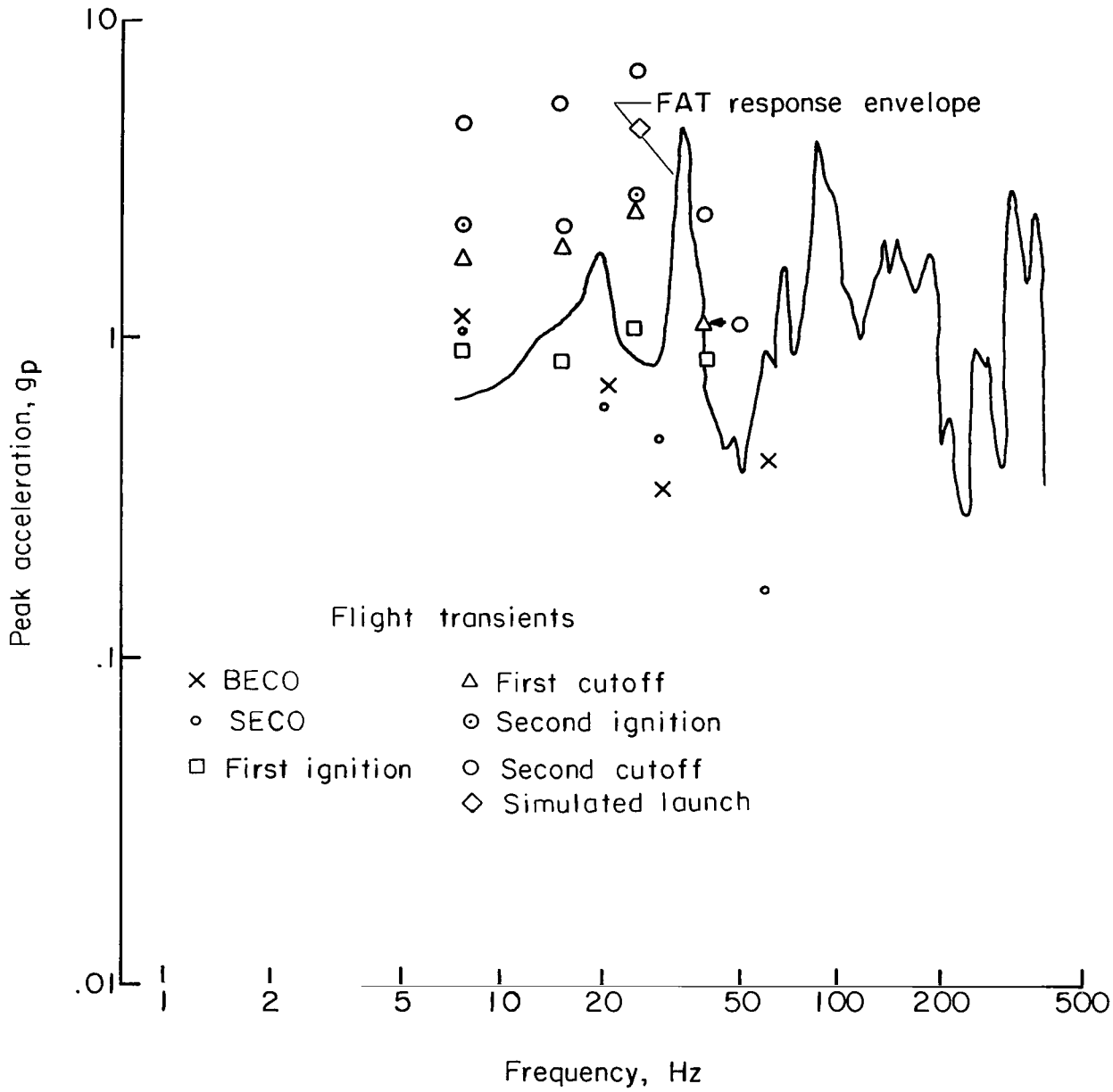

Figure 38.- Comparison of spacecraft longitudinal response $(A_{s,l})$ due to sinusoidal FAT and flight inputs. Lunar Orbiter V.

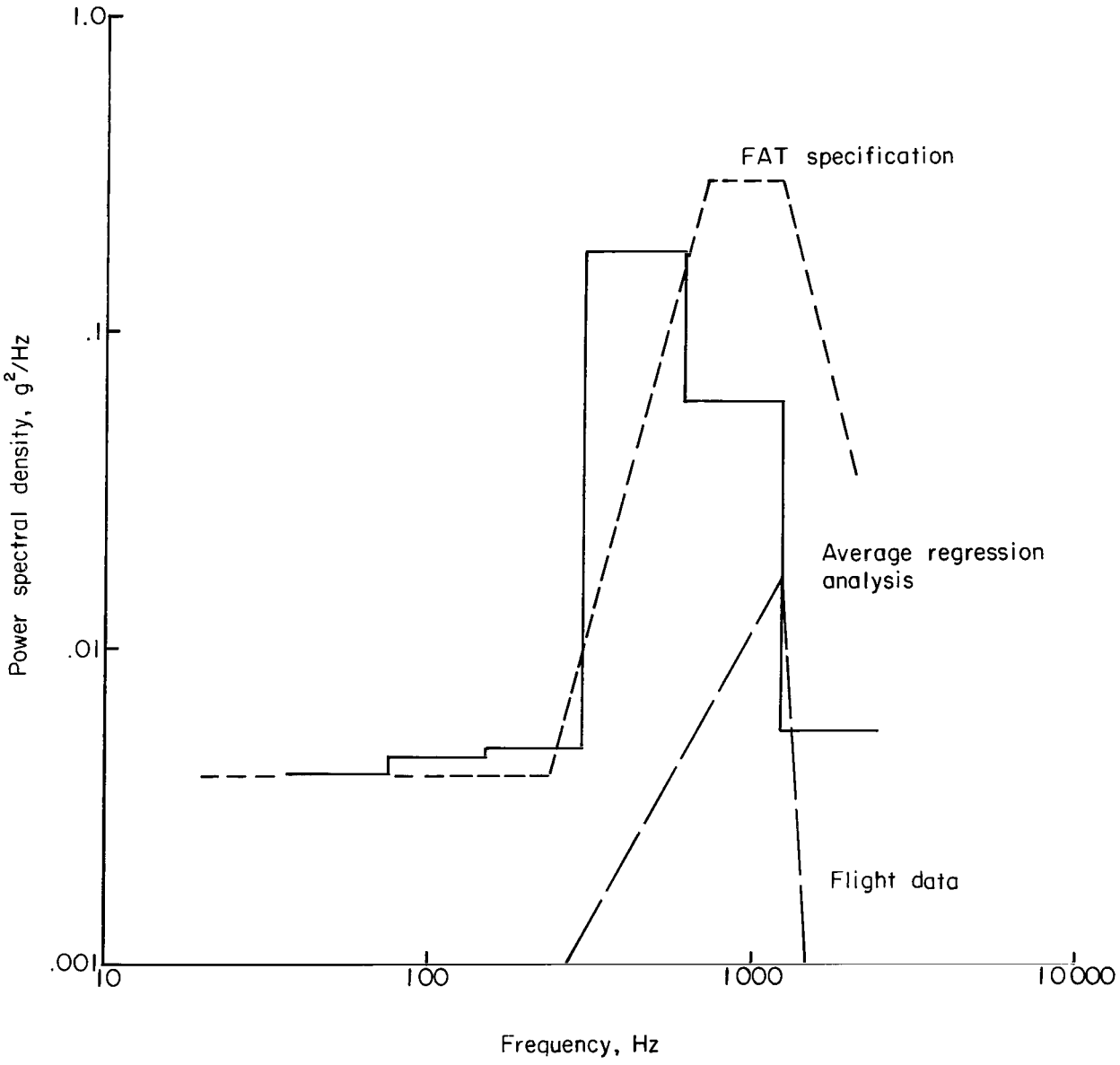

Figure 39.- Comparison of FAT, regression analysis, and flight data in the longitudinal direction $(A_{a,l})$ at lift-off.

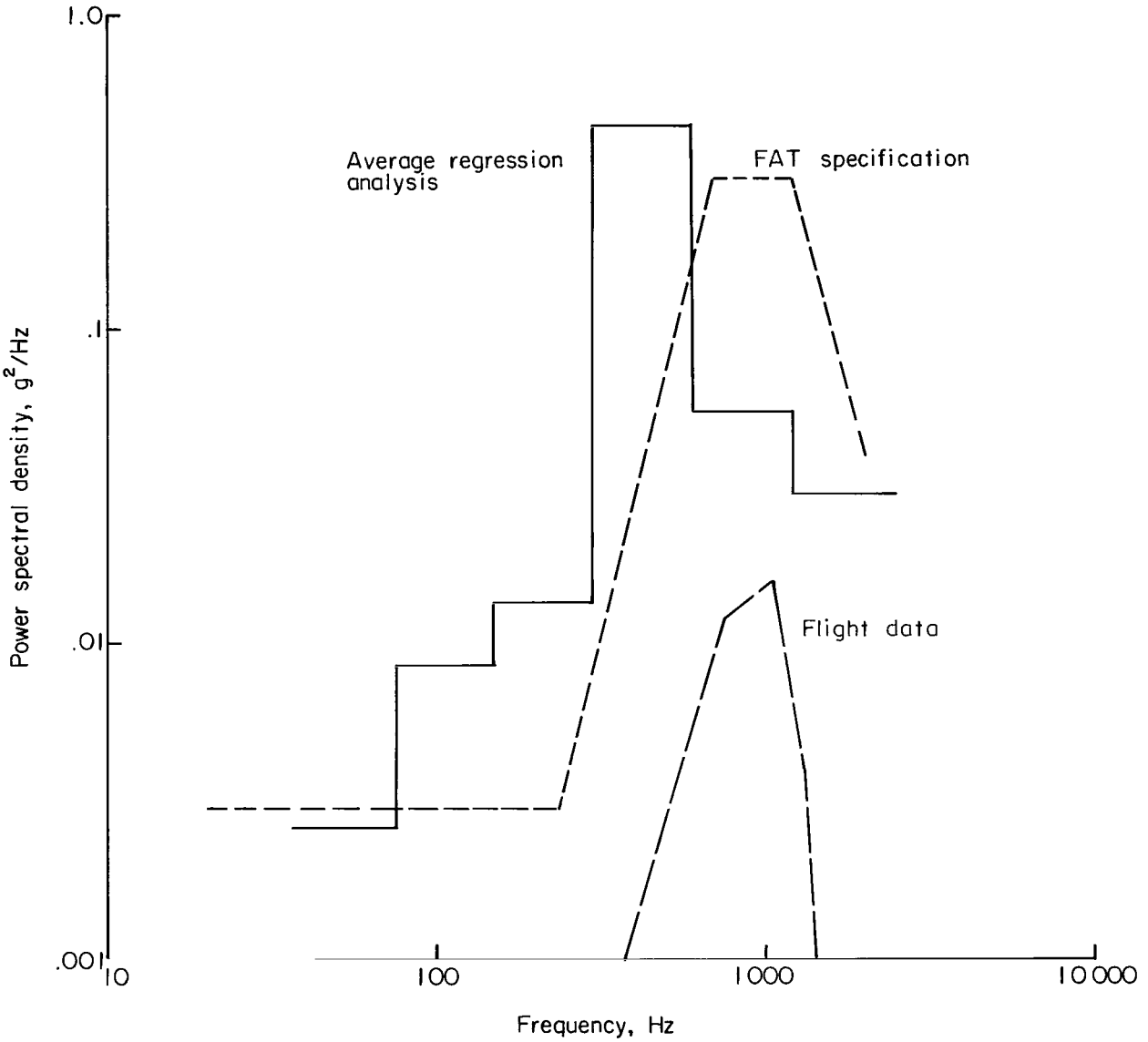

Figure 40.- Comparison of FAT, regression analysis, and flight data in the longitudinal direction $(A_{a,l})$ at transonic speeds.

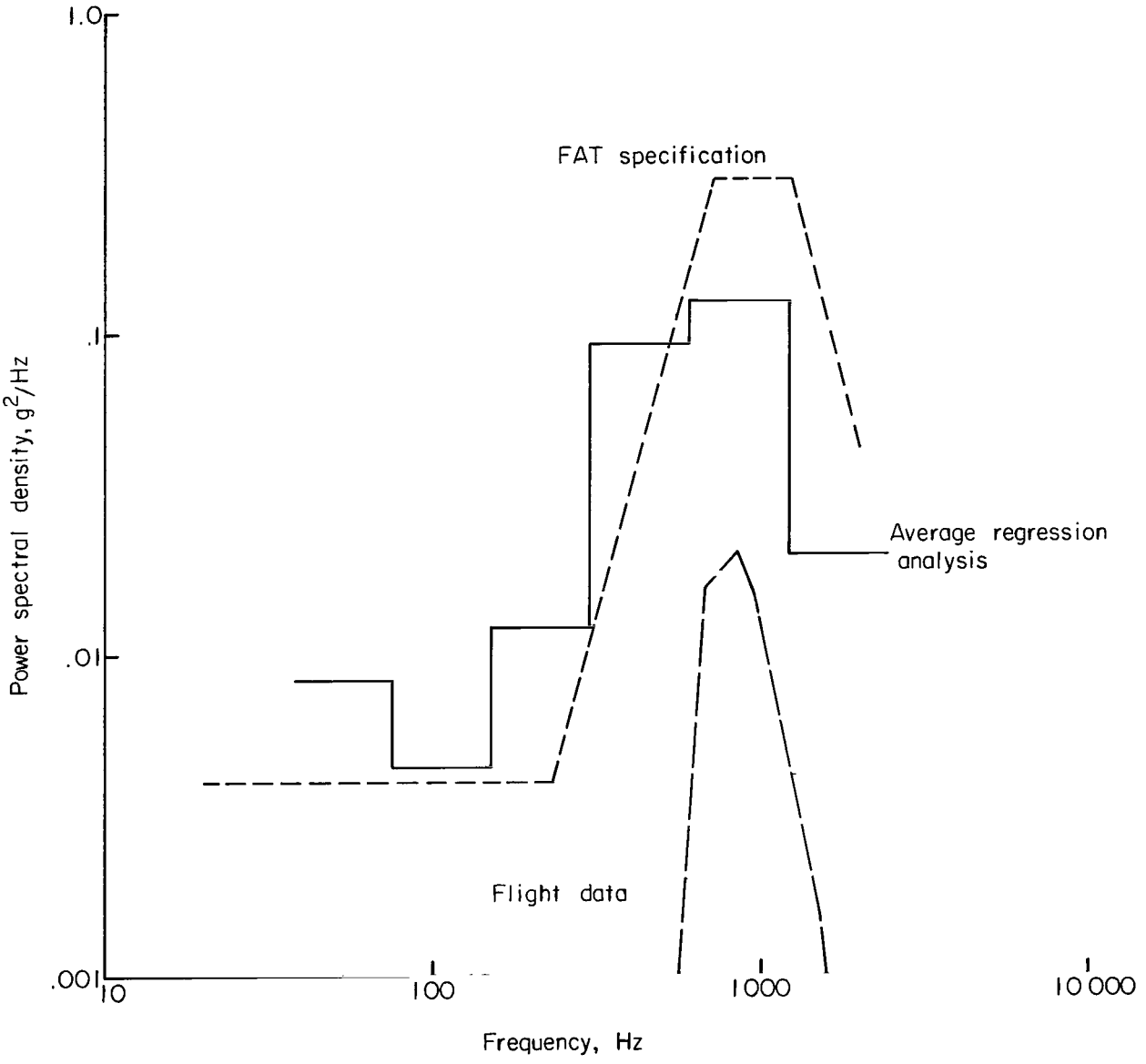

Figure 41.- Comparison of FAT, regression analysis, and flight data in the transverse direction $(A_{a,t})$ at lift-off.

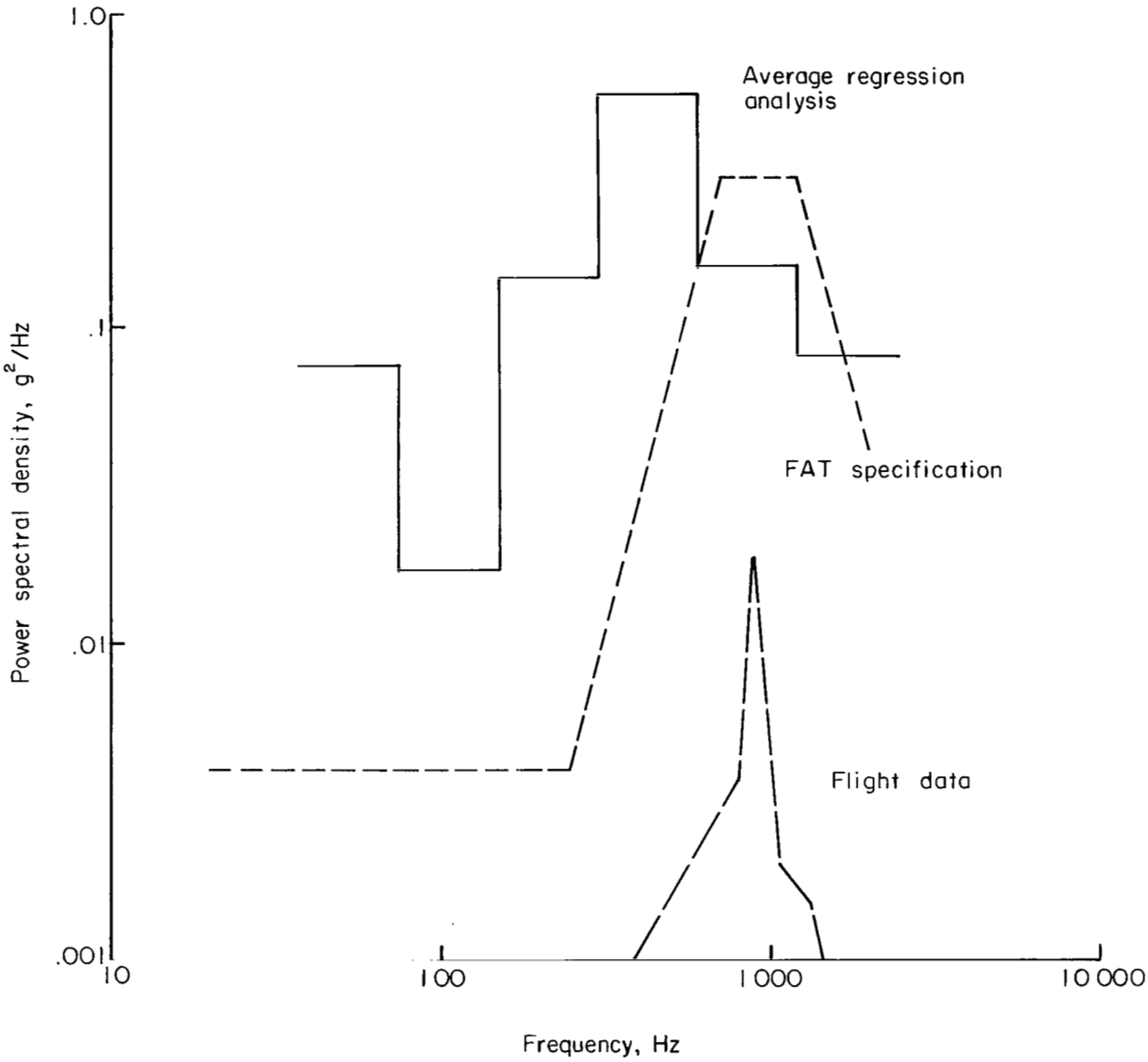

Figure 42.- Comparison of FAT, regression analysis, and flight data in the transverse direction $(A_{a,t})$ at transonic speeds.

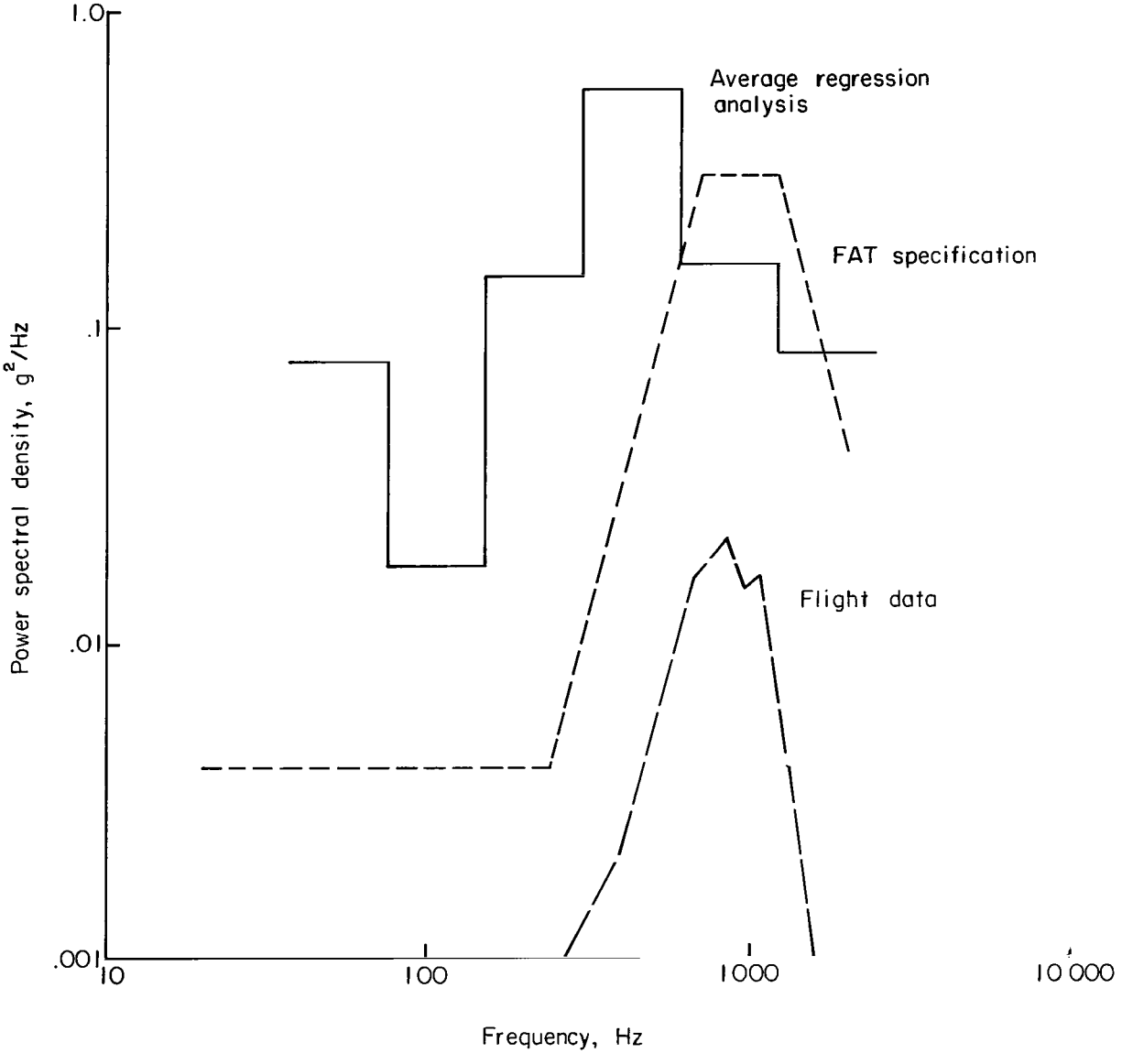

Figure 43.- Composite comparison of FAT, regression analysis, and flight data.

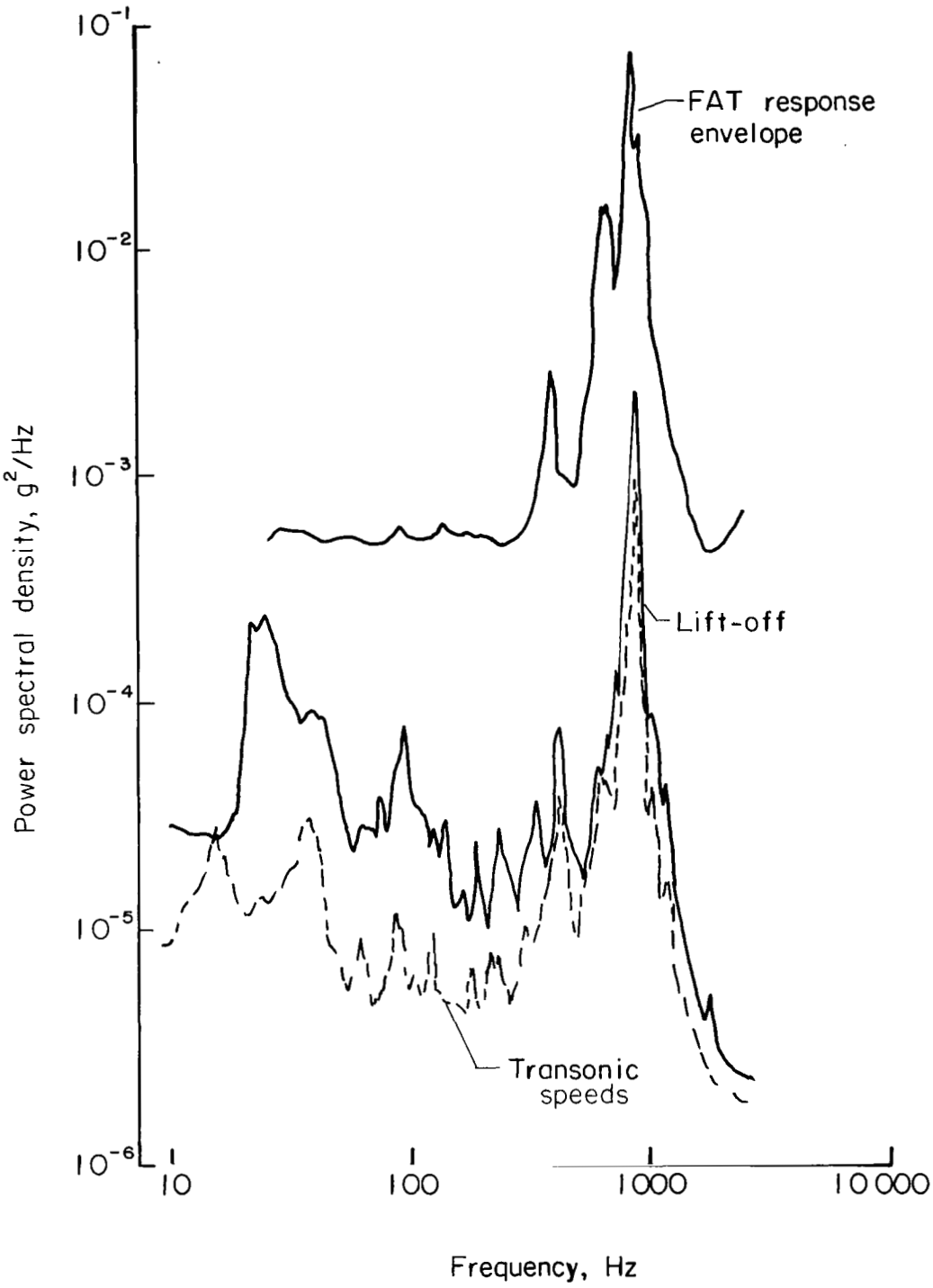

Figure 44.- Comparison of spacecraft transverse response due to random FAT and flight inputs $(A_{s,t})$.

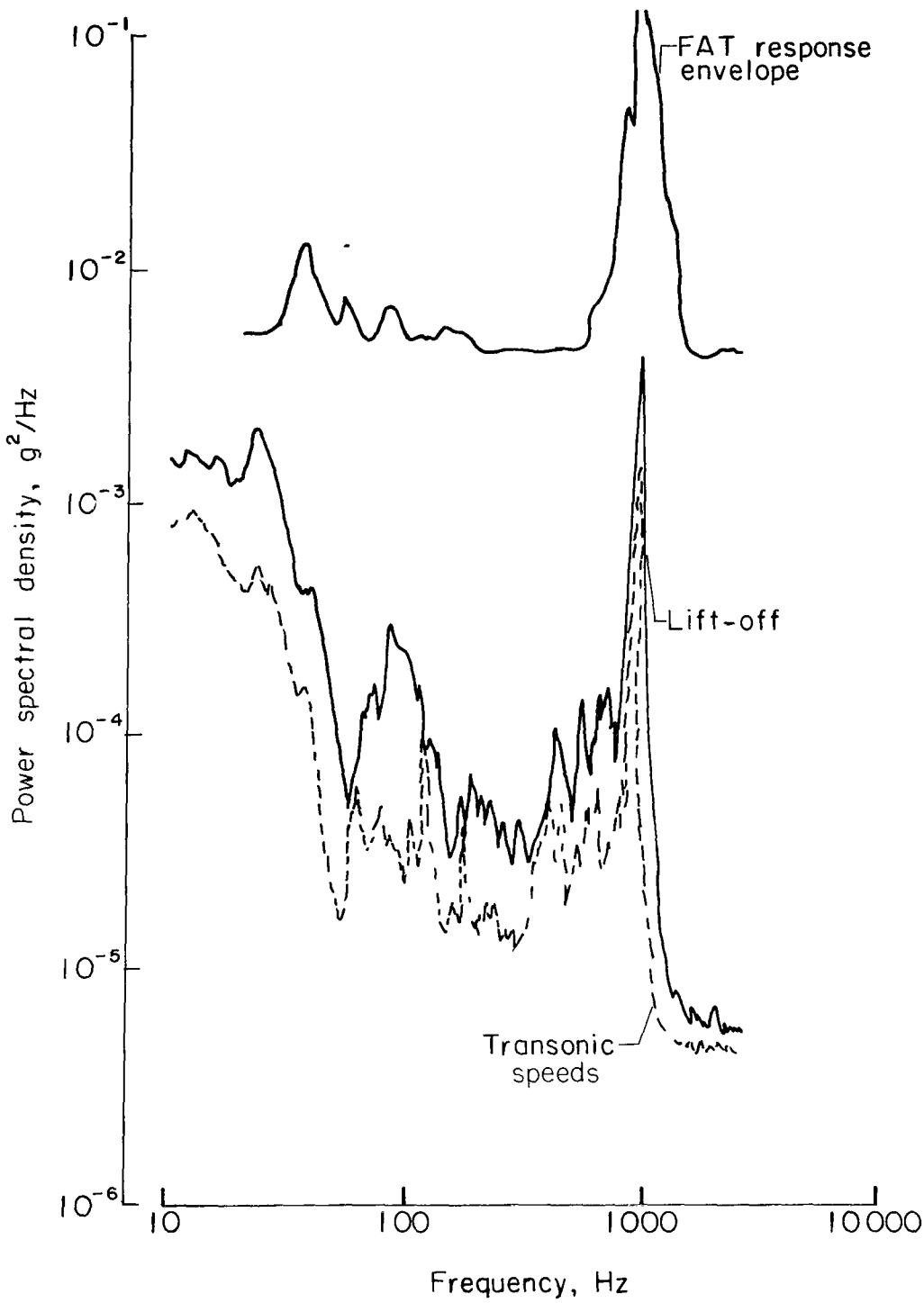

Figure 45.- Comparison of spacecraft longitudinal response due to random FAT and inputs $(A_{s,l})$.

NASA-Langley, 1970 — 31 L-6594

"The aeronautical and space activities of the United States shall be conducted so as to contribute . . . to the expansion of human knowledge of phenomena in the atmosphere and space. The Administration shall provide for the widest practicable and appropriate dissemination of information concerning its activities and the results thereof."

—NATIONAL AERONAUTICS AND SPACE ACT OF 1958

NASA SCIENTIFIC AND TECHNICAL PUBLICATIONS

TECHNICAL REPORTS: Scientific and technical information considered important, complete, and a lasting contribution to existing knowledge.

TECHNICAL NOTES: Information less broad in scope but nevertheless of importance as a contribution to existing knowledge.

TECHNICAL MEMORANDUMS: Information receiving limited distribution because of preliminary data, security classification, or other reasons.

CONTRACTOR REPORTS: Scientific and technical information generated under a NASA contract or grant and considered an important contribution to existing knowledge.

TECHNICAL TRANSLATIONS: Information published in a foreign language considered to merit NASA distribution in English.

SPECIAL PUBLICATIONS: Information derived from or of value to NASA activities. Publications include conference proceedings, monographs, data compilations, handbooks, sourcebooks, and special bibliographies.

TECHNOLOGY UTILIZATION PUBLICATIONS: Information on technology used by NASA that may be of particular interest in commercial and other non-aerospace applications. Publications include Tech Briefs, Technology Utilization Reports and Notes, and Technology Surveys.

Details on the availability of these publications may be obtained from:

SCIENTIFIC AND TECHNICAL INFORMATION DIVISION

NATIONAL AERONAUTICS AND SPACE ADMINISTRATION

Washington, D.C. 20546